N68-15698

NASA CR-72253
DAC-60975

INTERIM REPORT

HYPERGOLICITY OF F_2-H_2 AND REACTION PRODUCT FREEZING UNDER MAIN TANK INJECTION PRESSURIZATION CONDITIONS

by

E. C. Cady

prepared for

NATIONAL AERONAUTICS AND SPACE ADMINISTRATION

15 September 1967

CONTRACT NAS 3-7963

Technical Management
NASA Lewis Research Center
Cleveland, Ohio
Erwin A. Edelman

Douglas Aircraft Company
Missile and Space Systems Division
Santa Monica, California

FOREWORD

This report was prepared by the Douglas Aircraft Company under Contract No. NAS 3-7963. The contract is administered by the National Aeronautics and Space Administration, Lewis Research Center, Chemical and Nuclear Rocket Procurement Section, Cleveland, Ohio. The NASA Project Manager for the contract is Mr. E. A. Edelman. This is the Interim Report on the contract, summarizing technical effort from 30 June 1966 to 30 July 1967.

The contribution of W. G. Black, G. R. Compton, W. D. English, and W. J. Wachtler, Douglas Aircraft Company, to the technical effort described in this report is gratefully acknowledged.

Independent Research and Development (IRAD) funds from the Douglas Aircraft Company, resulting in Appendix A, Freezing Point Depression in LF_2 Systems, by W. A. Cannon, W. E. Crane, and W. D. English, Douglas Aircraft Company, and contributing to this report are acknowledged.

ABSTRACT

An experimental program is described which determined the effects of physical and chemical variables on the hypergolicity of F_2 - H_2 under conditions relevant to Main Tank Injection pressurization of the LH_2 tank. A concurrent program describes the characteristics of reacted HF and unreacted F_2 freezing in the LH_2 tank. Testing was done in small (5-in. diam) glass Dewars. Generally, hypergolic ignition was found with some variables inhibiting the reaction to a point of nonignition and freezing of the F_2. Several injection modes were tested, and criteria for reliable ignition and effective pressure rise were determined.

CONTENTS

INTRODUCTION 1

HYPERGOLICITY 3

- Parameter Definition 3
- Experiment Design 6
- Test Facility Description and Procedure 17
- Results 32

REACTION PRODUCT FREEZING 67

- Reacted Product 67
- Unreacted Product 72

CONCLUSIONS 73

REFERENCES 75

APPENDIX A 77

- Symbols 85
- References 87

LIBRARY CARD 89

DISTRIBUTION LIST 91

PRECEDING PAGE BLANK NOT FILMED.

FIGURES

1	MTI Hypergolicity Test Facility Schematic	18
2	MTI Hypergolicity Test Apparatus	22
3	Ullage Injection Test Apparatus	23
4	Submerged Injection Test Apparatus	24
5	Hypergolicity Test Setups	24
6	Special Test Setup	25
7	MTI Hypergolicity Control Schematic	28
8	Typical Fastax Movie Photos	29
9	Oscillograph of Typical Ullage Injection Without Reaction	40
10	Oscillograph of Typical Ullage Injection With Reaction	41
11	Specific Pressure Rise vs Injection Pressure (Warm Gas Injected Into Ullage)	43
12	Specific Pressure Rise vs Injection Pressure (Cold Gas or Liquid Injected Into Ullage)	44
13	Effect of O_2 Contaminant in Injectant on Specific Pressure Rise	45
14	Effect of O_2 Contaminant in Injectant on Minimum Ignition Energy	46
15	Oscillograph of Typical Enthalpic Pressure Rise With Submerged Injection	49
16	Oscillograph of Typical Submerged Injection Without Reaction	50
17	Oscillograph of Typical Submerged Injection With Reaction	52
18	Specific Pressure Rise vs Injection Pressure Differential (Submerged Injection with 10-psi He Pressure)	53
19	Specific Pressure Rise vs Injection Pressure Differential (Submerged Injection Without He Prepurge)	54
20	Specific Pressure Rise vs Injection Pressure Differential (Submerged Injection With Warm Gas for Different Injection Modes)	56

21 Pressure Rise vs Injected Mass for Three Heat Transfer Models 65

22 Photograph Showing Absence of Tyndall Effect After Reaction 68

23 Reaction-Product Effects 69

24 Injector Damage Caused by HF Attack 71

A-1 Freezing-Point Apparatus 81

A-2 Typical Cooling Curve 83

A-3 Phase Diagram OF_2 - F_2 84

TABLES

I	Summary of Parameters and Values	7
II	Enthalpy Effects--Gaseous Injectant	9
III	Enthalpy Effects--Liquid Injectant	10
IV	US Injector With Gaseous Reactive Injectant	12
V	US Injector With Liquid Reactive Injectant	13
VI	SS Injector With Gaseous Reactive Injectant	14
VII	SS Injector With Liquid Reactive Injectant	15
VIII	Supplemental Testing Conditions	16
IX	Valve Identification	20
X	Fluorine Analysis	30
XI	MTI-Hypergolicity Test Summary	33
XII	Pressure Rise Comparison Using Point-to-Point Technique (Warm Gas US Injection)	59
XIII	Pressure Rise Comparison Using Point-to-Point Technique (SS Injection With Purge)	60
XIV	Pressure Rise Comparison Using Point-to-Technique (SS Injection With Cold Gas or Liquid)	63
A-I	Observed Freezing Points, OF_2 - F_2 Mixtures	82

SUMMARY

A comprehensive series of 131 tests was performed to experimentally determine how physical and chemical variables affected the hypergolicity of fluorine and hydrogen at conditions relevant to the use of F_2 for Main Tank Injection (MTI) pressurization of the LH_2 tank of a space vehicle. A concurrent investigation studied the problem of reacted products (HF) or unreacted injectant (F_2) freezing in the LH_2 tank. The physical variables included injector location; F_2 phase (ambient gas, liquid, and saturated vapor), temperature (140° -520°R) and pressure (65 psia-195 psia); and H_2 condition (saturated at 25-55 psia). Chemical variables included propellant contaminants and catalytic effects. The tests were performed in small (5 in. diam. x 10 in.) glass Dewars, with pressure and temperature measurements and Fastax movies (at 4,000 pictures/sec) taken of each test. Expulsion of the LH_2 from the tank was not performed.

The following results were noted:

(1) Generally, hypergolic ignition of F_2 and H_2 was found; however, some variables inhibited the reaction to the point of nonignition, with resultant freezing of F_2 in the LH_2. Strong inhibition was caused by very low (~ 1.0 vol %) O_2 contamination of the F_2 injectant with the ullage injection mode, and by the use of an injector prepurge of helium with the submerged injection mode.

(2) Reliable ignition and effective pressurization were found with submerged injection without a helium prepurge, but problems of HF freezing in the injector occurred.

(3) The frozen HF and frozen unreacted F_2 behaved differently in the test tank. The HF suspended in the LH_2 and plated out on all internal tank surfaces; the F_2 settled loosely in the tank bottom where it occasionally detonated violently.

(4) Within the limits of small-scale testing, practical criteria were determined for the design of MTI pressurization systems for F_2-H_2 vehicles.

INTRODUCTION

Main Tank Injection (MTI) Pressurization is a technique for rocket vehicle propellant tank pressurization in which a hypergolic reactant is injected into the propellant tank, and the resultant reaction heat release is used to pressurize the tank. A great deal of work has been done with MTI as applied to hypergolic storable propellants (ref. 1, for example), but little has been done with hypergolic cryogenic propellants such as fluorine and hydrogen. This report presents the initial work performed in a program to analytically and experimentally determine the feasibility, limitations, and operating characteristics of a propellant tank pressurization system which utilizes the injection of fluorine into a liquid hydrogen tank to generate pressurizing gas by vaporizing hydrogen. This initial effort is a study of two problems peculiar to this cryogenic hypergolic system: the effect of a number of physical and chemical variables on the hypergolicity of fluorine injected into a liquid hydrogen tank; and the characteristics and behavior of the reaction products freezing in the hydrogen tank. The two problems fall naturally into two investigations with the following objectives:

(1) Hypergolicity Investigation--To establish, through a series of tests, the range of conditions over which fluorine will be hypergolic with hydrogen contained in a rocket propellant tank. Since the hypergolicity determination is specifically for operating conditions found in liquid hydrogen rocket propellant tanks, the selection and range of parameters used are limited accordingly, and include all parameters expected to affect such hypergolicity. Ignition lag and repeatability were determined by high-frequency-response instrumentation, including high-speed Fastax movie photography. This program was performed in small-scale glass tanks to provide maximum viewing capability. There was no expulsion of the liquid hydrogen during this phase.

(2) Reaction Product Freezing Investigation--To determine the modes and hazards of freezing of the reaction products during and after pressurization through analysis and experiments concurrent with that of the hypergolicity investigation. The behavior of unreacted injectant is included in this study. Location, type, size, and composition of frozen solids, buildup rate, particle settling rate, and propellant surging effects on the adherence of the particles were determined by visual observations and analysis of frames from motion pictures. Effects of vibration upon adherence could not be determined, and attempts at analytical sampling were not successful.

Based on the data determined from these two investigations, criteria for the design of the injectors and other MTI system components and characteristics are being established.

The actual injector design, fabrication, and expulsion testing in large-scale tankage are to be done during subsequent phases of the program.

HYPERGOLICITY

Parameter Definition

To design a rational experiment, it is necessary to define all of the parameters that affect F_2 - H_2 hypergolicity under the conditions found in a vehicle LH_2 tank. Analysis of the system suggested that there were a sufficient number of potentially important parameters to make imperative the design of the overall experiment in the form of a statistical test matrix. Using such a plan, it was possible to hold the number of levels of most variables to two and still develop adequate data. The parameters were separated into three classes: mechanical, physical, and chemical.

Mechanical Parameters.—Injector Location and Type: There were two basic injector locations: injection into the GH_2 ullage and submerged injection into the LH_2. Because only one propellant was injected, there were only two basic types of injection: simple injection through a single tube, and aspirated injection through an eductor tube to pump H_2 (with the F_2) into the combustion zone. The very small quantities of injectant (~0. 1 gm) and the very short injection times (50 to 100 msec), would probably make aspirated performance very difficult to obtain, particularly in the ullage space. However, the aspirated type could be effective in the submerged injector location. Accordingly, the location/types considered were ullage space/simple injection (US), submerged/simple injection (SS) and submerged/aspirated injection (SA). During supplementary tests,ullage space/aspirated injection (UA) was alsorun. Interface combustion was not considered as an independent uncoupled location/type, since it would occur as a natural consequence of ullage injection which penetrates the ullage without ignition but ignites at the interface. Thus, this mode was evaluated as it occurred during ullage space testing; if it had not occurred, it would be difficult to obtain this type of combustion with a practical vehicle system.

Injector Purge: Freezing of reactant fluorine (F_2) or product hydrogen fluoride (HF) in the injector may be a problem, or combustion inside the injector tube may cause ignition of the injector structural materials, hence it may be necessary to purge the injector with gaseous helium (GHe) before and/or after each use. A helium prepurge is particularly likely to be a requirement for the submerged injectors, because there will be gaseous or liquid hydrogen in the injector tube. Although it is clear that a helium prepurge may have a considerable effect on ignition, it is difficult to see, except for rapidly pulsed injections, how a post-injection purge would affect subsequent ignition (except as it diluted the ullage GH_2, covered under ullage composition below). Accordingly, a helium prepurge was a variable for the test series, while a post-purge was not used (because conditions did not demand it). The helium prepurge pressure was selected as 10 psig because, mechanically, this pressure gave an adequate purge with small chance of excessive F_2 dilution.

Physical Parameters.—Injectant Enthalpy: Injection of a relatively hot injectant into the LH_2 tank may cause pressure and temperature rise even without reaction. To isolate the enthalpic heat injection from the reaction heat injection, there were a series of "blank" tests with nitrogen as a non-reactive simulant for fluorine. Both gaseous nitrogen (GN_2) and liquid nitrogen (LN_2) at conditions comparable to those of the gaseous fluorine GF_2) and liquid fluorine (LF_2) were used; i.e., LN_2, saturated at 140°R and 180°R, and GN_2, superheated vapor at 160°R - 75 psia and gas at 400°R - 75 psia.

Fluorine Phase: This variable was partly controlled by the preconditioning of the injectant and partly affected by the injection velocity, since if injection were slow, the injectant would stay in contact with the cold injector parts longer. All three phases were originally suggested: solid, liquid, and gas. Injection of a solid, except in a carrier, is impractical, but contact of solid F_2 with LH_2 and GH_2 could be provided by some mechanical system, such as breaking an ampule containing F_2 inside the H_2 container. Very slow injection of F_2 could result in formation of solid F_2 in the injector, but effective injection of this plug would be chancy. It was felt that if injected F_2 froze without reaction, there would be subsequent opportunities to observe its behavior in LH_2. Thus, the solid phase was eliminated from consideration as an injectant. The conditions used for LF_2 and GF_2 injectant phase were as follows:

(1) LF_2--Saturated (or subcooled) at 140°R, 180°R.

(2) GF_2--Saturated vapor at 180°R - 75 psia.
Superheated vapor at 400°R - 75 psia.
Superheated vapor at 400°R - 150 psia.

These were selected as appropriately bracketing the conditions which would be used in an actual MTI pressurization system.

Hydrogen Phase: Although previously identified as a separate variable, this was not separable from injector location/type. The conditions of H_2 temperature and pressure were coupled at equilibrium saturated conditions, which were LH_2 and GH_2 - saturated at 40°R, 25 psia and saturated at 46°R, 55 psia. Immediately following pressurization or injectant reaction, the ullage could be hotter than the equilibrium liquid temperature. Some contingency tests were planned to investigate the effect of warm ullage (see below).

Injectant Quantity: The nature of the pressure pulse-peak height and duration depends on the quantity of F_2 injected. The quantities chosen to minimize the change of apparatus breakage were approximately 1.0×10^{-4} and 2.0×10^{-4} lb/slug injected. These approximate quantities were used for both liquid and gaseous injection.

Injector Valve Open Time: The injector valve open time was the only other easily controlled physical variable, and, together with system geometry, injectant phase, and pressure differentials, determined injectant flow rate and velocity which were derived variables that may be important to the hypergolic reaction. There were two valve-open times: 0.050 sec and 0.100 sec.

Ullage Volume: It was anticipated that ullage volume variation would have only a second-order effect on ullage injection. This effect was studied in conjunction with the special experiments for wall effects described below. Thus ullage volume was not a parameter for the main testing.

Chemical Parameters.—Ullage Composition: The principal variable was the effect of GHe dilution of the ullage. For an actual system, He might be used for ground- or prepressurization and could be present even after venting. Two levels of He in the ullage, 0% and 50%, were selected. The ullage composition was only important in the ullage (US location/type) tests, and was not a varaiable for the submerged (SS or SA) location/type tests.

Fluorine Purity: Two separate, independent variables were considered here: HF and oxygen (O_2) contaminants. HF was suspected of acting as a catalyst, speeding up the reaction (ref. 2), while O_2 has been shown to be an inhibitor under some conditions (ref. 3). HF concentration in F_2 was readily controlled down to the 0.02 (vol %) level reached with NaF scrubber traps. It was not practical to add HF to the F_2. The two levels were: natural HF content, and scrubbed to 0.02 vol %; and these only in GF_2 at the conditions of 400°R and 75 and 150 psia, since the HF will freeze out of saturated vapor or liquid.

O_2 is a common contaminant in F_2, and, since removal of O_2 is difficult and expensive, while addition of extra O_2 is easy, tests were performed with 1.0 vol % added O_2. Thus the levels tested were natural O_2 content and natural +1.0 vol % added O_2 in both LF_2 and GF_2.

Catalytic Effects: Catalysis by structural materials and combustion products was considered, and the following areas were tested:

(1) Combustion product catalysis--The effect of HF produced in a prior pulse on the ignition of subsequent pulses was coupled to the effects of the warm ullage gas discussed above and were to be studied in the same contingency tests. Again, this effect was only important for the ullage location/type (US) and was not a parameter for the submerged (SS or SA) location/type.

(2) Wall effects--The effect of typical structural materials for propellant tanks were studied in a separate series of tests (see below) with tube bundles of typical material placed in the glass reactor. Only ullage (US) location/type combustion was tested with no tubes, and with aluminum tubes, at two ullage levels (degree of wall exposure): 1/3 and 2/3 ullage. The no-tube condition has stainless steel present in the valve head.

(3) Injector materials effects--These effects could only be explored if complete injector apparatus sets including injector valve and valve

head exposed in the Dewar could be made of different materials. This is impractical and very expensive, and was therefore eliminated as a basic test variable. It was anticipated that if there were a material effect on the reaction, it would be detected during the wall effects tests described above.

A summarized list of pertinent variables and the number of levels investigated is shown in Table I. It will be noted that the large number of variables, together with the potential for two- and three-factor interactions, could make the number of tests very large. To minimize the number of tests and to maximize the amount of information, the test matrix was statistically designed. The experiment design contains contingency plans to be utilized as the need arises, based on the initial test data.

Experiment Design

If it is assumed that the important dependent variables of hypergolicity, namely, reaction (ignition delay time), pressure rise, and temperature rise, are continuous quantitative functions (at least over the range of concern) of the independent variables (factors) shown in Table I, then the fractional factorial approach to experiment design is the most efficient means of deriving information about main effects (the effects of a change in a specific independent variable on the dependent variables) and important interaction effects (ref. 4). Within the limits set by experimental error, fractional factorial design:

(1) Enables the main effects of every factor to be estimated independently of one another.

(2) Enables the dependence of the effect of every factor upon the levels of the others (the interactions) to be determined (where desired).

(3) Enables the effects to be determined with maximum precision.

(4) Supplies an estimate of the experimental error for the purpose of assessing the significance of the effects and enables confidence limits to be determined.

Three of the parameters of Table I make the experiments fall into natural groups. These are reactive or nonreactive injectant, ullage or submerged location/type, and gas or liquid injectant.

Nonreactive Injectant. — To evaluate the enthalpic effects of injecting warm fluid into the hydrogen tank, a series of tests were run with nitrogen as shown in Tables II and III. The subscripted letters refer to the code symbols for parameters and levels shown in Table I. The numbers in parentheses refer to actual tests run, shown in Table XI and discussed below. Since no reaction is involved, only thermodynamic variables are considered. Data from these tests give baseline pressure and temperature rise for comparison with the reactive tests with comparable conditions, and thermodynamic

TABLE I

SUMMARY OF PARAMETERS AND VALUES

	Code Symbol	Selected Level
A.	Location/Type	
	a_1	US (= Ullage, simple)
	a_2	SS (= Submerged, simple)
	a_3	SA (= Submerged, aspirated)
B.	Injector materials: comparison not practical	
C.	Enthalpy	
	c_1	N_2
	c_2	F_2
D.	Liquid injectant	
	d_1	140°R Saturated
	d_2	180°R Saturated
	d_3	180°R - 75 psia (Saturated vapor)
E.	Gaseous injectant	
	e_1	400°R - 75 psia
	e_2	400°R - 150 psia
F.	Hydrogen	
	f_1	40°R - 25 psia saturated
	f_2	46°R - 55 psia saturated
	f_3	Hot ullage & HF--Contingency test
G.	Injectant quantity	
	g_1	1.0×10^{-4} lb
	g_2	2.0×10^{-4} lb
H.	Injector valve open time	
	h_1	0.050 sec
	h_2	0.100 sec

TABLE I (Concluded)
SUMMARY OF PARAMETERS AND VALUES

	Code Symbol	Selected Level
I.	Ullage composition	
	i_1	0% He
	i_2	50% He
J.	HF contaminant in F_2	
	j_1	0.02 vol %
	j_2	Natural HF Content
K.	O_2 contaminant in F_2	
	k_1	Natural O_2 content
	k_2	1.0 vol % added O_2
L.	Injector purge	
	l_1	With prepurge
	l_2	Without prepurge
M.	Wall effects	
	m_1	No tubes
	m_2	Al tubes
N.	Ullage	
	n_1	1/3
	n_2	2/3
O.	Gaseous injectant (GN_2 only)	
	o_1	160°R - 75 psia
	o_2	400°R - 75 psia

TABLE II
ENTHALPY EFFECTS--GASEOUS INJECTANT

<table>
<tr><th>Independent variables and levels;</th><th>Constant parameters and levels</th></tr>
<tr><td>A: a_1, a_2
G: g_1, g_2
F: f_1, f_2
H: h_1, h_2
O: o_1, o_2</td><td>For a_1: c_1 i_1 l_2 m_1 n_1
For a_2: c_1 i_1 l_1 m_1 n_1</td></tr>
<tr><td colspan="2">Main effects and two-factor interactions that can be estimated</td></tr>
<tr><td colspan="2">All: A, G, F, H, O, AG, AF, AH, AO, GF, GH, GO, FH, FO, HO</td></tr>
<tr><td colspan="2">Combinations to be tested $1/2 \times 2^5 = 16$</td></tr>
<tr><td colspan="2">a_1 g_1 f_1 h_1 o_1
a_2 g_2 f_1 h_1 o_1
a_2 g_1 f_2 h_1 o_1
a_1 g_2 f_2 h_1 o_1
a_2 g_1 f_1 h_1 o_2
a_1 g_2 f_1 h_1 o_2
a_1 g_1 f_2 h_1 o_2
a_2 g_2 f_2 h_1 o_2
a_2 g_1 f_1 h_2 o_1
a_1 g_2 f_1 h_2 o_1
a_1 g_1 f_2 h_2 o_1
a_2 g_2 f_2 h_2 o_1
a_1 g_1 f_1 h_2 o_2 (1)
a_2 g_2 f_1 h_2 o_2
a_2 g_1 f_2 h_2 o_2
a_1 g_2 f_2 h_2 o_2
Note: Experiment number in parentheses</td></tr>
</table>

TABLE III

ENTHALPY EFFECTS--LIQUID INJECTANT

<table>
<tr><th>Independent variables and levels</th><th>Constant parameters and levels</th></tr>
<tr><td>A: a_1, a_2
F: f_1, f_2
D: d_1, d_2
G: g_1, g_2
H: h_1, h_2</td><td>For a_1: c_1 i_1 l_2 m_1 n_1
For a_2: c_1 i_1 l_1 m_1 n_1</td></tr>
<tr><th colspan="2">Main effects and two-factor interactions that can be estimated</th></tr>
<tr><td colspan="2">All: A, F, D, G, H, AC, AF, AD, AG, AH, FD, FG, FH, DG, DH, GH</td></tr>
<tr><th colspan="2">Combinations to be tested 1/2 x 2^5 = 16</th></tr>
<tr><td colspan="2">a_2 f_1 d_1 g_1 h_1 (46C)
a_1 f_2 d_1 g_1 h_1
a_1 f_1 d_2 g_1 h_1
a_1 f_1 d_1 g_2 h_1
a_1 f_1 d_1 g_1 h_2
a_2 f_2 d_2 g_1 h_1
a_2 f_2 d_1 g_2 h_1
a_2 f_2 d_1 g_1 h_2
a_2 f_1 d_2 g_1 h_1 (46D)
a_2 f_1 d_2 g_1 h_2 (46A)
a_2 f_1 d_1 g_1 h_2 (46B)
a_1 f_2 d_2 g_2 h_1
a_1 f_2 d_2 g_1 h_2
a_1 f_2 d_1 g_2 h_2
a_1 f_1 d_2 g_2 h_2 (2)
a_2 f_2 d_2 g_2 h_2</td></tr>
<tr><td colspan="2">Note: Experiment number in parentheses</td></tr>
</table>

interactions can be defined. These tests also provide some information on whether a purge is required to prevent freezing of injected fluid in the injector.

Reactive Injectant. — The reactive tests are broken down by location/type and gas/liquid injectant; the series is shown in Tables IV to VII. It will be noted that only US and SS location/types are specified. However, as shown in Table VI, tests with the SA location/type were performed.

In Table IV, all the obvious variables are evaluated except injectant quantity, injector purge, and wall effects. Injectant quantity is evaluated in all other tests and its interactions were well defined by these. Injector purge is evaluated as a variable in the submerged tests but is eliminated as a variable in the US tests with metal injector where it is felt to be of lesser importance. Some check tests were run, however.

In Table V, there are three levels of "liquid" condition, one of which is saturated vapor. This is lumped with the liquid test for convenience in reducing the test matrix since HF contamination (J) is not used in conjunction with either liquid or saturated vapor.

In Tables VI and VII, the ullage composition (I) is not a variable because submerged combustion is anticipated with this location/type. In Table VI, three of the two-factor interactions are assumed to be negligible, allowing a saving of 16 tests. These interactions can be determined in the tests in Table VII. If these interactions prove to be significant, additional tests will be performed.

In addition to the main effects and two-factor interactions listed in Tables II to VII, estimates can be made for the two- and three-factor interactions involving injectant phase and the following: F, G, K, H, FG, FK, FH, GK, GH, KH, I, FI, KI, and HI. Similarly, estimates can be made for the two- and three-factor interactions involving location/type (A) and the following: C, F, H, CF, CH, FH (with respect to nonreactive injectant) and F, D, G, K, H, FD, FG, FK, FH, DG, DK, DH, GK, GH, KH, E, J, FE, FJ, KE, KH, HE, HJ, and EJ (with respect to reactive injectant).

Wall Effects Testing. —The wall effects tests consisted of the insertion of a bundle of aluminum tubes in the basic apparatus to evaluate its catalytic effects. These tests basically evaluate parameters M and N (see Table I) but parameters F, G, H, I, J, K, and L and phase (D or E) may also be involved. To evaluate all the two-factor interactions, as many as 64 tests would be required if no prior knowledge existed. However, when these tests were reached, all of the tests shown in Tables II through VII had been performed, and most of the significant interactions were already identified. Therefore, it was anticipated that only about 8 tests would be required for the wall effects testing. These tests were performed as shown in Table IV.

Supplemental Testing.—Following the tests shown in Tables II through VII, specific problem areas were uncovered (see Results, below), indicating that supplemental tests would be desirable. These supplemental test conditions are shown in Table VIII and are not included in the factorial experiment

TABLE IV

US INJECTOR WITH GASEOUS REACTIVE INJECTANT

Independent variables and levels	Constant parameters and levels
F: f_1, f_2 E: e_1, e_2 J: j_1, j_2 I: i_1, i_2 K: k_1, k_2 H: h_1, h_2	a_1 c_2 g_2 l_2 m_1 n_1
Main effects and two-factor interactions that can be estimated	
-All-: F, E, J, I, K, H, FE, FJ, FI, FK, FH, EJ, EI, EK, EH, JI, JK, JH, IK, IH, KH	
Combinations to be tested 1/2 x 2^6 = 32	
f_2 e_1 j_1 i_1 k_1 h_1 m_2 (76)	f_1 e_2 j_2 i_2 k_1 h_1
f_1 e_2 j_1 i_1 k_1 h_2 (81); m_2 (78); l_1 m_2(80)	f_1 e_2 j_2 i_1 k_2 h_1 (12)
f_1 e_1 j_2 i_1 k_1 h_1 (5, 13B)	f_1 e_2 j_2 i_1 k_1 h_1 (13)
f_1 e_1 j_1 i_2 k_1 h_1 (8)	f_1 e_2 j_1 i_2 k_2 h_1 (16)
f_1 e_1 j_1 i_1 k_2 h_1 (9); m_2 (75)	f_1 e_2 j_1 i_2 k_1 h_2
f_1 e_1 j_1 i_1 k_1 h_2 (3)	f_1 e_2 j_1 i_1 k_2 h_1 (14)
f_2 e_2 j_2 i_1 k_1 h_1	f_1 e_1 j_2 i_2 k_2 h_1 (11)
f_2 e_2 j_1 i_2 k_1 h_1	f_1 e_1 j_2 i_2 k_1 h_2 (6)
f_2 e_2 j_1 i_1 k_2 h_1	f_1 e_1 j_2 i_1 k_2 h_2 (7); h_1 (12A)
f_2 e_2 j_1 i_1 k_1 h_2 m_2(77); l_1 m_2 (82)	f_1 e_1 j_1 i_2 k_2 h_2 (10)
f_2 e_1 j_2 i_2 k_1 h_1	f_2 e_2 j_2 i_2 k_2 h_1
f_2 e_1 j_2 i_1 k_2 h_1	f_2 e_2 j_2 i_2 k_1 h_2
f_2 e_1 j_2 i_1 k_1 h_2	f_2 e_2 j_2 i_1 k_2 h_2
f_2 e_1 j_1 i_2 k_2 h_1	f_2 e_2 j_1 i_2 k_2 h_2
f_2 e_1 j_1 i_2 k_1 h_2	f_2 e_1 j_2 i_2 k_2 h_2
f_2 e_1 j_1 i_1 k_2 h_2	f_1 e_2 j_2 i_2 k_2 h_2 (15)
Note: Experiment number in parentheses	

TABLE V

US INJECTOR WITH LIQUID REACTIVE INJECTANT

Independent variables and levels	Constant parameters and levels
F: f_1, f_2 D: d_1, d_2, d_3 G: g_1, g_2 K: k_1, k_2 H: h_1, h_2	a_1 c_2 i_1 l_2 m_1 n_1

Main effects and two-factor interactions that can be estimated
-All-: F, D, G, K, H, FD, FG, FK, FH, DG, DK, DH, GK, GH, KH

Combinations to be tested 3/4 x 2^4 x 3^1 = 36		
f_1 g_1 k_1 h_1 d_1 (28)	f_1. . . . h_1 d_2 (20)	f_1. . h_1 d_3 i_2 (32)
f_1 g_2 k_1 h_2 d_1	f_1. . . . h_2 d_2 (30)	f_1. . h_2 d_3 (31)
f_1 g_1 k_2 h_1 d_1 (17)	f_1. . . . h_1 d_2	f_1. . h_1 d_3
f_2 g_1 k_2 h_2 d_1	$f_1$$g_2$. . h_2 d_2 (22)	f_2. . h_2 d_3
f_1 g_1 k_1 h_2 d_1 i_2 (29)	f_1. . . . h_2 d_2 (23A) i_2 (23)	f_1. . h_2 d_3
f_1 g_2 k_2 h_1 d_1	f_1. . . . h_1 d_2 i_2 (21)	f_1. . h_1 d_3
f_2 g_1 k_2 h_1 d_1	f_2. . . . h_1 d_2	f_1. . h_1 d_3 i_2 (27)
f_1 g_2 k_1 h_2 d_1 (4)	f_2. . . . h_2 d_2	f_1. . h_2 d_3 i_2 (24)
f_1 g_1 k_2 h_2 d_1 i_2 (19)	f_1. . . . h_2 d_2	f_1. . h_2 d_3 (25)
f_1 g_2 k_1 h_1 d_1 i_2 (18)	f_1. . . . h_1 d_2	f_1. . h_1 d_3 (26)
f_2 g_1 k_1 h_2 d_1 (79)	f_2. . . . h_2 d_2	f_2. . h_2 d_3
f_2 g_2 k_2 h_2 d_1	f_2. . . . h_2 d_2	f_2. . h_2 d_3

Note: Experiment number in parentheses

TABLE VI

SS INJECTOR WITH GASEOUS REACTIVE INJECTANT

Independent variables and levels	Constant parameters and levels
F: f_1, f_2	a_2 c_2 m_1 n_1
E: e_1, e_2	
G: g_1, g_2	
J: j_1, j_2	
K: k_1, k_2	
H: h_1, h_2	
L: l_1, l_2	

Main effects and two-factor interactions that can be estimated

All except LG, LH, and LF, which must be assumed to be negligible. Hence, F, E, G, J. K, H, L, FE, FG, FJ, FK, FH, FL, EG, EJ, EK, EH, EL, GJ, GK, GH, GL, JK, JH, KH, KL, HL, JL can be estimated.

Combinations to be tested 1/4 x 2^7 = 32

f_1 e_1 g_1 j_1 k_1 h_1 l_1 (33)	f_2 e_1 g_1 j_1 k_2 h_2 l_1
f_1 e_1 g_1 j_1 k_1 h_1 l_2 (60) a_3 (72)	f_2 e_1 g_1 j_2 k_1 h_2 l_1
f_1 e_1 g_1 j_2 k_2 h_1 l_2 (66)	f_2 e_1 g_2 j_2 k_1 h_1 l_1
f_1 e_1 g_2 j_2 k_2 h_2 l_1	f_2 e_2 g_1 j_2 k_2 h_2 l_1
f_1 e_1 g_2 j_2 k_1 h_1 l_2	f_2 e_2 g_1 j_1 k_1 h_2 l_1
f_1 e_1 g_2 j_1 k_2 h_1 l_2	f_2 e_2 g_2 j_1 k_1 h_1 l_1
f_1 e_2 g_2 j_2 k_1 h_2 l_1 (36)	f_2 e_2 g_1 j_2 k_1 h_1 l_2
f_1 e_2 g_2 j_1 k_1 h_1 l_2	f_2 e_1 g_1 j_1 k_2 h_2 l_2 (62)
f_1 e_2 g_1 j_2 k_1 h_1 l_2 (67)	f_2 e_2 g_1 j_1 k_1 h_2 l_2 (63) a_3 (74)
f_1 e_2 g_1 j_2 k_2 h_2 l_2	f_2 e_1 g_2 j_1 k_1 h_2 l_2
f_1 e_2 g_2 j_1 k_2 h_2 l_1	f_2 e_1 g_1 j_1 k_1 h_1 l_2
f_1 e_1 g_2 j_1 k_1 h_2 l_1 (35)	f_2 e_2 g_2 j_2 k_1 h_2 l_2
f_1 e_1 g_1 j_2 k_2 h_1 l_1	f_2 e_1 g_2 j_1 k_2 h_1 l_1
f_1 e_2 g_1 j_1 k_2 h_1 l_2 (61) a_3 (73)	f_2 e_2 g_2 j_2 k_2 h_1 l_1
f_1 e_2 g_1 j_1 k_2 h_1 l_1 (46)	f_2 e_2 g_1 j_2 k_2 h_2 l_2 (65)
f_1 e_2 g_1 j_2 k_1 h_1 l_1 (37)	f_2 e_1 g_1 j_2 k_1 h_2 l_2 (64)

Note: Experiment number in parentheses

TABLE VII

SS INJECTOR WITH LIQUID REACTIVE INJECTANT

Independent variables and levels	Constant parameters and levels
F: f_1, f_2 D: d_1, d_2, d_3 G: g_1, g_2 K: k_1, k_2 H: h_1, h_2 L: l_1, l_2	a_2 c_2 i_1 m_1 n_1

Main effects and two-factor interactions that can be estimated

-All-: F, D, G, I, K, H, L, FD, FG, FI, FK, FH, FL, DG, DI, DK, DH, DL, GI, GK, GH, GL, IK, IH, Il, KH, KL, HL.

Combinations to be tested $1/4 \times 2^6 \times 3^1 = 48$

f_1 d_1 g_1 k_1 h_1 l_1 (34)	f_1 d_2 g_2 k_2 h_1 l_1 (47)	f_2 d_3 g_1 k_1 h_1 l_2
f_1 d_1 g_1 k_2 h_1 l_2	f_1 d_2 g_1 k_1 h_1 l_1 (44)	f_2 d_3 g_1 k_2 h_1 l_2 (69)
f_2 d_1 g_2 k_1 h_1 l_1 (49)	f_2 d_2 g_2 k_1 h_1 l_1 (51, 51A)	f_1 d_3 g_2 k_2 h_1 l_2 (57)
f_2 d_1 g_2 k_2 h_1 l_2	f_2 d_2 g_2 k_2 h_1 l_1	f_1 d_3 g_2 k_1 h_1 l_1 (42)
f_1 d_1 g_2 k_1 h_1 l_2 (53)	f_1 d_2 g_2 k_1 h_1 l_1 (43)	f_1 d_3 g_1 k_1 h_1 l_1 (41)
f_1 d_1 g_2 k_2 h_1 l_2 (58, 58A)	f_1 d_2 g_2 k_2 h_1 l_2 (56)	f_1 d_3 g_1 k_1 h_1 l_2 (55)
f_1 d_1 g_1 k_1 h_2 l_1 (39)	f_1 d_2 g_1 k_1 h_2 l_2	f_1 d_3 g_1 k_1 h_2 l_1 (40)
f_1 d_1 g_1 k_2 h_2 l_2	f_1 d_2 g_1 k_1 h_2 l_1 (45)	f_1 d_3 g_1 k_2 h_2 l_2
f_2 d_1 g_1 k_1 h_2 l_2	f_2 d_2 g_1 k_1 h_2 l_1	f_2 d_3 g_2 k_1 h_1 l_1 (48)
f_2 d_1 g_1 k_2 h_2 l_1	f_2 d_2 g_1 k_2 h_2 l_2	f_2 d_3 g_2 k_1 h_1 l_2 (68)
f_2 d_1 g_2 k_1 h_1 l_2 (59)	f_2 d_2 g_1 k_1 h_1 l_1 (50)	f_2 d_3 g_2 k_1 h_2 l_1
f_2 d_1 g_1 k_2 h_1 l_2 (71)	f_2 d_2 g_1 k_2 h_1 l_2 (70)	f_2 d_3 g_2 k_2 h_2 l_2
f_2 d_1 g_2 k_1 h_2 l_1	f_2 d_2 g_2 k_1 h_2 l_2	f_2 d_3 g_1 k_1 h_2 l_2
f_2 d_1 g_2 k_2 h_2 l_2	f_2 d_2 g_2 k_2 h_2 l_1	f_2 d_3 g_1 k_2 h_2 l_1
f_1 d_1 g_2 k_1 h_1 l_1 (38)	f_1 d_2 g_2 k_1 h_2 l_1	f_1 d_3 g_2 k_1 h_1 l_2 (52)
f_1 d_1 g_2 k_2 h_2 l_1	f_1 d_2 g_2 k_2 h_2 l_2	f_1 d_3 g_2 k_2 h_2 l_1

Note: Experiment number in parentheses

TABLE VIII

SUPPLEMENTAL TESTING CONDITIONS

Common Conditions: Hydrogen Pressure - 25 psia; Injectant Quantity 2.0×10^{-4} lb. *; Valve Open Time - 100 MS*; Percent Helium in Ullage - 0%; Natural HF and 0_2 content in F_2; no helium prepurge.

US Injector With GF_2 Injectant

F_2 Pressure, psia	65	105	145
F_2 temperature °R	500	500	500
	350	350	350
	200	200	200

Modified SA Injector With GF_2 Injectant

Each combination of					
F_2 pressure, psia	65		105		145
F_2 temperature, °R		180		500	
*Injectant Quantity, lb x 10^4		1.0		2.0	

UA Injector With GF_2 Injectant (500°R)

Each combination of		
F_2 pressure, psia	65	145
*Injectant Quantity, lb x 10^4	1.0	2.0

SS Injector With LF_2 Injectant For Detonation

F_2 pressure, psia		145		65
F_2 temperature, °R	180	160	140	140

HF Freezing

HF pressure, psia	65
Injector	US SA

*Valve open time - one minute

---

*Exceptions noted

design. The reasons for the parameter values selected are discussed in detail under Results, below.

Potential Problems in Experiment Design.—The initial assumption leading to the factorial experiment design was that the important dependent variables of reaction, ignition delay times, and pressure and temperature rise, are continuous quantitative functions of the variables of Table I. It was recognized at the outset that this might not be the case, and that there might be instances of "no reaction," i.e. infinite ignition delay time. If this occurs, it has an important effect on the statistical significance of the main effects and interactions, because such a situation leads to statistically unsatisfactory and meaningless conclusions. This problem is considered further when the results are discussed. It was decided to proceed with testing per the factorial design anyway since there was no attractive alternative.

It will also be noted from Tables II to VII, that all tests in the design were not performed. The reasons are discussed under Results. Basically it became clear, as the test series proceeded, that certain variables had little or no effect and further tests that varied such parameters were dispensed with.

The tests were not run in the order shown in Table II to VII, because some parameters were more difficult to vary than others. The matrix was reordered for convenience in testing, but the levels for each particular test were kept the same.

Test Facility Description and Procedure

Test Facility Description.— The overall layout of the hypergolicity and reaction products freezing test facility is shown schematically in fig. 1. The facility is designed to be completely flexible so that all the parameters in the test matrix can be varied to the desired level with precision and minimum effort and time. Further, the facility is fundamentally designed for safe operation: all oxidizer valves are either remotely-operated manual or remotely actuated; all valves which must be operated while F_2 and H_2 are in proximity are either sensor-controlled or remotely actuated; and the entire hazardous area is barricaded for personnel safety. Salient features of the facility are as follows:

(1) There are two basic loops, oxidizer and hydrogen, with the only point of contact at the injector valve.

(2) The oxidizer loop is GN_2- and vacuum-purged through a scrubber.

(3) The LH_2 loop is GHe purged to a remote disposal area. The LH_2 vacuum jacket is maintained by a different vacuum pump.

(4) Only gaseous oxidizers are stored and handled; they are liquefied with LN_2 just before injection.

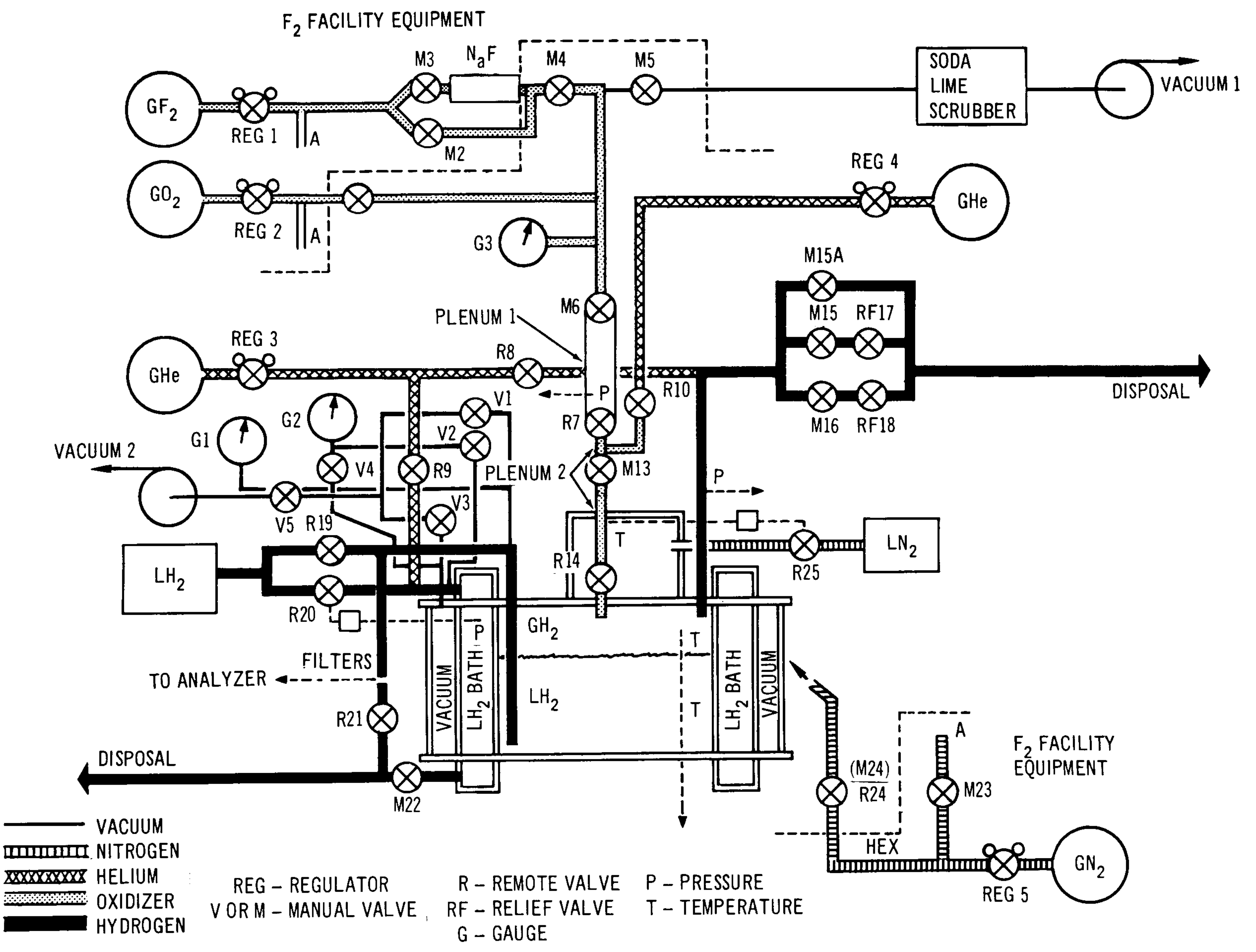

Figure 1. MTI Hypergolicity Test Facility Schematic

(5) A NaF scrubber is available to remove HF from F_2 to the 0.02 vol % level or it can be bypassed for supplying "dirty" F_2.

(6) O_2 can be added accurately when required by partial pressure fill of an isolated plenum of calibrated volume.

(7) The quantity of injectant is controlled by pressure fill of a calibrated volume plenum.

(8) The condition of the injectant is controlled by a temperature controlled LN_2 bath.

(9) GHe supplies driving pressure to the injectant, and can be supplied as a prepurge before injection.

(10) GHe can be supplied to dilute the H_2 ullage before injection.

(11) In the original apparatus, a LH_2 cooling bath was designed to flow continuously through the apparatus during the test. If the apparatus broke, a pressure switch closed the LH_2 bath supply valve.

(12) The test LH_2 saturated condition is controlled by a remotely set vent/relief valve.

(13) The LH_2 can be completely drained following a test by remotely actuated GHe purge valves.

(14) Reaction products are filter trapped and routed to the mass spectrometer for analysis.

Although the injection loop and valve is shown on top for ullage injection, the entire loop and valve can be mounted on the identical bottom plate for submerged injection tests.

The valves used in the test facility, with the exception of the injector valve, were all commercially available valves, as shown in Table IX. There were no lubricants used in any of these valves. Essentially identical Control Components, Inc. valves were used for both LH_2 and F_2 service and gave exceptionally good service under these severe operating conditions. Internal leakage through these valves remained undetectable throughout the test program. External leakage of F_2 through the Teflon® stem packing occurred on occasion, but was always stopped by tightening the packing. The injector valve was specially made to meet the test program requirements by the Fox Valve Development Co. These requirements included compatibility with LF_2, operability at LN_2 temperatures, zero internal or external leakage, and valve open and close times of 5 msec or less. The LF_2 compatibility requirement dictated the use of a soft metal seat, and an annealed copper seat material was chosen. Two valves were procured. The first valve was a solenoid operated valve of very fast response, which could meet the valve open/close time requirement, but which, because of the necessarily light seat loading, might have a tendency to leak. The second valve was a solenoid-actuated, pneumatically operated valve to act as a back up to the first valve in the event of excessive leakage. The pneumatic valve design permitted higher seat

TABLE IX
VALVE IDENTIFICATION

No.	Vendor	P/N
M1, V1	Control Components, Inc.	MV 3004T
M2, V2	" " "	"
M3, V3	" " "	"
M4, V4	" " "	"
M5, V5	" " "	"
M6	" " "	"
R7	" " "	CE 3008T with 4-way Solenoid
R8	Allied Control Co., Inc.	HH 20391 115/60
R9	" " "	"
R10	Control Components, Inc.	CE 3008T with 4-way Solenoid
M13	" " "	"
R14	Fox Valve Development Co., Inc.	610840 or 610851
M15, MI5A	Control Components, Inc.	ES 3008T
M16	" " "	"
RF17	" " "	RV 9008T-30
RF18	" " "	RV 9008T-75
R19	" " "	CE 3008T with 4-way Solenoid
R20	" " "	"
R21	" " "	"
M22	" " "	ES 3008T
M23	" " "	MV 3004T
R24	Allied Control Co., Inc.	HH 20391 115/60
R25	" " "	HH 20391 "

loads and less probability of leakage but also was expected to have a longer response time. The valves were satisfactory, with the pneumatic valve being superior to the solenoid valve. The latter tended to leak after very few reactive cycles. The pneumatic valve, on the other hand, lasted much longer and had equally good response (5 msec). External leakage from these valves was nonexistent. Seat leakage through the injector valve R14 resulted in a very hazardous and intolerable situation. Three violent detonations resulted when LH_2 was being charged into the reaction Dewar (step 7, Experiment Technique, below) after charging F_2 into plenum (2) (step 6) when valve R14 had "minor" seat leakage.

Test Apparatus Description.— The test tank apparatus was originally conceived to be a heavy-walled glass Dewar. The heavy walls were necessary to obtain a high initial pressure capability and still contain a normal reaction without breakage, and glass was required for adequate viewing and for the high-speed movies. The original apparatus also had three walls (to contain a flowing LH_2 bath for Dewar chilldown) and was quite expensive. To reduce the expense of possible frequent breakage of these costly Dewars, it was decided to retain the triple-walled heavy glass apparatus, but to use commercial glass pipe sealed into heavy stainless steel end plates. This concept is shown in the fabrication drawing of the original apparatus (fig. 2). The end plates contained penetrations for LH_2 fill, vent, and bath, and thermocouple and injection ports, and was vacuum jacketed. The end plates were interchangeable and could be turned over for submerged injection.

Numerous problems were encountered with this apparatus, the most persistent being LH_2 bath problems, seal leakage, and excessive heat leak and boiling at the bottom end plate. The initial LH_2 tests of the apparatus showed that the flowing LH_2 did not accomplish its purpose of chilling down the end plate to eliminate excessive boiling of the test volume of LH_2. Further, it obscured vision into the chamber because of turbulence in flowing through the glass walls. Modifications were made in attempts to solve these problems with little success; excessive heat leak through the bottom end plate continued to be a problem. Seal leakage through the glass-metal seal at the end plates was also a persistent and insoluble problem. The original "crescent rings" were quickly abandoned and replaced by Creavey® seals (Teflon coated steel spring O-rings) which had been used in previous LH_2 applications with success. The Creavey seals also leaked before or, at best, after an LH_2 chilldown cycle because of adverse differential expansion in the end-sealing configuration, so modifications were made to provide a side-sealing configuration to alleviate adverse differential expansion. Assembly problems resulted because of the rigidity of the Creavey seals, which resulted in tearing of the seals and subsequent leakage. Softer silicone O-rings and Teflon-coated metal v-seals were also tried without success.

After reaching an apparent impasse with the problems of seal leakage and excessive heat leak, it was decided to obtain commercial unsilvered Dewars of the appropriate size and, at least, perform the low-pressure hydrogen tests shown in the test matrix. It was hoped that these Dewars would hold sufficient pressure to contain the pressure rise of a normal reaction. The

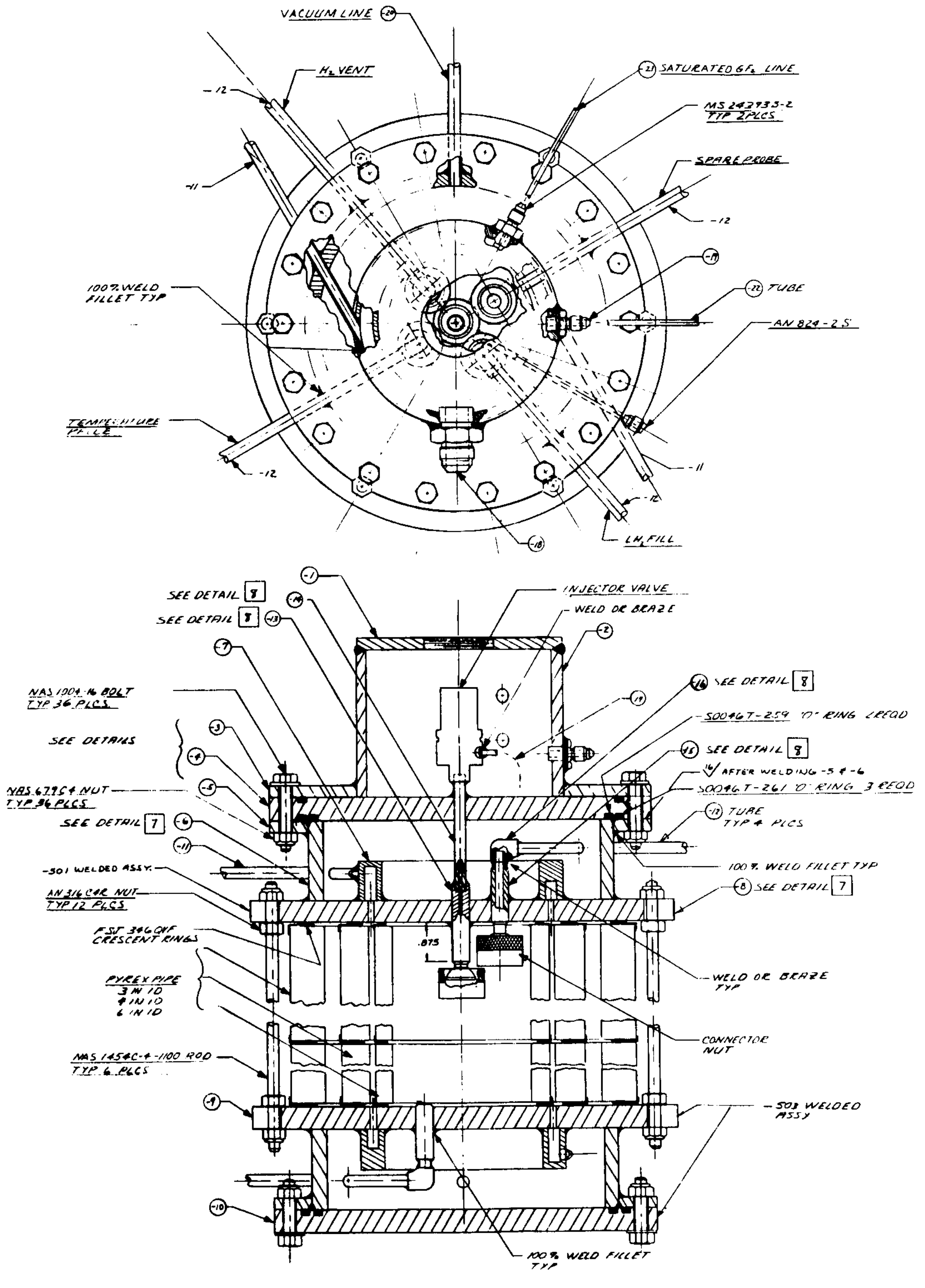

Figure 2. MTI Hypergolicity Test Apparatus

resulting injector loop and apparatus configuration for the US tests is shown in figs. 3A and 3B. The Dewar was sealed to the original end plate with a flat gasket fabricated from 1/4-in. sheet silicone rubber to specification MIL-R-5847D class I grade 32 (low-temperature silicone with 32 durometer hardness). This seal worked amazingly well, lasting through as many as 25 LH_2 chilldown cycles (with 11 reactions) before cracking and leaking. This apparatus gave excellent results for the low-pressure LH_2 tests, often containing reactive pressure rises to as high as 50 psi. This experience gave enough confidence in the Dewar strength to try the high pressure LH_2 series. Again, results were excellent, with the Dewars containing reactive pressure rises to over 110 psia without breakage or leakage.

This success led to the procurement of special unsilvered Dewars with a bottom penetration for the SS location/type test series. The injector loop and apparatus configuration is shown in figs. 4A and 4B. This bottom penetration, of necessity, had a coil of glass tubing to allow thermal contraction of the inside Dewar shell, and this resulted in a longer injection path for the SS (and SA) injection than for the US injection. The possible consequences of this are discussed below under Experiment Technique. The results with this Dewar configuration were also excellent, and a complete series of low- and high-pressure tests were run with the SS configuration. The US and the SS test apparatus' are shown installed in the test facility in fig. 5.

The Dewar with bottom penetration was also used for the original and modified SA configuration tests (see figs. 6A and 6B). The design criteria used in sizing the SA injectors shown are discussed in Results, below.

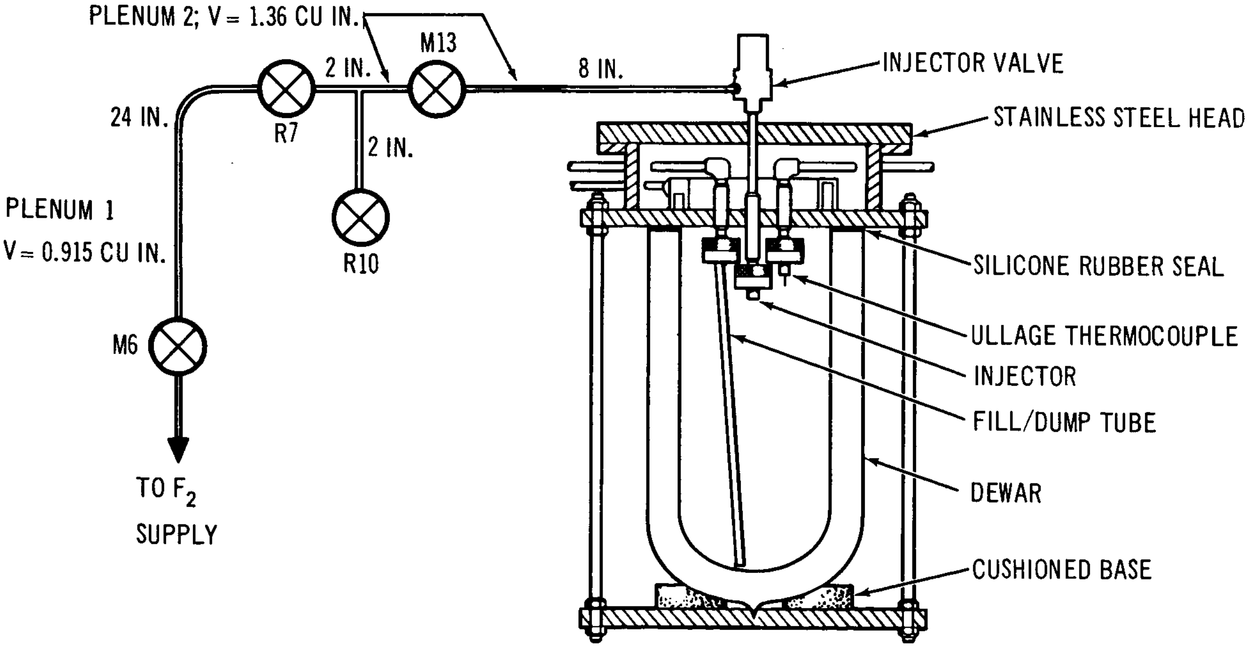

(a) INJECTION LOOP DIMENSIONS

(b) TEST APPARATUS CONFIGURATION

Figure 3. Ullage Injection Test Apparatus

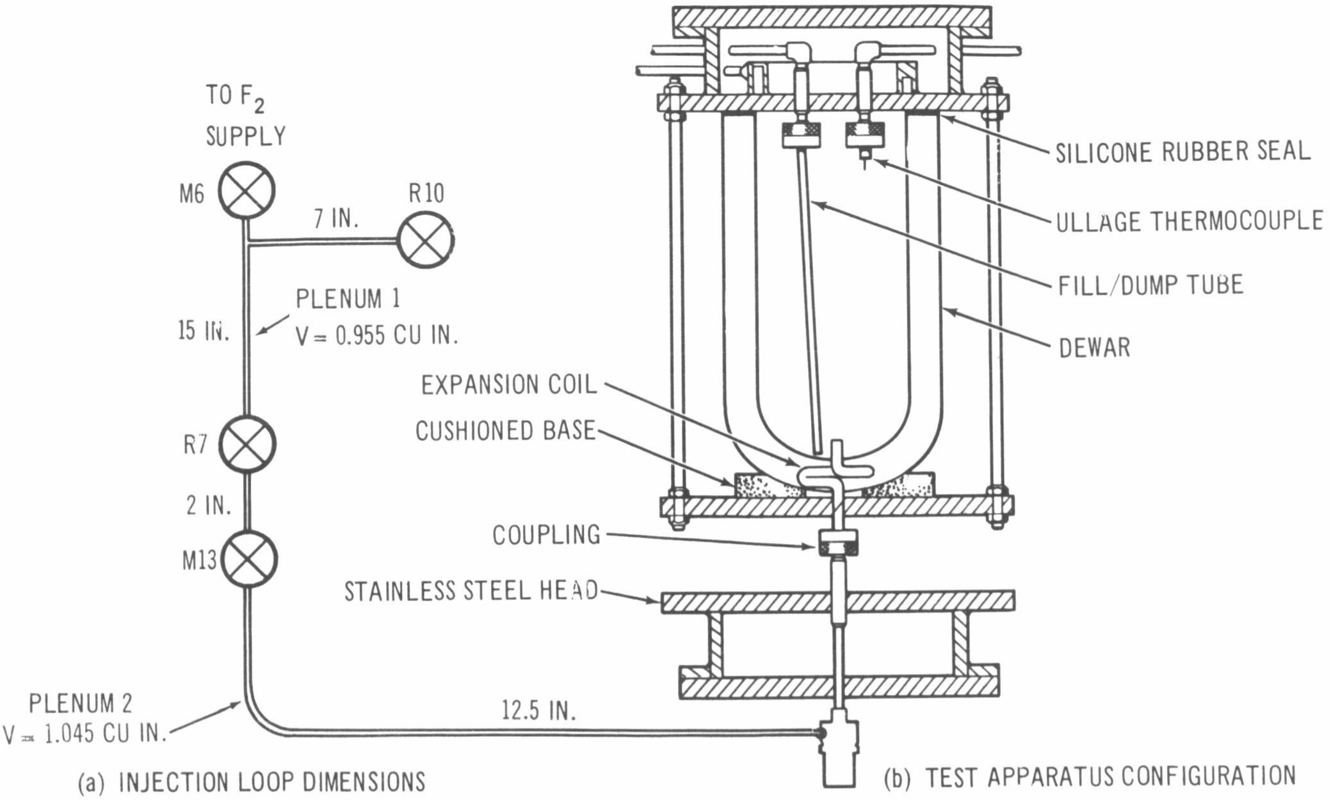

(a) INJECTION LOOP DIMENSIONS (b) TEST APPARATUS CONFIGURATION

Figure 4. Submerged Injection Test Apparatus

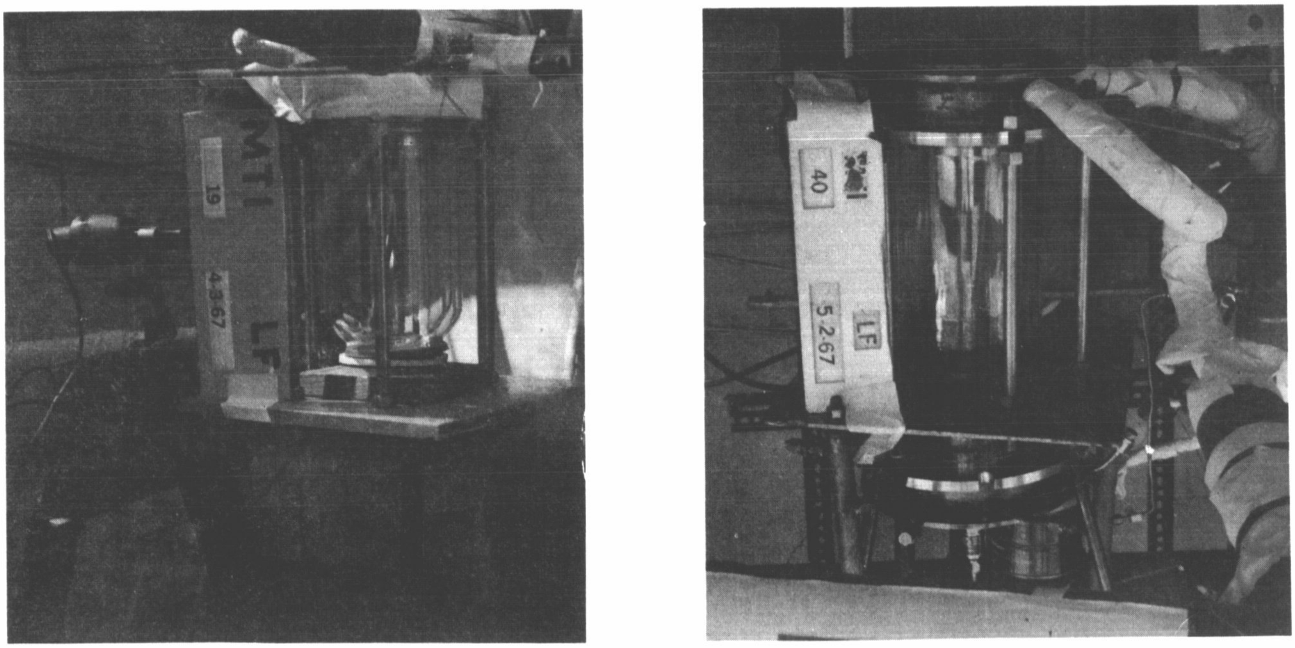

(A) ULLAGE INJECTION (B) SUBMERGED INJECTION

Figure 5. Hypergolicity Test Setups

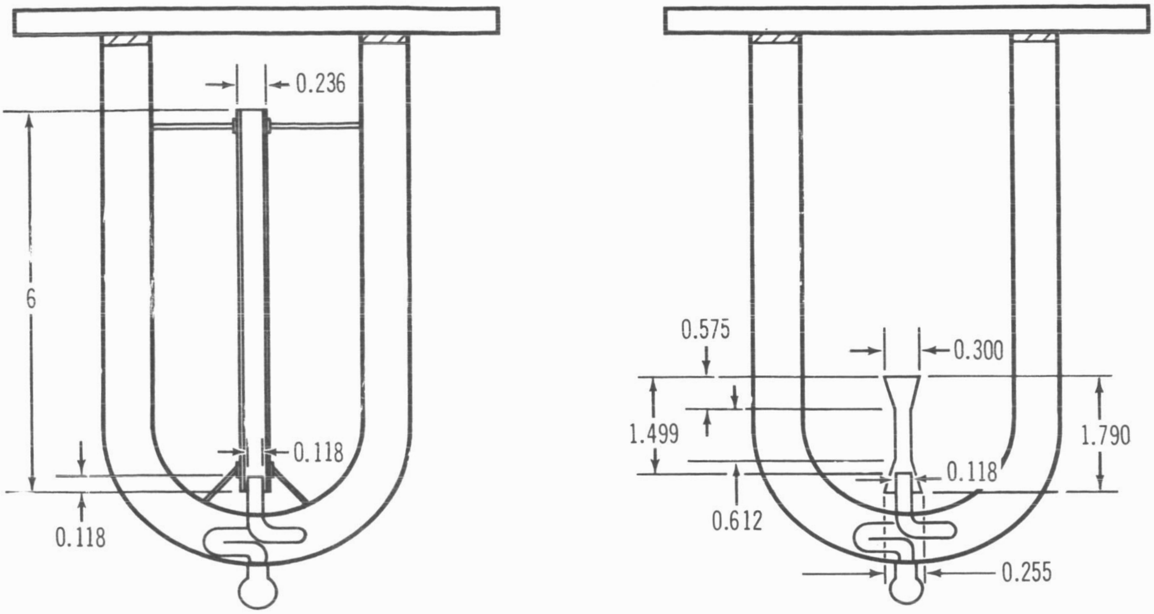

(a) SA INJECTOR — CONFIGURATION NO. 1

(b) SA INJECTOR — CONFIGURATION NO. 2

NOTE: ALL DIMENSIONS ARE IN INCHES

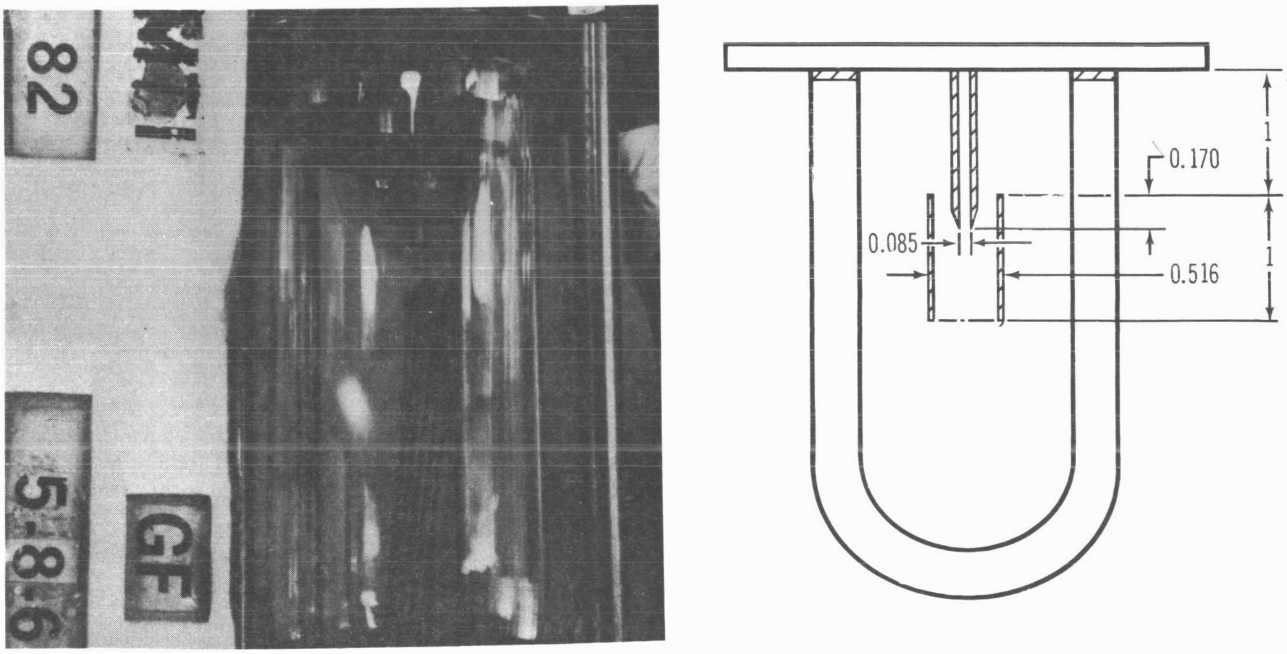

(c) ULLAGE INJECTION WITH TUBE BUNDLE

(d) UA INJECTOR CONFIGURATION

Figure 6. Special Test Setup.

The wall effects testing was done in the US configuration with a bundle of aluminum tubes (see fig. 6C), and in the UA configuration with a bundle of copper tubes. The aluminum tubing bundle had the following characteristics: 24 tubes of 6.0 in. length, 0.125 in. o.d., 0.055 in. i.d., total surface area of 81.5 sq in. The copper tubing bundle had the following characteristics: 10 tubes of 4.75 in. length, 0.250 in. o.d., 0.188 in. i.d., total surface area of 65 sq in. The results of the wall effects testing are discussed below.

The ullage/aspirated (UA) configuration tested is shown in fig. 6D. The results of these tests (performed as part of the supplemental tests) are discussed below.

Instrumentation.—Because of the potentially destructive nature of the test series, it was decided that use of ultrahigh response (but costly and fragile) instrumentation to measure temperature and pressure rise was not warranted. Instead, ordinary Statham PG 146 TC-100-350 transducers were used to detect pressure rise, and copper-constantan thermocouples were used to detect temperature changes. The thermocouples were made of 36-gage wire and had response times of the order of 200 msec, which was considered adequate for this application. CEC recording oscillographs were used to record the transducer outputs. It was anticipated that ignition lag and other high-speed phenomena could be observed with high-speed movies.

The chamber pressure transducer was mounted in the chamber vent line and was thermally isolated from the cold vented GH_2. The chamber thermocouple protruded into the chamber from a fitting in the metal end plate (see figs. 3B and 4B). In this location it was subject to considerable heat leak from the metal end plate, but it gave adequate relative temperature changes. The fluorine temperature thermocouple was mounted on the injector valve outlet where its readings were largely affected by ambient temperature. The fluorine LN_2 bath temperature was measured, but was not recorded, and was used for bath temperature control.

The most important instrumentation requirements were for visual equipment. It was initially hoped that a Schlieren system could give useful information on the reactive flow field. It was quickly determined, however, that the curved glass obliterated the Schlieren field, so this system was dropped from further consideration. A Wollensak WF4 16 mm Fastax camera with 400 ft film capacity was used to take high-speed color movies of the hypergolicity testing. The camera has built-in timing and frame-rate signals and has the following speedup and event time characteristics:

Pictures/Sec	Delay-Sec	Event Time-Sec
2000	3.10	4.78
3000	3.00	2.32
4000	2.73	2.03
5000	1.66	1.68

A framing rate of 4000 pictures/sec was found to be satisfactory and was used throughout the testing. Backlighting of the test Dewar was supplied by four mercury vapor arc lamps, shining through frosted glass.

It was originally proposed to take high-speed "streak" pictures, in addition to high-speed framed pictures if consistent ignition and flame pattern could be obtained. In the test series no favored ignition location was found, and consequently, no streak movies were obtained.

In addition to high-speed movies, real-time movies of each test were taken at 24 pictures/sec with a Milliken 16 mm camera.

Because of the 2.73 sec of delay in obtaining speed-up of the Fastax camera to 4000 pictures/sec, a control system was designed to ensure that injectant pressurization valves and the injector valve were operated at the proper times to provide reactant injection after the Fastax had reached the correct operating speed. This control system is shown schematically in fig. 7. The basic operation is as follows: the Fastax camera is started manually with a switch. When the camera reaches 4000 pictures/sec, a relay in the camera closes a circuit which opens the helium valve to pressurize the injectant and which starts a timer (T1). When T1 runs out it energizes a relay which opens the injector valve and starts a time-delay-relay (TDR1). When TDR1 runs out, it closes a relay which closes the injector valve. Thus, the valve open time is conveniently set on TDR1, while the helium pressurizing lead time is set on T1.

The Fastax camera generally produced excellent movies of each test. Typical frames showing the coverage of the movie film are shown in fig. 8.

Propellants.—The propellants used in the testing were ordinary and commercially obtained. The liquid hydrogen was 99.995% pure hydrogen delivered in a standard portable 1000-liter Dewar, and obtained from Union Carbide Corp., Linde Division, Ontario, California.

The fluorine used was obtained from Air Products,Inc. and was analyzed by mass spectrometry at Douglas Aircraft Company. The pertinent contaminants are shown in table X. The fluorine was supplied as gas in standard 400 psig cylinders.

The oxygen used as an additive was "Aviators Breathing Oxygen" at 99.6% purity and was obtained as gas in standard 2500 psig cylinders from Air Products, Inc.

The helium used as a pressurant for the hydrogen and the fluorine was commercial water-pumped (12 ppm H_2O) and was obtained in standard 2500 psig cylinders from Air Products, Inc.

Experiment Technique.—Because of the large number of varying parameters, the experiment operating procedure was necessarily complex. The complexity was eased somewhat by following a standard written procedure (Douglas Drawing 1T13845) and keeping a log of the settings of the variables. Each movie film was identified by test number, date, and injectant on a sign board as shown in fig. 8. The following general procedure applied for each test (refer to fig. 1).

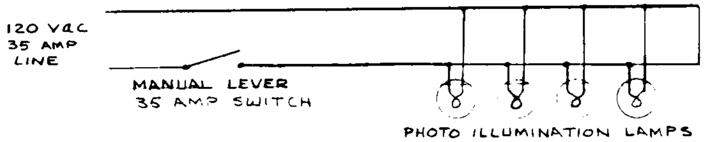

LAMP CIRCUIT

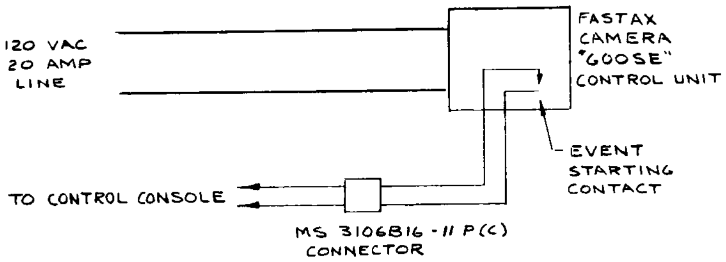

FASTAX CAMERA INTERLOCK

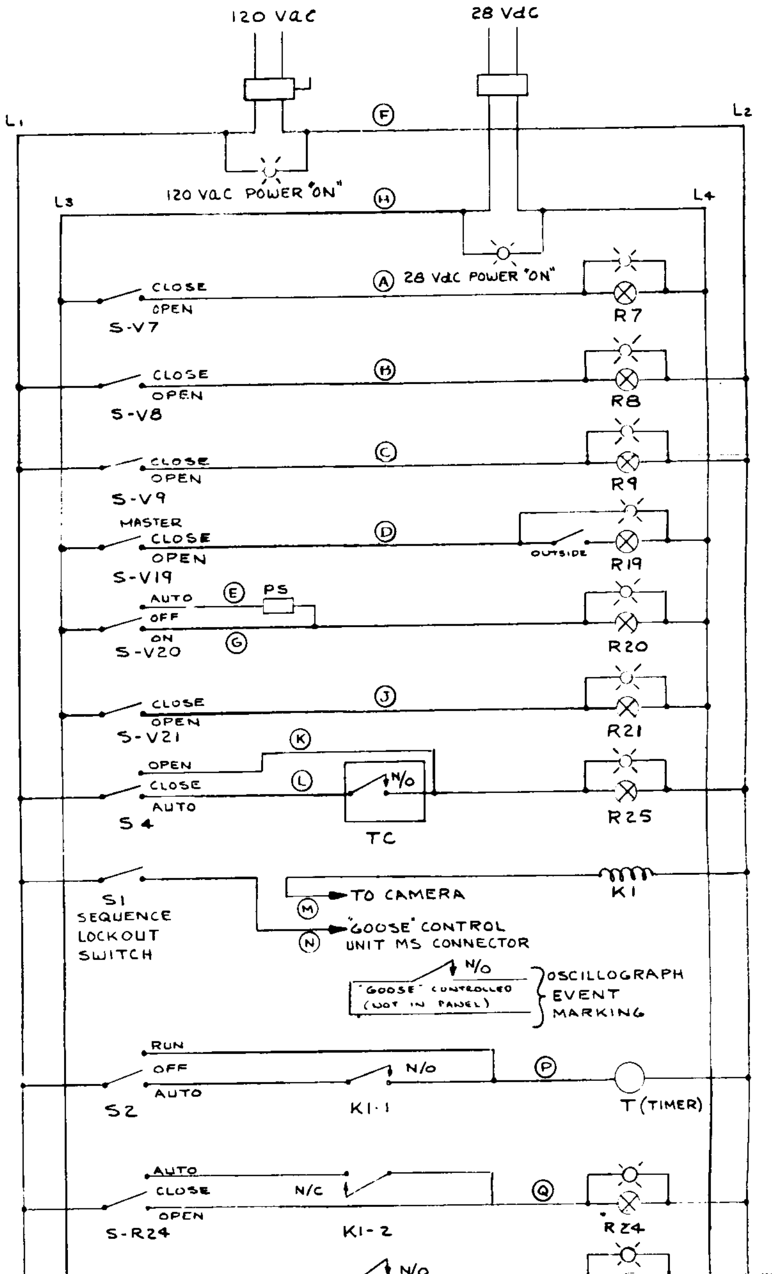

LIST OF PARTS

—	Switch, manual lever, minimum rating 35 amp, 120 VAC (for lamps).
R	Remote valve, electric solenoid actuated.
T	Timer, cam, single revolution.
PS	Pressure Switch.
TC	Temperature controller, thermocouple actuated.
☼	Light, panel mounted.
—•⁄ o—	Switch, single pole single throw, rating 6 amps, 120 VAC/DC.
—o⁄ •—	Switch, single pole, 3 throw, rating 6 amps, 120 VAC/DC
IRD	Infrared detector.
TDR1	Time delay relay, 5 to 100 millisecond. 2 N/O contacts, 2 separate N/C contacts.
TDR2	Same as TDR1 but 1 N/O and 1 N/C contact.
K1	Relay, 120 VAC, general purpose 3 N/O, 1 N/C.
K2	Relay, 120 VAC, general purpose 2 N/O.
K3	Relay, 120 VAC, general purpose 2 N/O.
K4	Relay, 120 VAC, general purpose 3 N/O.
K5	Relay, 120 VAC, general purpose 1 N/O.

SEQUENCE OF OPERATIONS

- Circuit breakers control 120 VAC and 28 VDC power. Indicating lights show "power on."
- Remote valves R7, R8, R9, R19 and R21 are opened and closed by manual switch.
- Remote valve R20 is controllable either by a manual switch or by a pressure switch.
- Remote valve R25 is controlled either by a manual switch or by a temperature controller.
- Photo lamps are turned on manually. After enough lamp warm-up time the cameras are manually started. An interlock contact in the Fastax "Goose" control unit makes contact when the camera has attained speed. This contact closes R24 (if it is open) opens R10 (if R10 is needed in the sequence) and starts the cam timer.
- After a predetermined time the timer opens R14.
- A time delay relay closes R14.
- After R14 closes, if there has been an infra red radiation R14 again opens.
- A time delay relay closes R14.

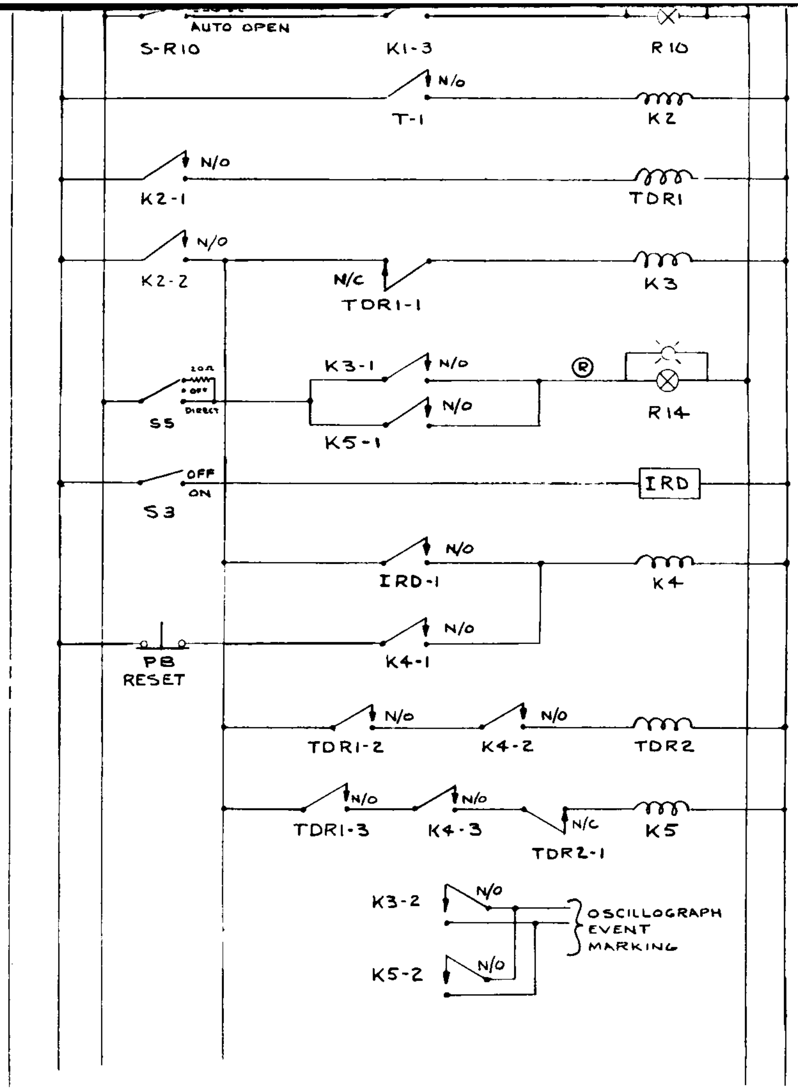

Figure 7. MTI Hypergolicity Control Schematic

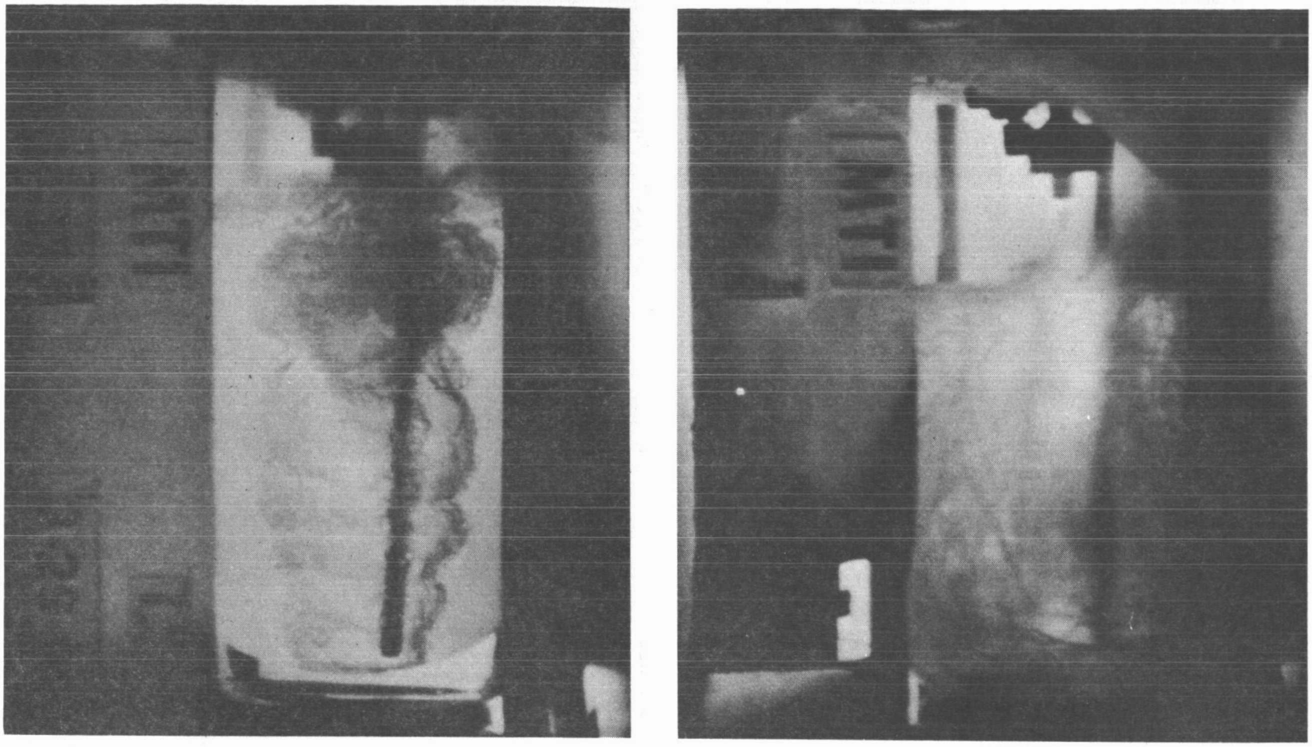

(A) TYPICAL REACTIVE ULLAGE INJECTION

(B) VERY FAST DETONATION (<1/4,000 SEC)

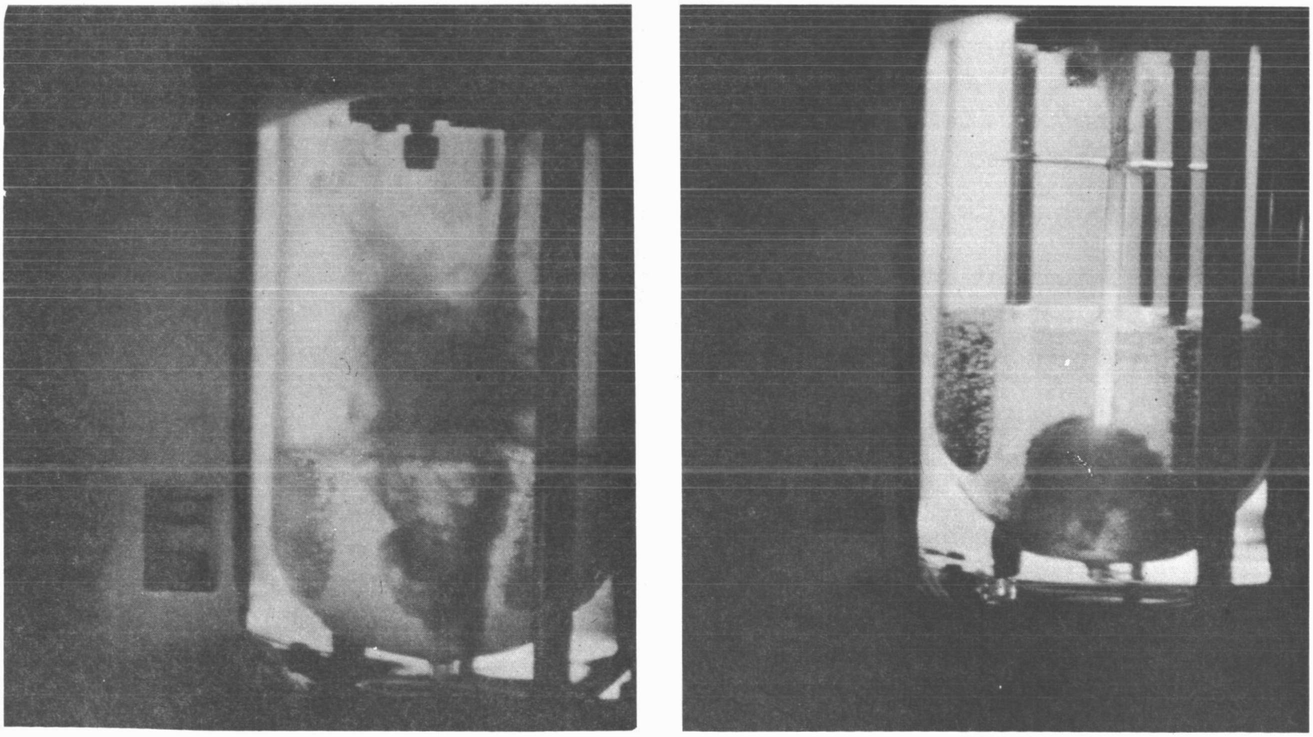

(C) TYPICAL REACTIVE SUBMERGED INJECTION

(D) TYPICAL REACTIVE SUBMERGED/ASPIRATED INJECTION

Figure 8. Typical Fastax Movie Photos

TABLE X
FLUORINE ANALYSIS

Cylinder No.	2994	12195	12092
Test No.	3-27	15', 16', 17', 18'	28-110
% F_2	98.0*	98.0*	98.0*
Vol % O_2	0.10	0.34	0.54
Vol % N_2	0.145	0.20	0.14
Wt % HF	0.193	0.006	0.018
Wt % HF (after scrubbing)	0.004	---	---

* Air Products, Inc. guaranteed minimum

(1) Load Fastax and real-time cameras; calibrate oscillograph.

(2) Pressurize the LH_2 storage Dewar; set appropriate pressure levels on regulators for O_2, He pressurant for injectant, He purge, and valve operating N_2 (or He).

(3) Evacuate, purge with He, and re-evacuate test Dewar and LH_2 transfer system.

(4) Evacuate injectant loop; set LN_2 bath controller to required temperature (if required) and allow to stabilize.

(5) If required, load O_2 by partial pressure to 1.0 vol % into plenum (1) upstream of R7 (by observing G3 - a Heise gage with 0.1% accuracy); add F_2 (scrubbed or unscrubbed, as required) to plenum to pressure required to obtain suitable quantity in plenum (2) between R7 and R14. Close M6.

(6) Allow time for mixing of O_2 and F_2, then open R7 and allow flow from plenum (1) to chilled plenum (2) then close R7.

(7) Open R19, LH_2 storage Dewar hand valve, and vent valve 15A and allow flow of LH_2 into Dewar (it usually took 5 - 10 minutes to obtain the proper amount of LH_2 in the Dewar).

(8) Close R19 and throttle vent valve 15A to obtain and maintain proper pressure in test Dewar.

(9) Retire to blockhouse and operate sequence, cameras, and oscillograph from control panel.

(10) Examine oscillograph record to see if reaction had occurred.

(11) Examine and/or photograph reacted or unreacted products. Analyze reacted products if appropriate.

(12) Dump LH_2 remaining in Dewar and purge apparatus with warm GHe.

A particular problem of technique which arose with this apparatus was the difficulty of determining the condition of injected liquid F_2 or saturated F_2 vapor. For mechanical and compatibility reasons it was impractical to install a thermocouple inside the injector tube downstream of the injector valve. A thermocouple was placed on the outside of the injector tube but it was greatly affected by ambient temperature. The LN_2 bath temperature is maintained within less than ± 5°R from the set temperature which results in the F_2 injectant being subcooled to at least the following degree:

d_1	LF_2	64.7 PSIA	140°R	42°R Subcooled
d_2	LF_2	149.7 PSIA	185°R	17°R Subcooled

In the US configuration the LF_2 has to pass through about 3 inches of tubing at 350°R and 2 inches of tubing at 50°R before entering the Dewar. Approximate heat transfer calculations indicate that in the d_1 case about 7% of the LF_2 would be revaporized, and for the d_2 case, about 30% would be revaporized.

In the SS configuration the LF_2 has to pass through about 6 inches of tubing at 500° R, 11 inches of tubing with an average temperature of 300° R and 3 inches of tubing with an average temperature of 100° R before entering the Dewar. Comparable calculations show that for the d_1 case about 37% of the LF_2 would be revaporized, and for the d_2 case, about 70% would be revaporized.

Thus the LF_2 injectant is probably not pure liquid but a mixture of cold gas and liquid. This condition not only eases the problem of injectant freezing, but may significantly affect the results of the hypergolicity experiment. This problem is discussed further in Results, below.

Results

General. – Performance of the large number of tests required for the test matrix, with an oscillograph record and several hundred feet of high-speed movies for each test, resulted in large quantities of interesting and important data which cannot be practically included in this report. Accordingly, only typical samples of oscillograph records which show significant variations are included. Similarly, typical frames from the Fastax movies (see fig. 8) are shown to give a general idea of the viewability. These excellent color films obtained in 90% of the tests were the most useful and interesting type of data, and the sample frames give only a poor example of their quality. Data summarizing the test series are shown in Table XI. The test numbers also reflect the order in which the tests were performed. Tests (1) and (2) are shown as "typical enthalpic runs." Although numerous GN_2 and LN_2 enthalpic runs were made for test facility checkout, the results were virtually identical, and these runs were picked as representative. This is discussed further below. The gross pressure rise (ΔP) shown includes the enthalpic pressure rise (if any) which is shown in parentheses. Words defining the reaction such as "no", "weak", "mild", "yes", and "strong" must be defined. "Yes" and "strong" indicate that an incandescent blue-white flame persisting throughout injection was visible in the high-speed movies. "No" and "weak" indicate that no such flame was visible, even though there may have been color changes and pressure rise indicative of a low-order reaction. "Mild" indicates that the flame was visible only briefly. "Detonation" indicates a very fast explosion or detonation, always with a flame and usually resulting in test apparatus destruction.

Ignition delay time recorded in Table XI is not the actual ignition delay time; it is the delay between the time the injectant first entered the test Dewar, and the appearance of flame. In the US tests, this time was often difficult to measure; because of backlighting, the time of entrance of the injectant into the Dewar was difficult to detect until color changes and/or ignition occurred, revealing its presence. In many cases, the flame was the first thing observed entering the Dewar, resulting in zero ignition delay time. Of course, in those cases where strong reaction did not occur, it was effectively "infinite". Otherwise, the ignition delay time showed a definite trend, except for the following anomalous cases of interest:

(1) The longest ignition delay following which a detonation occurred was 490 msec in the US configuration (#4) and 2940 msec in the SS configuration (#106).

(2) The shortest ignition delay following which a detonation occurred was 47 msec in the US configuration (#17) and 4 msec in the SS configuration (#104).

(3) The longest ignition delay following which a smooth reaction occur occurred was 6 msec in the US configuration (#26) and 40 msec in the SS configuration (#65).

Test No.	Mode	Injectant	Vol. % O_2	Helium Ullage ~%	Helium Prepurge at 10 psi	Wt. % HF	Valve Open Time msec	Injectant Quantity lb x 10^4
1*	US	GN_2	0	0		0	100	1.42
2*	US	LN_2	0	0		0	100	U**
3'	US	GF_2	U	0		U	100	3.04
3	US	GF_2	U	0		U	100	1.45
4	US	LF_2	U	0		U	100	4.26 (
5	US	GF_2	0.1	0		0.193	50	0.8
6	US	GF_2	0.1	50		0.193	100	1.128
7	US	GF_2	1.1	0		0.193	100	1.408
8	US	GF_2	0.1	50		0.004	50	0.831
9	US	GF_2	1.1	0		0.004	50	0.84
10	US	GF_2	1.1	50		0.004	100	1.085
11	US	GF_2	1.1	50		0.193	50	0.717
12	US	GF_2	1.1	0		0.193	50	3.44
12A	US	GF_2	1.1	0		0.193	50	0.68
13	US	GF_2	0.1	0		0.193	100	3.41
13B	US	GF_2	0.1	0		0.193	100	0.647
14	US	GF_2	1.1	0		0.004	50	3.41
15	US	GF_2	1.1	50		0.193	100	3.41
15'	US	GF_2	1.34	50		0.006	100	3.41
16	US	GF_2	1.1	50		0.004	50	3.41
16'	US	GF_2	1.34	50		0.006	50	3.41
17	US	LF_2	1.1	0		0.004	50	3.41
17'	US	LF_2	1.34	0		0.006	50	3.41
18	US	LF_2	0.1	50		0.004	50	3.41
18'	US	LF_2	0.34	50		0.006	50	3.30
19	US	LF_2	1.1	50		0.004	100	5.49
20	US	LF_2	0.1	0		0.004	50	5.7
21	US	LF_2	1.1	50		0.004	50	5.7
22	US	LF_2	1.1	0		0.004	100	3.46

(A) Temperature in parentheses is bath temperature.

(B) Pressure in parentheses is enthalpic contribution.

(C) Ignition Delay Tim

U Indicates Unobser

TABLE XI
MTI-HYPERGOLICITY TEST SUMMARY

Injectant Velocity ft/sec	P_{F_2} Initial psia	(A) T_{F_2} Initial °R	P_{H_2} Initial psia	Reaction	(B) P_{Rise} psi	T_{Rise} °R
U	75.0	400**	30.0	--	0	0
U	90.0	150	32.0	--	0	0
U	104.7	400*	25.2	Yes	39.0	4.5
11.1	60.2	400*	20.7	No	--	--
I) 3.125	40	(170)	23.2	Detonation	--	--
U	65.2	467	33.7	Yes	23.5	47.5
U	65.7	455	36.2	Yes	26.5	150.3
U	65.7	447	29.2	No	1.5	0
U	67.7	420	26.2	Yes	17	118.5
18.3	63.2	500	26.7	No	0.5	0
8.0	65.7	493	18.7	Mild	3.0	-11.5
7.5	65.2	519.5	26.2	Mild	1.0	-9.0
15.8	139.7	504	27.7	Mild	6.0	22.0
7.3	65.7	514.5	24.7	No	1.0	-5.5
48.3	138.7	497.5	25.2	Yes	13.5	-60.0
6.7	65.7	504	27.2	Yes	26.5	247.5
21.7	140.2	494	21.9	Yes	13.0	-44.5
U	135.2	514.5	26.1	No	2.4	0
20.8	135.2	499.5	28.2	Yes	16.0	-61.
U	138.2	513	28.7	No	2.5	0
28.3	138.7	504	26.2	No	2.5	0
U	68.7	209 (140)	19.2	No	2.7	0
7.8	66.7	211.5 (140)	14.9	Detonation	0.8	113.
U	67.2	204 (140)	26.2	Yes	29.3	-47.
14.9	61.2	210 (140)	37.1	Detonation	1.1	57.
U	62.7	200 (140)	17.2	Mild	9.5	-25.
14.3	138.0	411.5 (180)	23.9	Yes	37.3	-34.
17.9	138.0	435 (180)	23.9	No	2.8	0
10.4	138.2	443 (180)	23.3	No	2.2	0

--Milliseconds

ed

(C)

IDT	Photo Coverage	Remarks	
--	O. K.	*Typical Enthalpic Run	**Approx.
--	None	*Typical Enthalpic Run	**LN_2 Froze in Injector
U	No Lights	*Approx.	
--	O. K.	*Approx.	
490	O. K.	(M)-Max.	
U	Out of Focus	See No. 13B	
U	Out of Focus		
--	Out of Focus	See No. 12A	
U	Out of Focus		
--	O. K.		
--	O. K.		
--	O. K.		
1.5	O. K.	Valve Leak	
--	O. K.	See No. 7	
0	O. K.		
0	O. K.	See No. 5	
3.5	O. K.		
--	None		
--	O. K.		
U	None		
--	O. K.		
U	None		
47	O. K.	Very Fast Detonation <1/4000 sec	
U	None		
95	O. K.		
U	None		
2	O. K.		
--	O. K.		
--	O. K.		

				Helium			Valve
Test No.	Mode	Injectant	Vol. % O_2	Ullage ~ %	Prepurge at 10 psi	Wt. % HF	Open Ti mse
23	US	LF_2	0.1	50		0.004	100
23A	US	LF_2	0.1	0		0.004	100
24	US	SVF_2	0.1	50		0.004	100
25	US	SVF_2	1.1	0		0.004	100
26	US	SVF_2	0.1	0		0.004	50
27	US	SVF_2	1.1	50		0.004	50
28	US	LF_2	0.54	0		0.018	50
29	US	LF_2	0.54	50		0.018	100
30	US	LF_2	0.54	0		0.018	100
31	US	SVF_2	0.54	0		0.018	100
32	US	SVF_2	0.54	50		0.018	50
33	SS	GF_2	0.54		Yes	0.018	50
34	SS	LF_2	0.54		Yes	0.018	50
35	SS	GF_2	0.54		Yes	0.018	100
36	SS	GF_2	0.54		Yes	0.018	100
37	SS	GF_2	0.54		Yes	0.018	50
38	SS	LF_2	0.54		Yes	0.018	50
39	SS	LF_2	0.54		Yes	0.018	100
39A	SS	LF_2	0.54		Yes	0.018	100
40	SS	SVF_2	0.54		Yes	0.018	100
41	SS	SVF_2	0.54		Yes	0.018	50
42	SS	SVF_2	0.54		Yes	0.018	50
43	SS	LF_2	0.54		Yes	0.018	50
44	SS	LF_2	0.54		Yes	0.018	50
44A	SS	LF_2	0.54		Yes	0.018	50

(A) Temperature in parentheses is bath temperature.

(B) Pressure in parentheses is enthalpic contribution.

(C) Igni

U Indi

TABLE XI (Cont'd)

MTI-HYPERGOLICITY TEST SUMMARY

me c	Injectant Quantity lb x 10^4	Injectant Velocity ft/sec	P_{F_2} Initial psia	(A) T_{F_2} Initial °R	P_{H_2} Initial psia	Reaction
	3.35	8.9	137.7	380 (180)	21.2	Yes
	3.41	38.7	137.7	451 (180)	24.2	Yes
	3.46	3.3	69.7	391 (180)	19.7	Yes
	3.46	4.1	70.2	371.5 (180)	38.2	No
	3.41	38.7	64.7	365.5 (180)	28.4	Yes
	3.41	4.2	64.7	353 (180)	21.4	No
	3.42	U*	67.7	356 (140)	36.0	Yes
	1.71	10.4	64.7	(140)	29.4	No
	1.71	20.8	147.0	308 (180)	18.1	Yes
	1.71	20.8	64.7	268 (180)	17.2	No
	3.42	10.4	64.7	338 (180)	18.1	Mild
	1.71	28.3	74.7	492	25.2	No
	1.71	27.8	74.7	380 (140)	27.2	No
	1.72	U*	74.7	530	29.7	No
	1.72	62.5	159.7	532	31.2	No
	1.72	365	159.7	532	26.2	Mild
	1.98	29.7	74.7	467 (140)	36.2	Mild
	1.24	74.4	74.7	482 (140)	28.2	Yes
	1.24	44.4	74.7	480 (140)	28.2*	No
	1.24	52.9	74.7	498 (180)	28.3	Yes
	1.24	59.5	74.7	498 (180)	22.2	Mild
	1.98	31.9	74.7	510 (180)	23.2	No
	1.98	66.7	159.7	513 (180)	22.8	Yes
	1.24	104	159.7	519 (180)	19.9	No
	1.24	71.4	159.7	516 (180)	24.5	Yes

ion Delay Time--Milliseconds

cates Unobserved

(B) P Rise psi	T Rise °R	(C) IDT	Photo Coverage	Remarks
42.1	26.5	3	O. K.	
42.2	10.5	3	O. K.	Reaction Accelerated Velocity
44.0	71.5	6	O. K.	
.5	0	--	O. K.	
39.8	-42	5	O. K.	Reaction Accelerated Velocity
1.3	0	--	O. K.	
32.2	U	0	O. K.	*Velocity Obscured by Reaction
2.8	-13.5	--	O. K.	
39.6	25	0	O. K.	Reaction Accelerated Velocity
2.3	0	--	O. K.	
4.6	-47	--	O. K.	
.8	0	--	O. K.	SS Injection from Top for Checkout
1.5	0	--	O. K.	SS Injection from Top for Checkout
10.5 (10.5)	-19.5	--	O. K.	*No Injection--Possible Injector Plugging
24* (24)	-40*	--	O. K.	*Estimated
8.5 (5.0)	-41	--	O. K.	
16.5 (7.2)	-36.5	--	O. K.	
U*	U*	10	O. K.	*Oscillograph Malfunction
U**	U**	--	O. K.	*Estimated **Oscillograph Malfunction
16.0 (10.7)	-20	19	O. K.	
U*	U*	--	O. K.	*Oscillograph Malfunction
10.7 (7.2)	-32.5	--	Good	
27.3 (10.4)	-45.5	7	O. K.	
13.3 (10.4)	-33.3	--	O. K.	
21.4 (10.4)	-51.5	15	O. K.	

Test No.	Mode	Injectant	Vol. % O_2	Helium		Wt. % HF	Valve Open Time msec	Injectant Quantity lb x 10^4
				Ullage ~ %	Prepurge at 10 psi			
45	SS	LF_2	0.54		Yes	0.018	100	1.24
46	SS	GF_2	1.54		Yes	0.018	50	1.25
46A	SS	SVN_2	0		Yes	0	100	0.90
46B	SS	SVN_2	0		Yes	0	100	0.90
46C	SS	SVN_2	0		Yes	0	50	0.90
46D	SS	SVN_2	0		Yes	0	50	0.90
47	SS	LF_2	1.54		Yes	0.018	50	1.98
48	SS	SVF_2	0.54		Yes	0.018	50	1.24
49	SS	LF_2	0.54		Yes	0.018	50	1.98
50	SS	LF_2	0.54		Yes	0.018	50	1.24
51	SS	LF_2	0.54		Yes	0.018	50	1.98
51A	SS	LF_2	0.54		Yes	0.018	50	1.98
52	SS	SVF_2	0.54		No	0.018	50	1.98
53	SS	LF_2	0.54		No	0.018	50	1.98
54	SS	LF_2	0.54		No	0.018	50	1.24
55	SS	SVF_2	0.54		No	0.018	50	1.24
56	SS	LF_2	1.54		No	0.018	50	1.98
57	SS	SVF_2	1.54		No	0.018	50	1.98
58	SS	LF_2	1.54		No	0.018	50	1.98
58A	SS	LF_2	1.54		No	0.018	50	1.98
59	SS	LF_2	0.54		No	0.018	50	1.98
60	SS	GF_2	0.54		No	0.018	50	1.72
61	SS	GF_2	1.54		No	0.018	50	1.72
62	SS	GF_2	1.54		No	0.018	100	1.72

(A) Temperature in parentheses is bath temperature.

(B) Pressure in parentheses is enthalpic contribution.

(C) Ignition Delay Time

U Indicates Unobserve

TABLE XI (Cont'd)
MTI-HYPERGOLICITY TEST SUMMARY

Injectant Velocity ft/sec	P_{F_2} Initial psia	(A) T_{F_2} Initial °R	P_{H_2} Initial psia	Reaction	(B) P_{Rise} psi	T_{Rise} °R
69.5	159.7	524 (180)	24.5	No	8.7 (8.7)	-38.3
51.5	159.7	523	25.4	Mild	13 (10.4)	-34.5
48.6	159.7	486 (160)	32.3	--	24.0	-39.7
U	74.7	481 (160)	22.2	--	10.7	-20
U	74.7	467 (160)	22.5	--	7.2	-14
U	159.7	467 (160)	17.6	--	10.4	-38.5
62.5	159.7	505 (180)	25.1	No	15.6 (10.4)	-23.5
44.6	104.7	466 (180)	60.8	No	12.4 (7.2)	-33
50.6	104.7	342 (140)	57.9	No	14.3 (7.2)	-28.5
68.0	189.7	433 (180)	58.9	No	18.5 (10.4)	-25
55.1	189.7	496 (180)	54.7	Yes	24.4 (10.4)	-19
67.0	189.7	492 (180)	58.2	U*	22.9 (10.4)	-28
56.6	64.7	502 (180)	20.2	Yes	47.7 (7.2)	-26
78.9	64.7	465 (140)	22.7	Yes	59.6 (7.2)	-74.5
37.2	64.7	447 (140)	19.5	Yes	30.0 (7.2)	-65.5
68.5	64.7	464 (180)	19.2	Yes	28.3 (7.2)	-57.5
31.2	149.7	466 (180)	19.2	Yes	47.3 (10.4)	-57.5
52.1	64.7	460 (180)	19.8	Yes	47.7 (7.2)	-71.5
37.2	64.7	374 (140)	20.8	Yes	U*	-19
70.9	64.7	487 (140)	22.2	Yes	26.0 (7.2)	U
75.0	94.7	477 (140)	59.6^*	Yes	33.1 (7.2)	U
47.2	64.7	526	21.5	Yes	13.1 (3.6)	U
67.0	149.7	530	19.3	Yes	15.9 (6.5)	U
52.8	94.7	534	55.1	Yes	29.0 (10.1)	U

--Milliseconds

(C)

IDT	Photo Coverage	Remarks
--	O. K.	
9	O. K.	
--	O. K.	
--	None	
--	None	
--	None	
--	O. K.	
--	O. K.	
--	Good*	*Shows F_2 Snow Forming
--	O. K.	
9	O. K.	
--	O. K.	*No Visible Reaction--But High ΔP
16	O. K.	
11	O. K.	
7	Good	
9	O. K.	
5	O. K.	
13	Good	
10	O. K.	*Broke Dewar Penetration
7	Good	
13	Great	*Initial Leakage up from 55. 3 psia
14	Good	
5	Great	
12	Great	

Test No.	Mode	Injectant	Vol. % O_2	Helium Ullage ~ %	Helium Prepurge at 10 psi	Wt. % HF
63	SS	GF_2	0.54		No	0.018
64	SS	GF_2	0.54		No	0.018
65	SS	GF_2	1.54		No	0.018
66	SS	GF_2	1.54		No	0.018
67	SS	GF_2	0.54		No	0.018
68	SS	SVF_2	0.54		No	0.018
69	SS	SVF_2	1.54		No	0.018
70	SS	LF_2	1.54		No	0.018
71	SS	LF_2	1.54		No	0.018
72	SA	GF_2	0.54		No	0.018
73	SA	GF_2	1.54		No	0.018
74	SA	GF_2	0.54		No	0.018
75	US*	GF_2	1.54	0	No	0.018
76	US*	GF_2	0.54	0	No	0.018
77	US*	GF_2	0.54	0	No	0.018
78	US*	GF_2	0.54	0	No	0.018
79	US*	LF_2	0.54	0	No	0.018
80	US*	GF_2	0.54	0	Yes	0.018
81	US*	GF_2	0.54	0	No	0.018
82	US*	GF_2	0.54	0	Yes	0.018
83	US	GF_2	0.54	0	No	0.018
83A	US	GF_2	0.54	0	No	0.018
84	US	GF_2	0.54	0	No	0.018
85	US	GF_2	0.54	0	No	0.018
86	US	GF_2	0.54	0	No	0.018

(A) Temperature in parentheses is bath temperature.

(B) Pressure in parentheses is enthalpic contribution.

TABLE XI (Cont'd)
MTI-HYPERGOLICITY TEST SUMMARY

ve Time ec	Injectant Quantity lb x 10^4	Injectant Velocity ft/sec	P_{F_2} Initial psia	(A) T_{F_2} Initial °R	P_{H_2} Initial psia	Reaction
0	1.72	58.3	179.7	534	56.1	Yes
0	1.72	55.5	94.7	547	56.1	Yes
0	1.72	86.3	179.7	545	55.5	Yes
0	1.72	34.2	64.7	551	19.9	Yes
0	1.72	67.0	149.7	549	20.2	Yes
0	1.24	20.8	94.7	(180)	60.7	No
0	1.24	59.5	94.7	(180)	56.4	Mild
0	1.24	75.9	179.7	(180)	56.1	Yes
0	1.24	46.1	94.7	(140)	53.8	Mild
0	1.72	20.8	64.7	524	20.9	Yes
0	1.72	32.7	149.7	524	21.9	Yes
0	1.72	66.9	179.7	532	53.5	Yes
0	1.22	57.3	64.7	522	24.7	Yes
0	1.22	38.2	94.7	512	58.6	No
0	1.69	27.2	179.7	512	54.7	Yes
0	1.69	201.5**	149.7	512	24.7	Yes
0	1.22	13.9	94.7	197.5 (140)	22.2	No
0	1.69	187.5**	159.7	503	20.2	Yes
0	1.69	111.0**	149.7	500	22.2	Yes
0	1.69	145.5**	189.7	497	52.7	Yes
0	2.0	28.3	159.7	538	40.0	Yes
0	2.0	18.0	144.7	547	18.0	Yes
0	2.0	23.6	119.7	531	31.9	Yes
0	2.0	10.4	119.7	425 (200)	26.1	Yes
0	2.0	U*	64.7	178 (200)	23.8	Yes

nition Delay Time--Milliseconds

dicates Unobserved

(B) P_{Rise} psi	T_{Rise} °R	(C) IDT	Photo Coverage	Remarks
20.5 (9.1)	U	5	O. K.	
16.6 (6.8)	U	19	O. K.	
16.6 (7.8)	U	40	O. K.	
13.7 (2.3)	U	18	O. K.	
14.7 (6.8)	U	5	O. K.	
1.0* (1.0)	0	--	O. K.	*Leaky Valve--Probably Plugged Injector
5.3 (2.7)	0	--	O. K.	
32.2 (5.5)	-9	7	Great	
2.3 (0)	0	11	O. K.	Injector Tube Broke--HF Attack
10.4 (1.9)	0	12	Good	
10.4 (2.0)	-18	4	Good	
12.1 (2.9)	0	6	Great	17 psi/sec Pressure Rise Due to Valve Leak
6.9	0	0	O. K.	*With Al Tubes
1.2	0	--	O. K.	*With Al Tubes
U**	U**	--	O. K.	*With Al Tubes **Oscillograph Malfunction
3.0	-28.9	0	O. K.	*With Al Tubes **Flame Velocity
1.0	-9.5	--	O. K.	*With Al Tubes
8.1	-55.8	0	O. K.	*With Al Tubes **Flame Velocity
5.5	-64.3	0	O. K.	*With Al Tubes **Flame Velocity
3.9	-22	0	O. K.	*With Al Tubes **Flame Velocity
9.5	-69	0	O. K.	
7.5	-41.5	0	O. K.	
5.9	-26.4	3.5	O. K.	
20.8	-49.5	3	O. K.	
31.5	-18.5	0	O. K.	*Velocity Obscured by Reaction (But Low)

Test No.	Mode	Injectant	Vol. % O_2	Ullage %	Prepurge at 10 psi	Wt. % HF	Valve Open Time msec	Injectant Quantity lb x 10^4
86A	US	GF_2	0. 54	0	No	0. 018	100	2. 0
87	US	GF_2	0. 54	0	No	0. 018	100	2. 0
87A	US	GF_2	0. 54	0	No	0. 018	100	2. 0
88	US	GF_2	0. 54	0	No	0. 018	100	2. 0
89	US	GF_2	0. 54	0	No	0. 018	100	2. 0
90	US	GF_2	0. 54	0	No	0. 018	100	2. 0
91	US	GF_2	0. 54	0	No	0. 018	100	2. 0
92	SA	GF_2	0. 54		No	0. 018	100	2. 0
93	SA	GF_2	0. 54		No	0. 018	100	2. 0
94	SA	GF_2	0. 54		No	0. 018	100	2. 0
95	SA	GF_2	0. 54		No	0. 018	100	1. 0
96	SA	GF_2	0. 54		No	0. 018	100	1. 0
97	SA	GF_2	0. 54		No	0. 018	100	1. 0
98	SA	GF_2	0. 54		No	0. 018	100	1. 0
99	SA	GF_2	0. 54		No	0. 018	100	1. 0
100	SA	GF_2	0. 54		No	0. 018	100	1. 0
101	SA	GF_2	0. 54		No	0. 018	100	2. 0
102	SA	GF_2	0. 54		No	0. 018	100	2. 0
103	SA	GF_2	0. 54		No	0. 018	100	2. 0
104	SS	LF_2	0.54		No	0.018	100	2.0
105	SS	LF_2	0.54		No	0.018	100	2.0
106	SS	LF_2	0.54		No	0 018	100	2.0
107	SS	LF_2	0.54		No	0.018	100	2.0
108	UA	GF_2	0.54	0	No	0.018	100	2.0
109	UA	GF_2	0.54	0	No	0.018	100	2.45*
110	UA	GF_2	0.54	0	No	0 018	100	1.0
HF1	US	HF	--	0	No	100.0	2.0 sec*	U
HF2	SA	HF	--		No	100.0	2.75(+1.25)* sec	U

(A) Temperature in parentheses is bath temperature.

(B) Pressure in parentheses is enthalpic contribution.

(C) Ignition Delay Time--Mill

U Indicates Unobserved

TABLE XI (Concluded)
MTI-HYPERGOLICITY TEST SUMMARY

Injectant Velocity ft/sec	P_{F_2} Initial psia	(A) T_{F_2} Initial °R	P_{H_2} Initial psia	Reaction	(B) P_{Rise} psi
8.2	64.7	545 (200)	23.9	Yes	24.5
40.3	144.7	169 (200)	31.2	No	0
40.3	144.7	541 (200)	19.3	Yes	10.1
20.8	119.7	547 (350)	24.2	Yes	10.1
20.8	64.7	558 (350)	23.2	Yes	9.5
33.3	144.7	545 (350)	21.9	Yes	11.8
20.8	64.7	537	21.2	Yes	23.5
113*	64.7	555	23.7	Yes	11.5
439*	104.7	552	20.0	Yes	10.5
469*	144.7	558	24.3	Yes	11.5
417*	144.7	564	19.3	Yes	10.6
223*	104.7	560	24.3	Yes	9.9
182*	64.7	560	21.9	Yes	7.3
189*	64.7	541 (180)	20.0	Yes	8.9
338*	104.7	539 (180)	23.6	Yes	12.2
403*	144.7	535 (180)	20.0	Yes	14.5
428*	144.7	531 (180)	20.3	Yes	25.8
366*	104.7	535 (180)	21.6	Yes	14.5
205*	64.7	533 (180)	21.6	Yes	20.2
58.3	144.7	(180)	20.5	Detonation	11.6 (10.0)
37.5	144.7	(164)	20.5	Detonation	14.5 (4.2)
40.3	144.7	(140)	20.8	No*	13.9 (12.9)
40.2	64.7	(140)	20.8	Detonation	3.9 (3.9)
274*	144.7	532	20.2	Yes	7.7
25.6	144.7	532	19.5	No*	3.2
142.5*	64.7	523	19.2	Yes	5.8
U	64.7**	630**	20.4	---	0
U	64.7**	630**	20.3	---	33.7

seconds

ise R	(C) IDT	Photo Coverage	Remarks
90.5	0	O. K.	
0	--	O. K.	
2.2	0	O. K.	
7.5	0	O. K.	
-9	0	O. K.	
1	0	O. K.	
5	4.5	O. K.	
13.5	24	Good	* Aspirator Velocity
U	5	O. K.	* Aspirator Velocity
U	5	O. K.	* Aspirator Velocity
U	3	O. K.	* Aspirator Velocity
U	5	O. K.	* Aspirator Velocity
U	7.5	O. K.	* Aspirator Velocity
U	14	O. K.	* Aspirator Velocity
15	7	O. K.	* Aspirator Velocity
45	3	O. K.	* Aspirator Velocity
2	5	O. K.	* Aspirator Velocity
8	6	O. K.	* Aspirator Velocity
2	13	Good	* Aspirator Velocity
2	4	Good	Very fast detonation 1/4000 sec
5.7	9(+7)*	O. K.	* Detonation followed by subsequent reaction
4.8	--	O. K.	* Frozen F_2 detonated 2.94 sec after injection
9.8	7	O. K.	
U	0	O. K.	* Flame Velocity (with cu tubes)
U	--	O. K.	* Leaky valve-probably plugged injector (with cu tubes)
U	0	O. K.	* Flame velocity (with cu tubes)
2	--	O. K.	* HF Flow time before injector freezing **HF conditions
U	--	O. K.	* HF Flow time before injector freezing **HF conditions

In the SS and SA tests, where the ignition delay time was easily observed and measured, it was noted that the delay time decreased as a function of increasing ΔP (injectant static pressure minus Dewar static pressure). Close examination of the US tests revealed the same trend (except for those cases where the delay was zero). In general, the delay for the US tests was shorter than for the SA or SS tests. It was theorized that ignition first occurred at the injector valve seat (where the propellants first came in contact), and that the dependence on ΔP was due to the fact that the injectant velocity, V_g, was a function of ΔP. What was being observed as ignition delay time was the difference between V_g and the vector sum of V_g and the flame velocity V_f, with the sum V_{f+g} being slower than V_g. Requiring V_g to be propagating against the flow of gas explained the observed ΔP dependence of the ignition delay time as follows:

(1) With low ΔP, V_g was low, V_{f+g} was very low, and ignition delay time was long.

(2) With high ΔP, V_g was high, V_{f+g} was lower than V_g but much higher than V_{f+g} of case (1), and thus ignition delay time was short.

This velocity assumption is also substantiated by the fact that zero delay was only observed in the US tests, never in the SS and SA tests. If it is assumed that the absolute ignition delay at the injector valve is very short (~ 0 msec), then the reason for the zero delay is that the short length of the US injector tube (0.4 ft) allows the flame, on occasion, to be pushed ahead of the gas. But the longer length of the SS injector (1.4 ft) does not permit the flame front to be sustained ahead of the gas flow. Rather, the flame ahead of the gas is quenched while the flame following the gas flow remains. Based on these assumptions, the velocity of gas and gas + flame was analyzed for the US and SS-SA cases in an attempt to determine the absolute ignition delay and flame velocity.

There was great difficulty in accurately determining the gas velocity in the injector tube, since it was only visible after leaving the tube. Thus, there was considerable scatter in the data. However, analysis of this data indicated an absolute ignition delay time of 2.75 msec and a maximum flame velocity of 130 ft/sec. In one case, the actual ignition delay time was observed because reaction clearly initiated in the vessel at the LH_2 surface (US injection). This delay was 3 msec, which agrees well with the calculated time above. The computed flame velocity, on the other hand, appears quite high and may be in error by as much as 50%, judging from the velocity data scatter.

Ullage Tests - Enthalpic tests: The enthalpic series of tests (injection of N_2 rather than F_2) for the ullage configuration gave the following results:

(1) In all cases of GN_2 injection the enthalpic pressure rise was less than the limit of detectability of the pressure instrumentation (of the order of 0.5 psi). This implies that the enthalpy pressure rise is negligible compared to that expected following reaction (~50 psi). The temperature rise was also undetectable.

(2) In all cases of LN_2 injection the LN_2 froze in the injector. However, the liquidus range of LN_2 (25.4°R) is much less than the liquidus range of LF_2 (56.6°R), and it was expected that the LF_2 could be injected without freezing.

The reason for the negligible enthalpic pressure and temperature rise is evident from the movies. Although the injectant penetrates the LH_2 forming a central cavity, the cavity quickly fills up again, forcing the injectant GN_2 back up into the ullage space and out the vent. There is little opportunity for energy transfer and only moderate agitation of the LH_2. This is in contrast to the submerged enthalpic tests discussed below.

Low-Pressure Tests: The ullage injection tests into low-pressure hydrogen were characterized by erratic reaction. The difference between reaction and nonreaction was easily seen in the films. Fig. 8A shows a typical reactive ullage injection which was characterized by an incandescent blue-white flame (not visible in the figure). The injectant enters the Dewar, either already ignited or igniting upon reaching the LH_2 surface, and the hot ignited core penetrates the LH_2 to the Dewar bottom, where it comes back up the sides causing considerable turbulence in the LH_2. (Note the LH_2 surface has been displaced upward from its original position.) After some delay, the turbulence decreases and the LH_2 returns to its previous level, but it is now cloudy-looking, rather than clear, due to the HF suspension. Markedly different in appearance and behavior was a typical "nonreactive" test, in which no flame appeared, and in which the injectant penetrated the LH_2 surface and turned brown. Again a cavity was formed (due to injectant velocity) but it did not usually penetrate to the Dewar bottom. The LH_2 rapidly filled this cavity up again, forcing the brown reactant cloud up into the ullage where it finally settled to form a dense brown layer on top of the LH_2. The oscillograph records of the two cases were very different. Fig. 9 shows a typical oscillograph for the case of no reaction (Test #22). Although the F_2 plenum pressure drops, indicating flow and injection, the H_2 pressure rises but little (rising pressure to the right). This small pressure rise is due to the slow low-order reaction which also causes the injectant color change. Contrast this with fig. 10 (for Test #23), which shows a dramatic pressure spike (rising pressure upward) as well as a temperature jump. Note that the pressure decays rapidly following valve closure. This indicates that pressure rise was due to heating of the ullage with subsequent heat transfer and pressure collapse.

For the US runs, the pressure rise shown in Table XI was the peak pressure rise, rather than a steady-state value. This was done to avoid the indeterminate variable of heat transfer in the Dewar. In most US cases, no "steady-state" pressure was reached, and the pressure continued to decay from a combination of pressure collapse and venting. In many cases, an obvious temperature drop was noted. This was due to a combination of two effects: pressurization of the ullage resulting in condensation and cooling; or, more likely, rapid thermocouple cooling caused by sloshing of LH_2 against it during the turbulent portion of the reactive injection.

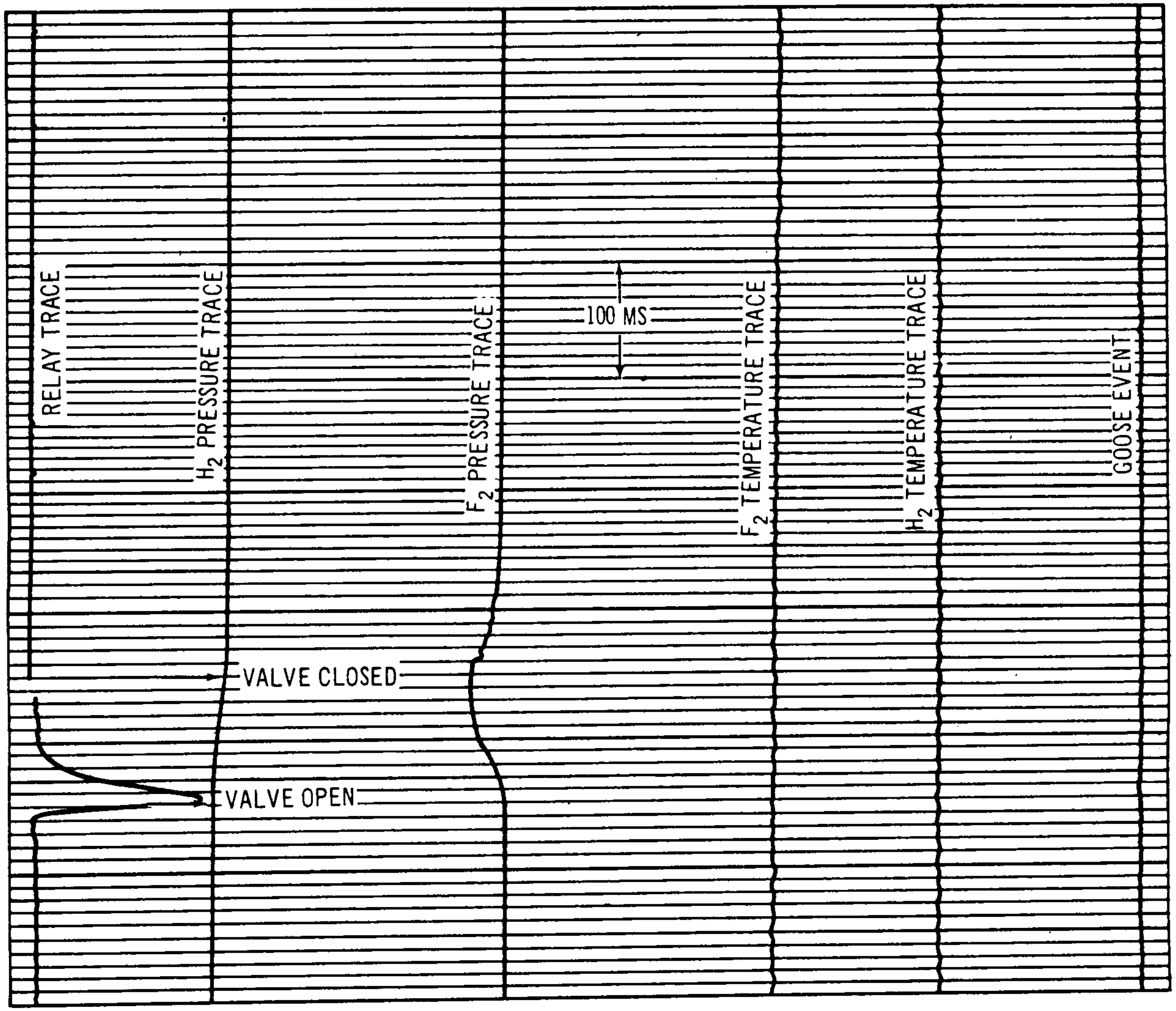

Figure 9. Oscillograph of Typical Ullage Injection Without Reaction

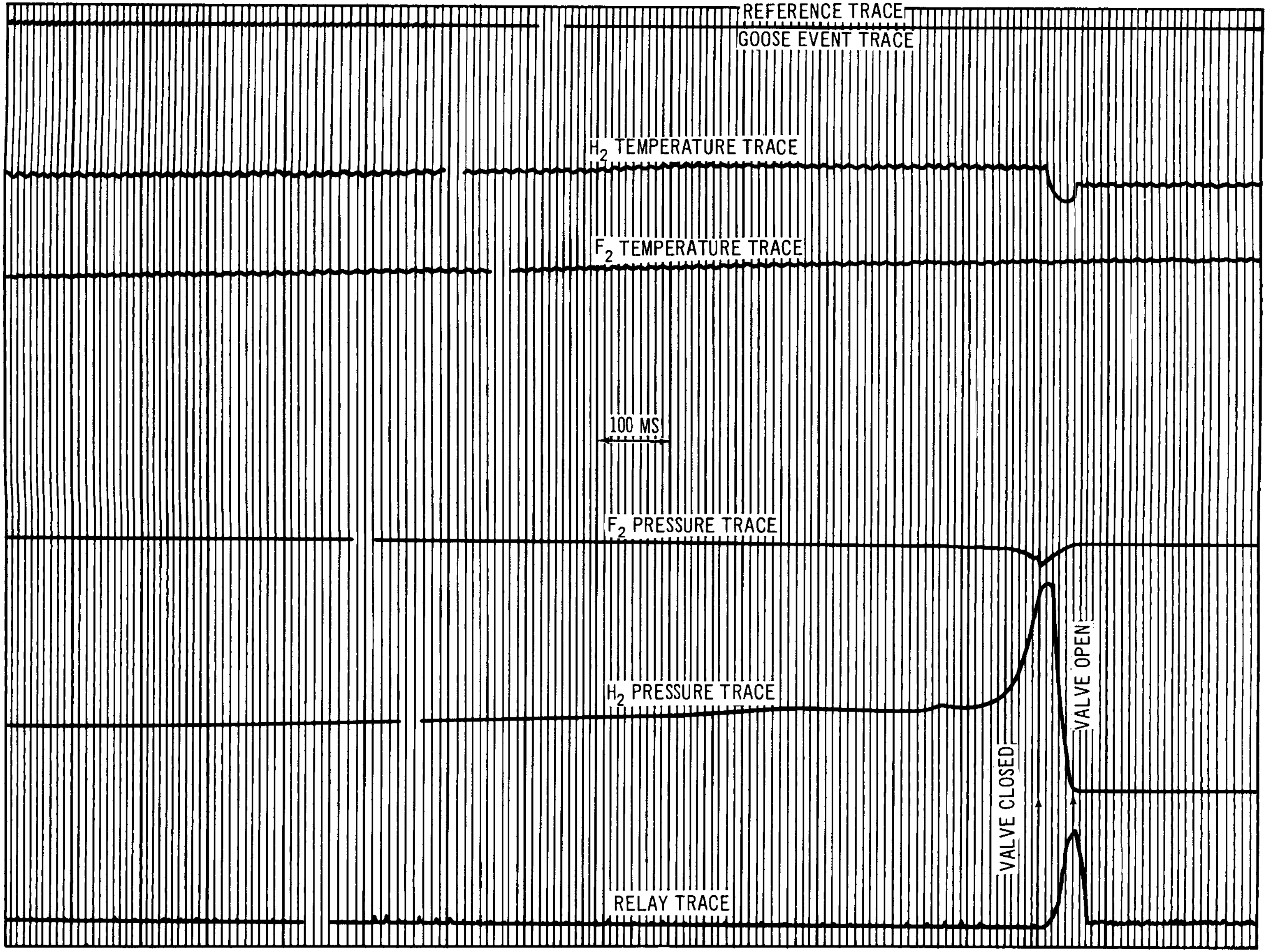

Figure 10. Oscillograph of Typical Ullage Injection with Reaction

In order to determine relative reaction efficiency and eliminate injectant quantity as a variable, the gross pressure rise was converted to specific pressure rise by dividing by injectant quantity and plotted versus injection pressure for warm gaseous injection (fig. 11) and cold gas or liquid injection (fig. 12). It should be noted that this parameter (specific pressure rise) is probably highly dependent on Dewar size, and thus should not be scaled to larger vessels. Also note that the 1.0 vol % O_2 addition had a significant effect on specific pressure rise, causing an order of magnitude suppression of the specific pressure rise. When this effect was noted, the fluorine used was analyzed for O_2 content (see Table IX). It was found that the uncontaminated F_2 (bottle #2994) used for most of the ullage tests was fortunately quite pure (0.1 vol % O_2), and the addition of only 1.0 vol % resulted in an order-of-magnitude change in O_2 content. The final low-pressure ullage tests were done with a different fluorine (bottle #12092) which analyzed fortuitously to an uncontaminated value of 0.54 vol % O_2. This value was midway between the reactive value (0.1 vol % O_2) and the nonreactive value (1.1 vol % O_2) of the previous F_2 and resulted in erratic ignition in the uncontaminated state (see fig. 12). The inhibiting effect of O_2 on the F_2-H_2 reaction was observed previously (see ref. 3) where small amounts of O_2 (~3%) sharply reduced the reaction rate. It was theorized (refs. 5 and 6) that the reaction $H + O_2 + M \rightarrow HO_2 + M$ competes with the reaction $H + F_2 \rightarrow HF + F$ to reduce the rate. What was unexpected was that addition of as little as 1.0 vol % O_2 would result in no reaction, under the conditions of the MTI tests.

The effect of oxygen contamination on specific pressure rise for US injection is shown in fig. 13. Following the US runs in the supplemental tests (discussed further below) all of which were done at a level of 0.54 vol % O_2, it was discovered that the erratic ignition seemed to depend on injectant temperature and injection rate. It appeared that warm (high-temperature) gas or large injection rate ignited, while cold gas or small injection rate did not. It was thought that the LH_2 acted like an "infinite" heat sink, rapidly draining energy from the injectant. The higher the injectant energy (enthalpy) injection rate, the more apt the injectant was to overcome the O_2-imposed reaction rate reduction and react before freezing in the LH_2. The absolute enthalpy (relative to absolute zero) was computed (based on the data of reference 7) and multiplied by the injection rate for each case of US injection. The results are plotted vs. vol % O_2 level in fig. 14. The shaded points indicate nonignition. Shown for reference only are lines of vapor, liquid, and solid enthalpy multiplied by the average injection rate at each level of O_2 contamination. Note that the individual points were not necessarily at the conditions implied by their relation to these lines, (i.e., vapor or liquid). A definite transition region between ignition and nonignition (shaded region) is observed. It lies above the reference line for vapor, with increasing energy required for increased O_2 level. This substantiates the thesis that O_2-imposed reaction rate reduction causes freezing of low-energy injection of F_2 prior to ignition.

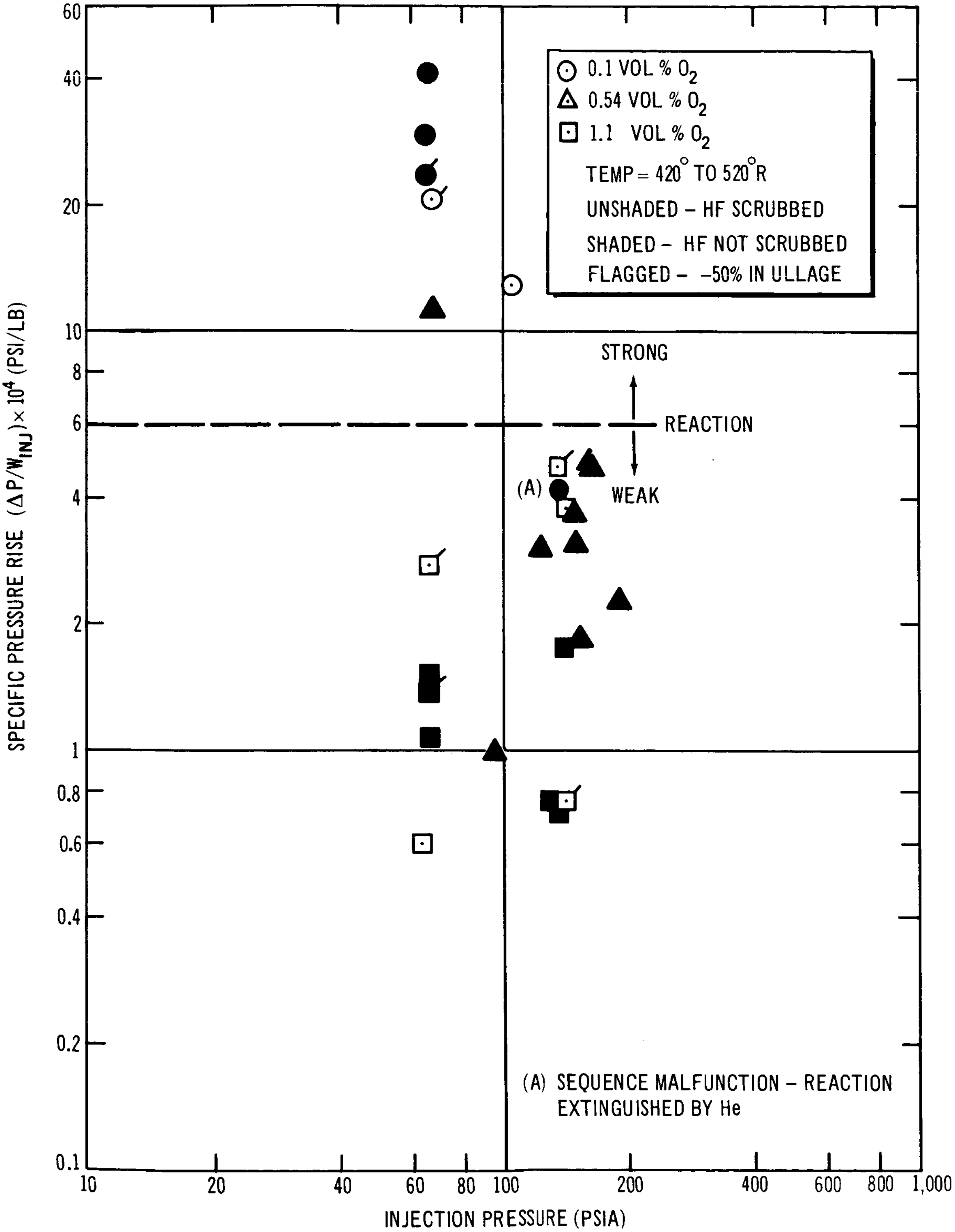

Figure 11. Specific Pressure Rise vs Injection Pressure (Warm Gas Injected into Ullage)

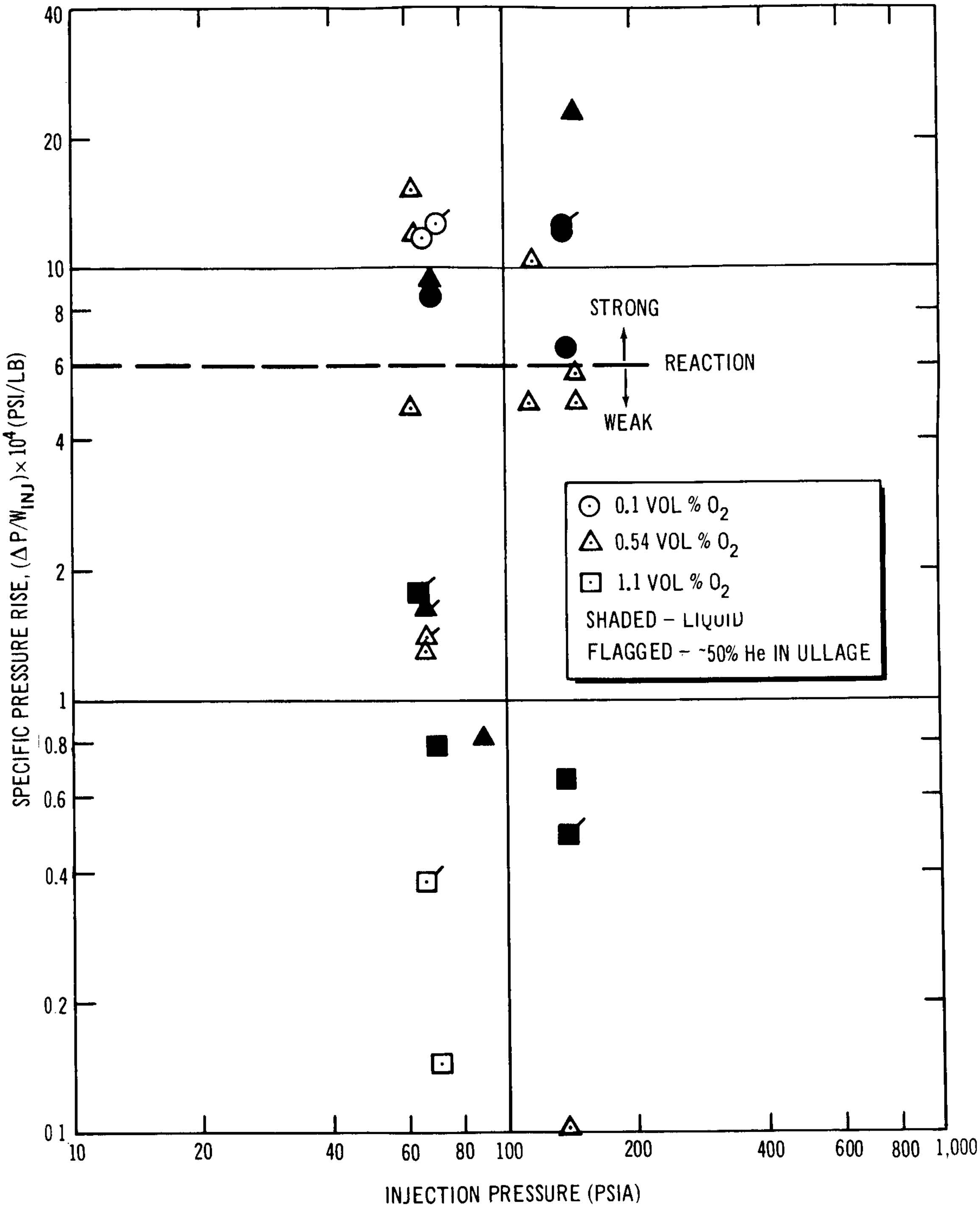

Figure 12. Specific Pressure Rise vs Injection Pressure (Cold Gas or Liquid Injected into Ullage)

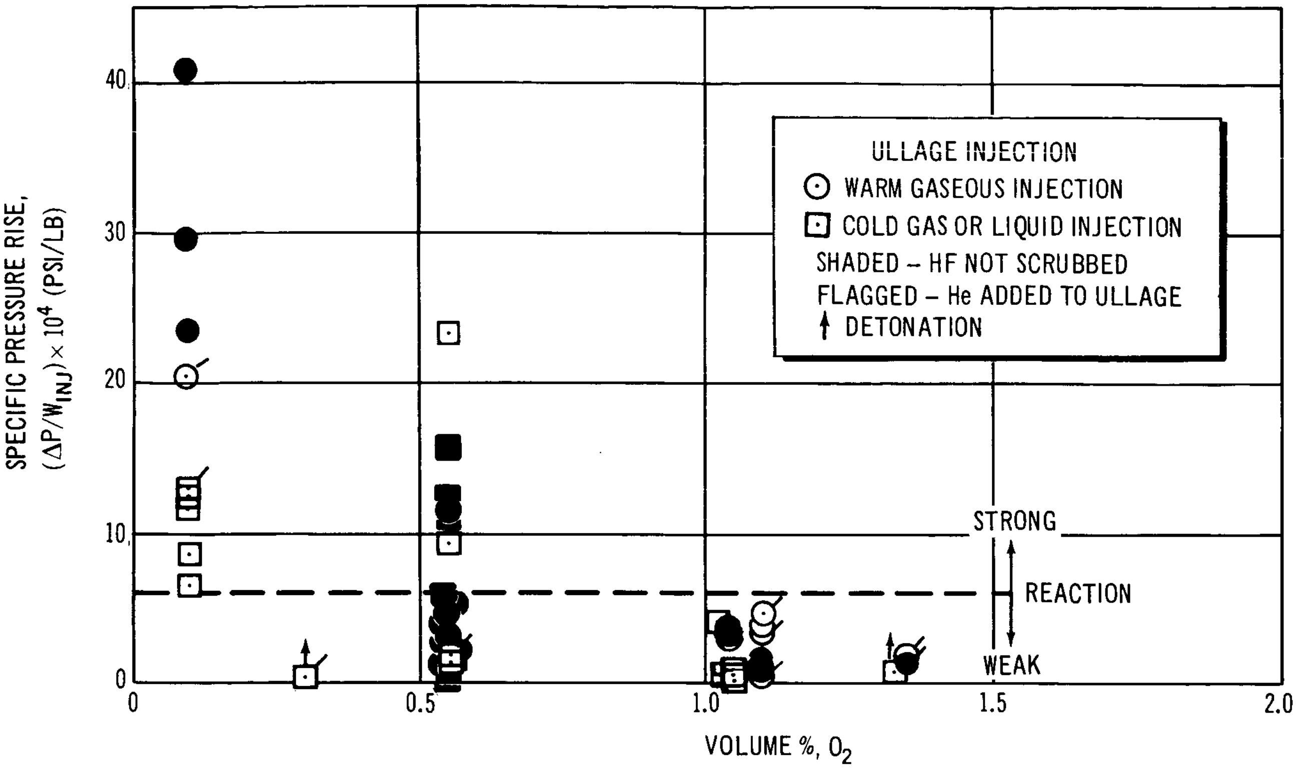

Figure 13. Effect of O_2 Contaminant in Injectant on Specific Pressure Rise

This frozen F_2, however, is capable of detonation in LH_2, as evidenced by occurrences during this program and during other testing under NASA Contract NAS3-2574. Further, this reaction rate reduction can cause sufficient ignition lag to lead to detonation in the test apparatus before the reactant freezes. Fig. 8B shows a very fast detonation which was visible for only 1/4000 sec. Note the cracks in the inside Dewar shell. Of the 5 detonations which occurred during the US tests, 2 occurred during dumping several minutes after injection, and are discussed under Reaction Products Freezing, below. The other 3 all occurred following a liquid injection with delay times of 47, 95, and 490 msec (there were also 8 LF_2 US injections which failed to react at all). The injectant was still obviously fluid, and had not frozen solid (except perhaps in the last case where viewing was obscured by boiling in the original apparatus). Detonation never followed a warm gas injection, although 9 warm gas US injections also failed to visibly react. This was probably due to the fact that the gas injectant was well-diffused through the LH_2 shortly after injection, while the liquid (in the 3 cases above) was confined to a smaller, denser slug.

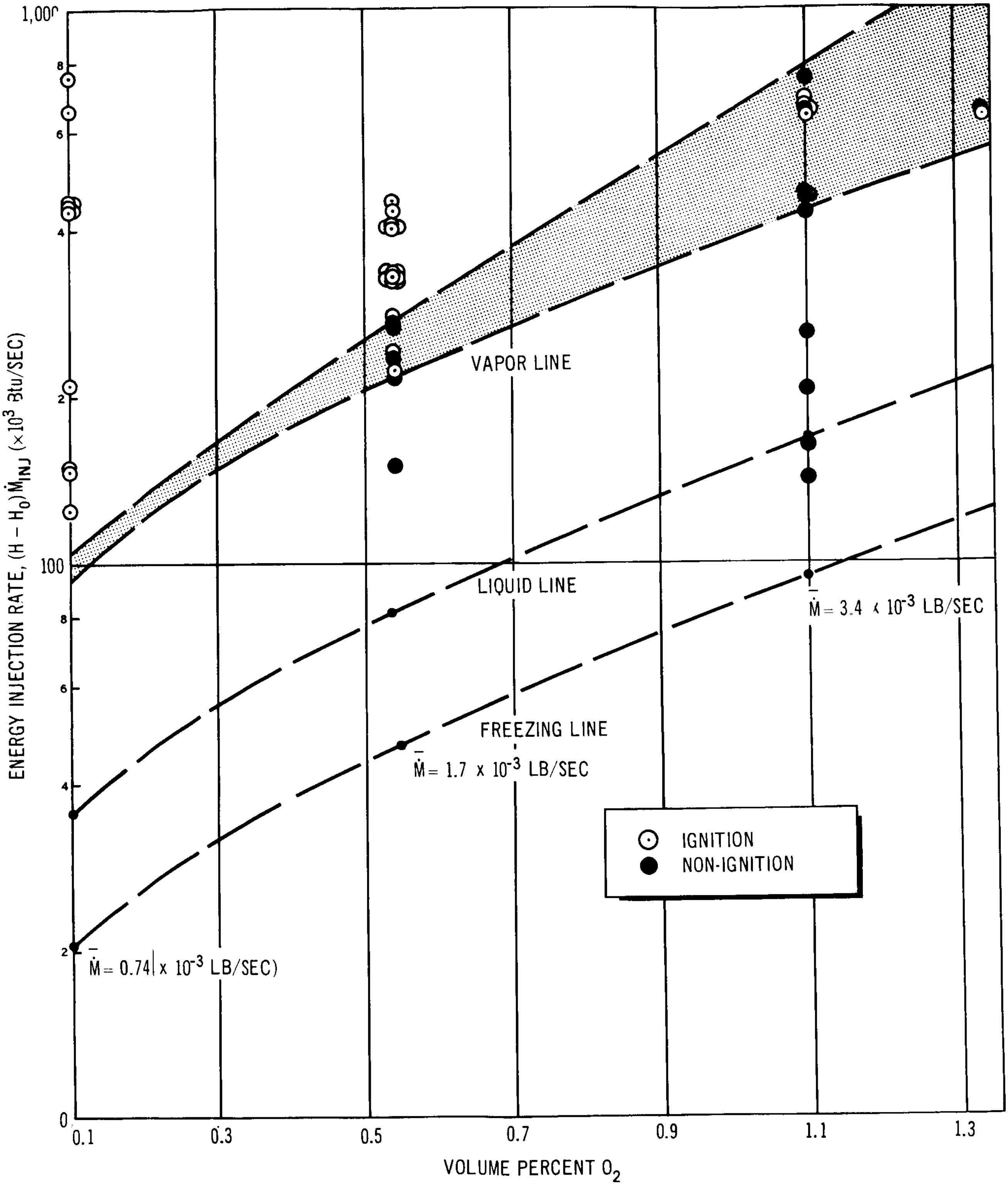

Figure 14. Effect of O_2 Contaminant in Injectant on Minimum Ignition Energy

It can be seen from figs. 11 and 12 that there is no obvious effect of HF contamination in the injectant or of helium dilution of the ullage. The HF was expected to stimulate the reaction, but obviously the O_2 inhibition effect was many times more powerful and completely overshadowed any HF catalysis. Helium in the ullage had no particular effect because in those cases where it was present, the injectant simply penetrated to the LH_2 surface and ignited there. The absence of these effects is verified in the results of the statistical analyses below.

High-Pressure Tests: The ullage injection tests into high-pressure hydrogen showed no particular differences from the low-pressure tests except a mild suppression effect, possibly in interaction with the increased natural O_2 content (0.54 vol %) of the F_2 used in these tests. This high-pressure suppression effect was found in a more positive manner in the SS tests and is discussed further below. The effect of a helium prepurge similar to that discussed below in the SS tests was evaluated for the high pressure tests, and checked with a low pressure test. In both cases there was no effect; the injectant ignited upon reaching the LH_2 surface.

Wall Effects and Supplemental Tests: An initial series of tests was run to evaluate the catalytic effect of an aluminum surface, represented as a bundle of tubing. There was no discernible effect, and in no case did the reaction appear to originate near the tube bundle. In all cases the reaction, if it occurred, was visible as soon as the injectant reached the LH_2 surface. Similarly, the level of ullage, which varied by 30%, also appeared to have no effect.

In the supplemental test series described above, additional tests were run to evaluate the catalytic effect of a copper surface, also represented as a bundle of tubing. Again, there was no discernible effect, the reaction being visible on injectant entry or upon the injectant reaching the LH_2 surface. These tests were coupled with tests of the ullage/aspirated (UA) injection mode, configured as shown in fig. 6D. The UA mode was not expected to give performance discernably different from US; in fact, this mode showed no tendency to aspirate. These tests showed that the UA mode performed no useful pressurization function compared to the US mode.

Submerged Tests. — SS Test Matrix Reduction: Before proceeding with the submerged tests the data from the ullage tests were examined to see if some of the variables which had shown no effect could be eliminated from the SS test matrices. Ullage helium had shown little effect, but was not a variable for the SS tests. HF concentration in the GF_2 had been shown to have little effect and was present in the fluorine used to only 0.018 wt % (see Table X) so it was eliminated as a variable. O_2 content had been shown as a significant parameter when varied between 0.1 and 1.1 vol %. However, the present fluorine had a natural concentration of 0.54 vol % (see Table X) and had given both reaction and nonreaction in the final ullage tests. It was judged pointless to perform a whole series of tests at the 1.54 vol % O_2 level when 1.1 vol % O_2 had shown such strong inhibition. However one GF_2 test (#46) and one LF_2 test (#47) were run at the 1.54 vol % O_2 level as a check in the runs with helium prepurge. In the runs without helium prepurge, consistent ignition led to the reinstallation of k_2 as a variable and a number of runs were made at the 1.54 vol % O_2 level. (See results below.) It had also been determined that in the US runs the valve-open time, h, had had little effect on the LF_2 injection runs, since effective injection occurred in less time than the minimum valve open time of 50 msec. Accordingly, most of the LF_2 runs with and without prepurge were made at the h_1 level of 50 msec. However, h was kept as a variable for the GF_2 injection tests. Finally, although injectant quantity, g, was to be a variable in the SS GF_2 injection test matrix, it was not a variable for the US GF_2 injection tests. Accordingly, it was retained as a variable only for the SS LF_2 injection tests. These reductions resulted in just the tests run as shown in Tables V and VI, with, it is thought, no loss of important interaction data.

Enthalpic Tests: The enthalpic tests injecting cold N_2 rather than F_2 for the submerged configuration gave results very different from those of the ullage configuration. Fig. 15 shows a typical oscillograph record for an enthalpic injection (#46D). There is an obvious smooth pressure rise to a "steady-state" value with an accompanying temperature drop. The "steady-state" pressure rise and minimum temperature drop for the enthalpic tests are shown in Table XI. The "steady-state" pressure rise is not steady, but decays slowly with time to approximately the pre-injection pressure level. The reason for the differences between US and SS enthalpic tests lies in the injection technique. Fig. 8C shows a typical SS injection with reaction--a nonreactive injection is similar in appearance. The injectant enters the Dewar with sufficient energy to throw large quantities of LH_2 into the warmer ullage. Some of this LH_2 strikes the thermocouple, which is quickly chilled and shows a temperature drop. Much of this LH_2 is vaporized in the warm ullage--resulting in a significant smooth pressure rise. When the remaining LH_2 falls back out of the ullage, the thermocouple quickly returns to its original temperature, and the pressure slowly decays back to its original value. It is important to note that this dynamic effect also occurs during reactive injection, and the "enthalpic" pressure rise is significant during and shortly after injection. In Table XI the "enthalpic" contribution to the gross pressure rise shown is given in parentheses.

Tests with Helium Prepurge: Because of the apparent fragility of the glass tubing injector used in the SS Dewar configuration, it was decided to run the initial series of SS tests with a 10 psi helium prepurge entering the tubing and Dewar just ahead of the injectant. The injection pressures were also raised 10 psi for mechanical reasons of keeping relatively constant flow compared to tests without prepurge. The helium prepurge mass was about 3% of the injected F_2 mass and the sole purpose of the prepurge was to prevent ignition in (and breakage) of the glass injector external to the inner Dewar shell.

These tests were similar to the US test series in that they were characterized by erratic ignition. Again, reaction was characterized by an incandescent blue-white flame. Fig. 8C shows a typical reactive SS injection. The injectant enters from the bottom and penetrates the LH_2 to the ullage. After an obvious (and easily measured) delay the flame appears, sometimes in the tube, sometimes just above the tube outlet. After reaction there is considerable and persistent turbulence in the LH_2. The case of no reaction was generally similar (except for absence of flame) with perhaps milder turbulence following injection. Again, the oscillograph records for the two cases show obvious differences. Fig. 16 shows a typical oscillograph for the case

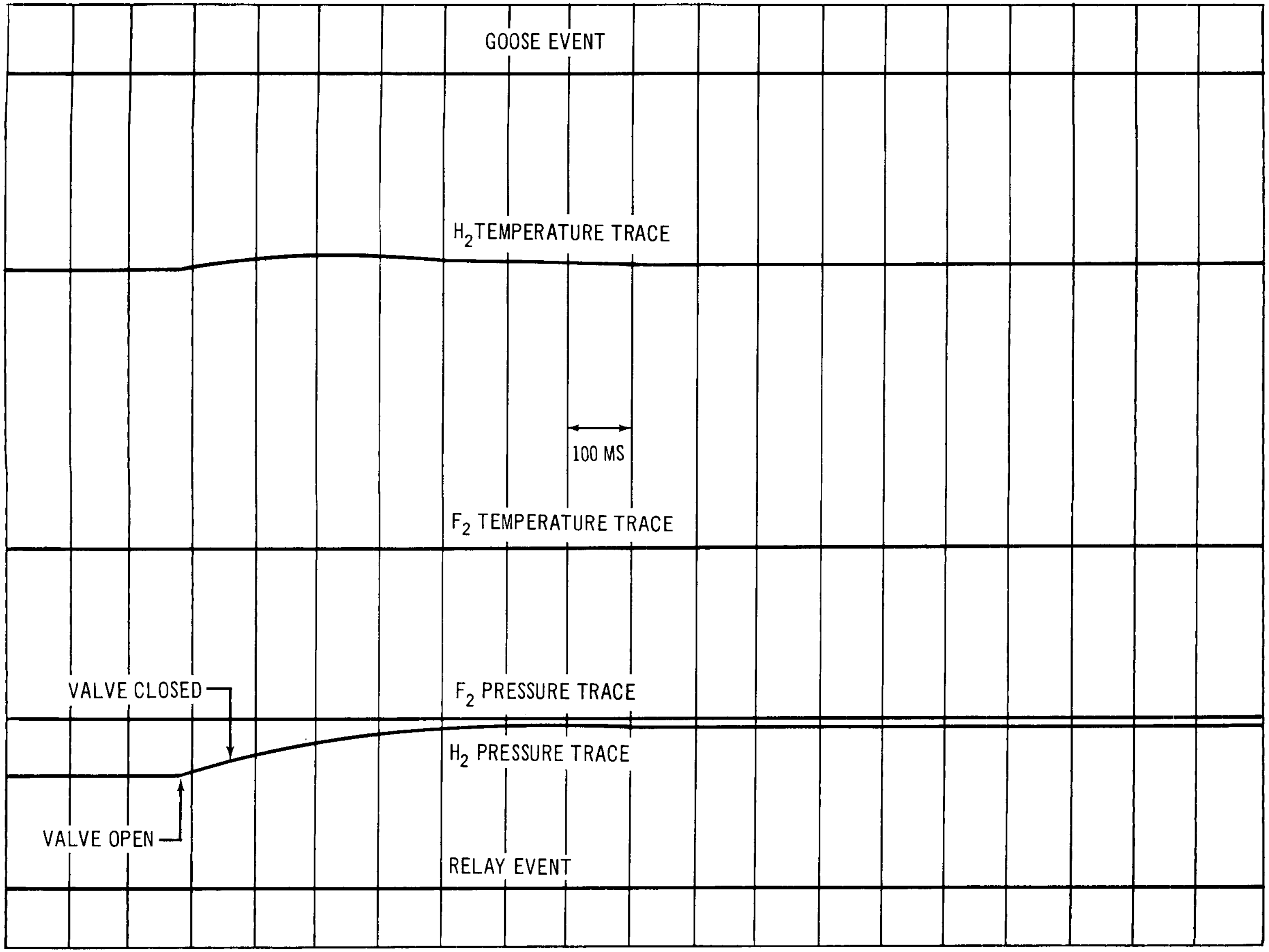

Figure 15. Oscillograph of Typical Enthalpic Pressure Rise with Submerged Injection

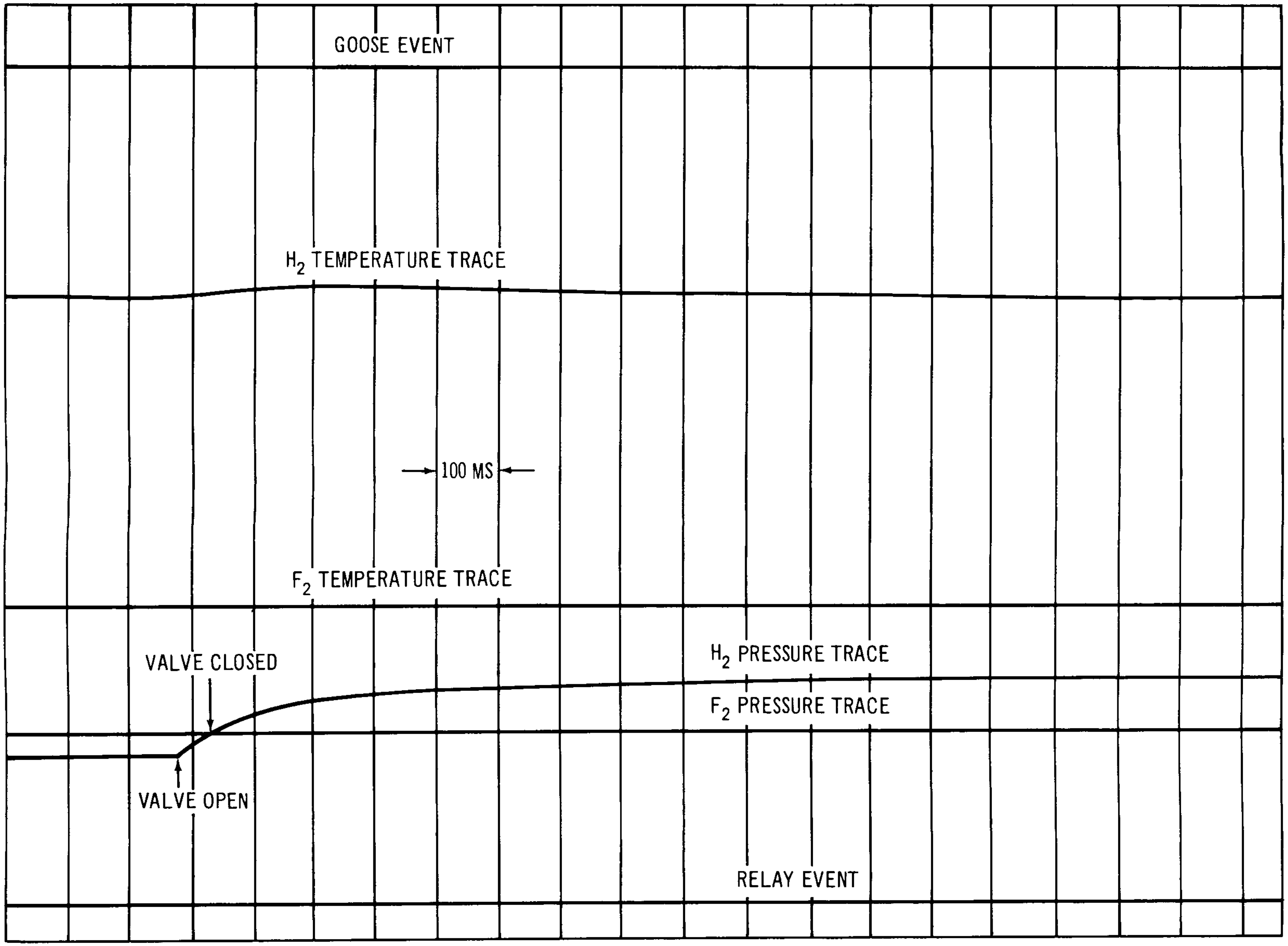

Figure 16. Oscillograph of Typical Submerged Injection without Reaction

of no reaction (test #47). It is virtually identical to the oscillograph for enthalpic injection (fig. 15), showing a temperature drop which quickly recovers, and a smooth pressure rise which gradually decays. Compare this with fig. 17 (for test #44A) which shows an immediate sharp pressure jump, followed by a smooth pressure rise to a steady state value which does not then decay. For the reactive tests, the "enthalpic" pressure rise shown in parentheses was taken as the difference between the steady-state pressure and the pressure of the initial sharp jump. The net pressure rise (subtracting the "enthalpic" contribution) was again converted to specific pressure rise and plotted against injectant pressure minus initial LH_2 pressure (to allow uniform presentation of high and low pressure LH_2 tests) as shown in fig. 18. It will be noted that there is a mild interaction with both injection pressure and injectant phase. This is verified in the statistical results below. Again the increased pressure increases the injectant internal energy, improving the tendency for reaction, while the LF_2 phase improves the tendency for reaction due to favorable density effects.

An interesting effect which showed the greater capacity for injectant energy transfer in the SS tests compared to the US tests was the appearance of brown "snow" (i. e., frozen F_2) following nonreaction in several of the SS injection Fastax films. This injectant freezing would have had to occur in less than 1. 5 sec to appear in the high-speed movies. This effect was never seen during the US injection tests, which verifies that energy transfer was more efficient in the SS tests.

Tests Without Helium Prepurge: A series of SS tests without the 10 psi helium prepurge was run to complete the SS test matrices. These tests were characterized by consistent, vigorous reaction. Of 21 tests run, there were only 2 which reacted in a "mild" fashion, and only 1 which did not react. This non-reaction was due to frozen HF plugging of the injector which sharply reduced the injectant flow rate. For these tests, the specific pressure rise is plotted vs the injection pressure differential in fig. 19. It can be seen that there is no noticeable pressure effect (as was the case with prepurge), but there is again a definite phase effect. O_2 contaminant was again introduced as a variable to include 0. 54 and 1. 54 vol %, and it can be seen that there is no discernible inhibition effect even at this high O_2 percent. The highly reliable ignition, regardless of inhibiting factors, can be explained through examination of the high-speed movies for these tests. In 15 of the 18 tests with strong reaction, the initial reaction occurred in the injector tube outside the Dewar, and the flame raced up the injector tube into the Dewar. In the other 3 tests reaction occurred just above the mouth of the injector. Clearly, in this test configuration, the injectant had opportunity to react with warm GH_2 just downstream of the injector valve. Failing this, it had opportunity to ignite upon reaching the LH_2. In this test series many interesting flame patterns were observed with the high-speed movies including cases of the "blowtorch effect", in which the flame roared out of the injector, through the previous penetration through the LH_2, and into the ullage without pause. This reliable ignition engendered other problems, however, the most severe of which was frozen HF buildup in the injector with subsequent plugging of the injector. This problem is discussed below under Reaction Products Freezing.

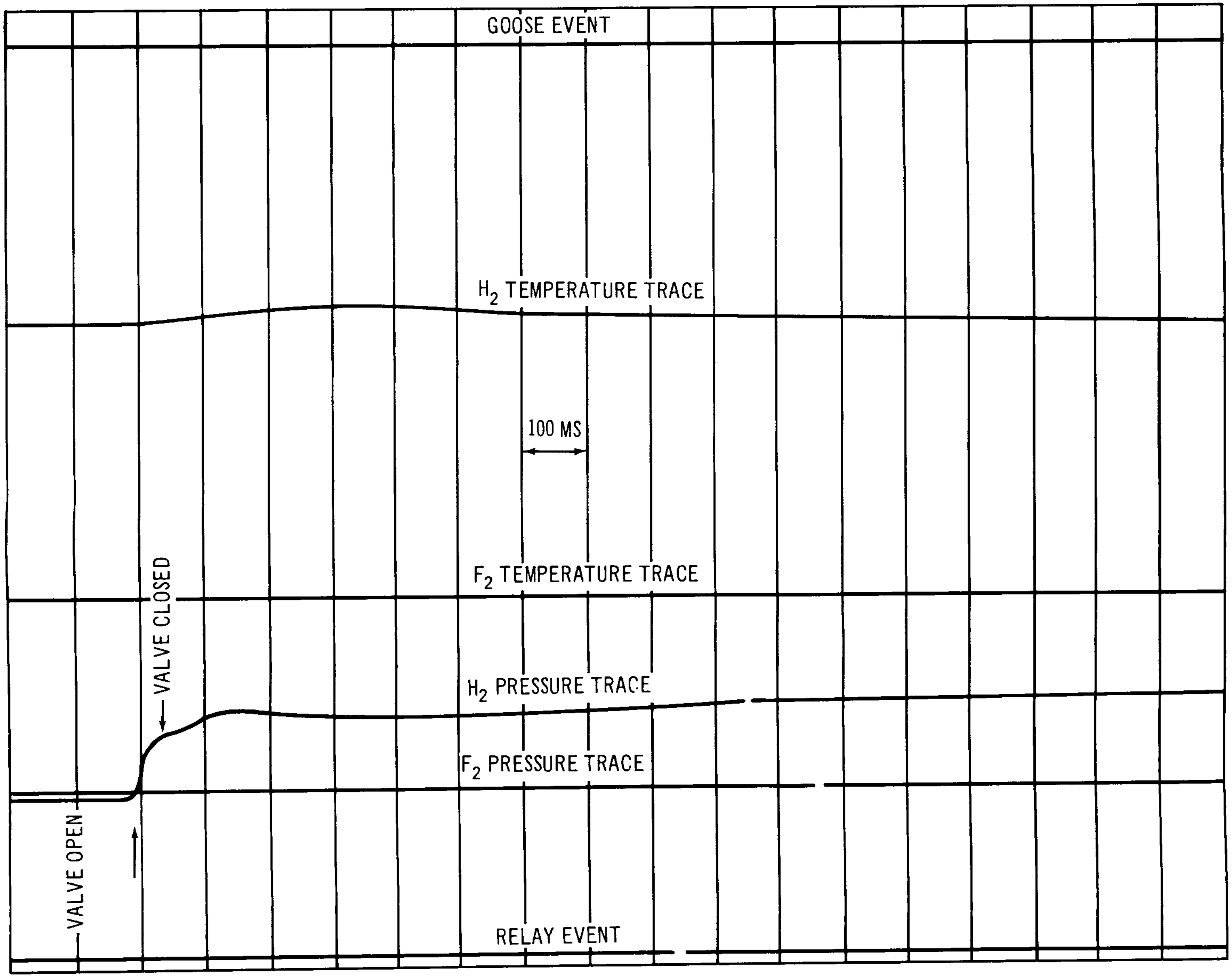

Figure 17. Oscillograph of Typical Submerged Injection with Reaction

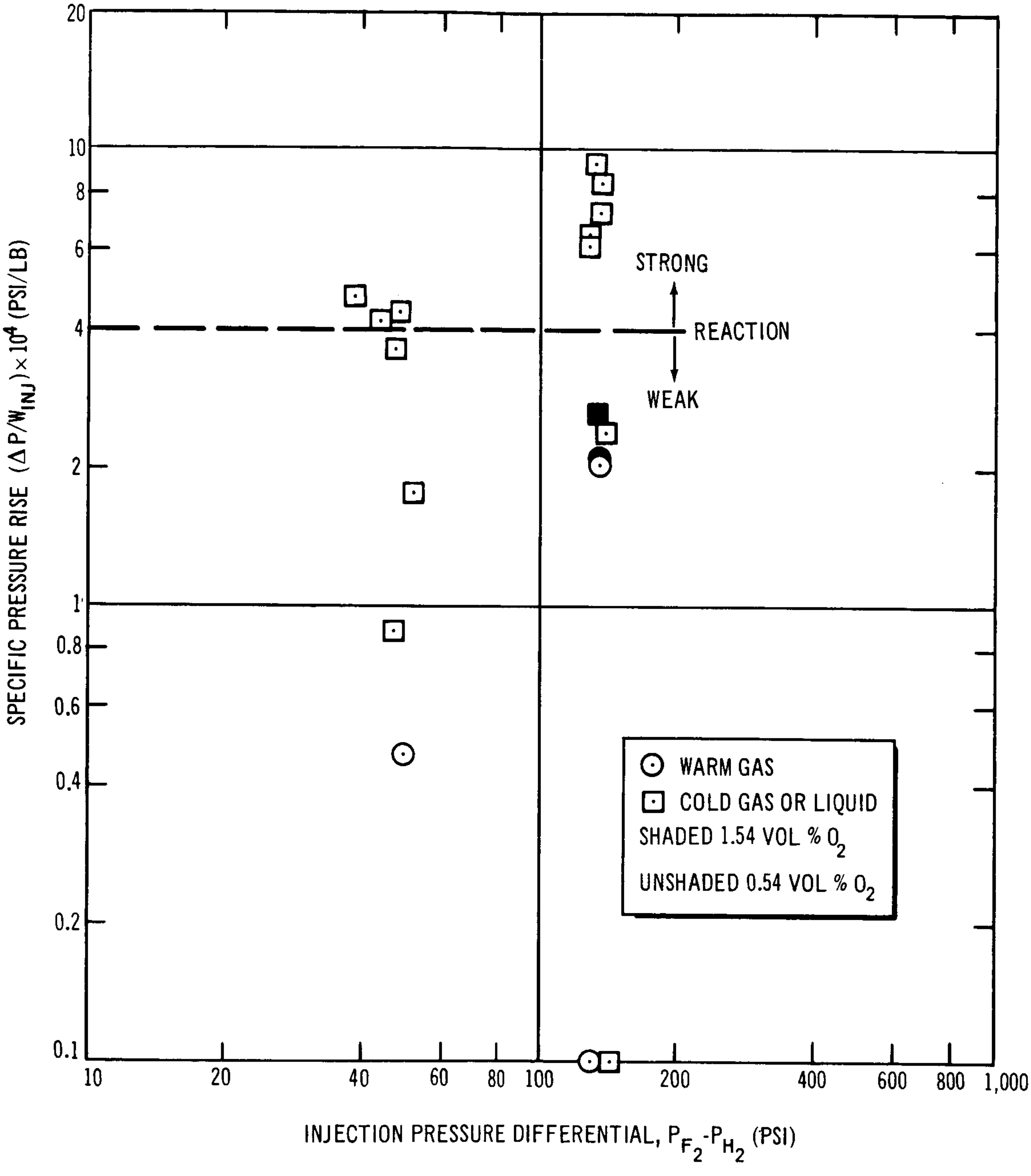

Figure 18. Specific Pressure Rise vs Injection Pressure Differential (Submerged Injection with 10-Psi He Pressure)

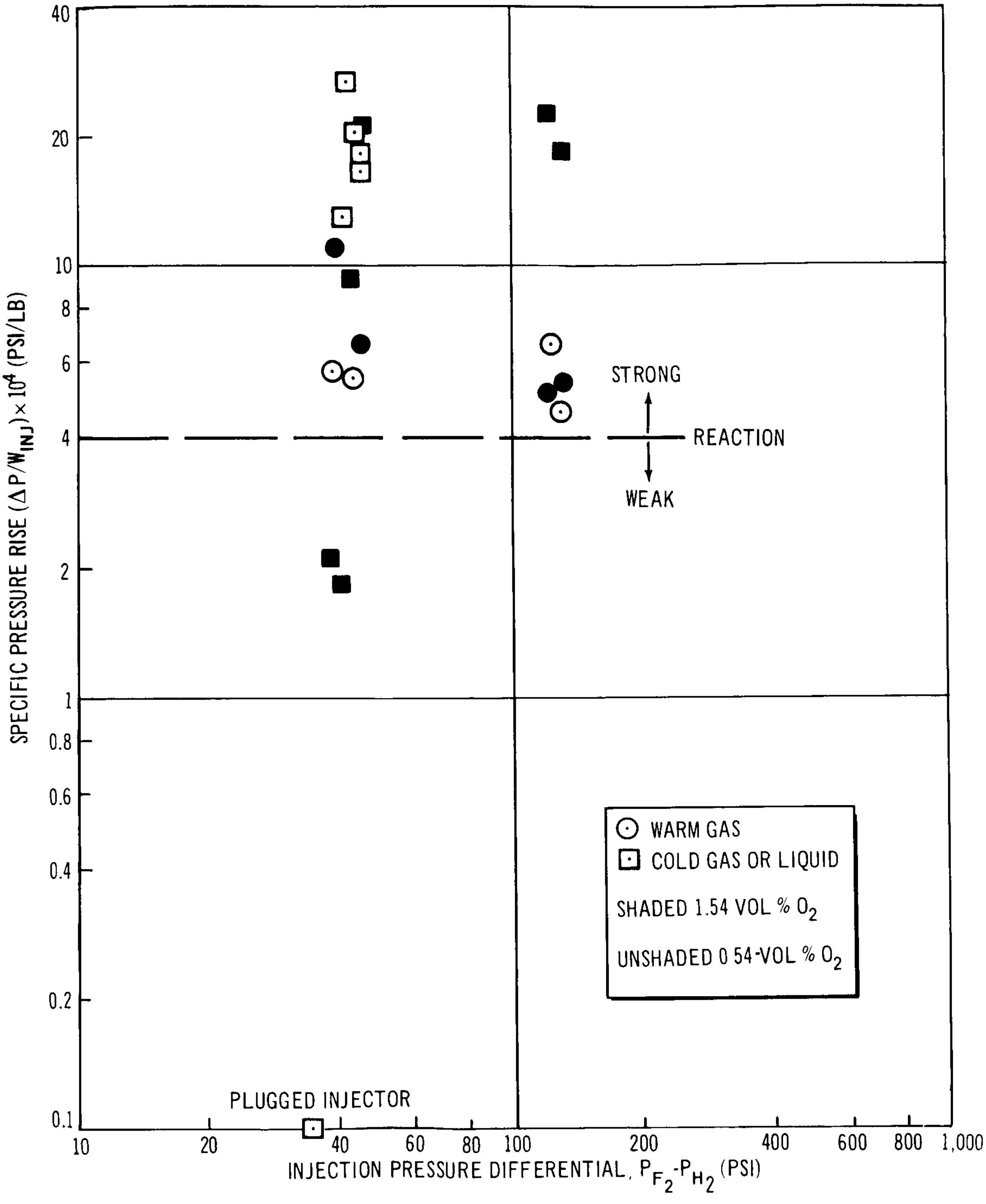

Figure 19. Specific Pressure Rise vs Injection Pressure Differential (Submerged Injection without He Prepurge)

Submerged/Aspirated and Supplemental Tests: The initial tests were made with the SA configuration shown in fig. 6A, and were all done without helium prepurge to insure reliable ignition. These tests were at high and low injection pressures and high and low hydrogen pressures. The oscillograph records for these tests were virtually identical to those of the SS tests. The pressure rise for the SA tests was remarkable similar to that for the SS tests under otherwise similar conditions. This is shown in fig. 20 which compares 3 SA tests with 3 SS tests with prepurge, and with 3 SS tests without prepurge, all tests being run at essentially identical conditions.

Fig. 8D shows an initial SA reactive test (all of the SA tests had reaction). Note the following features:

(1) The bright flame inside the aspirator tube, below the LH_2 surface.

(2) The vigorous injection of LH_2 into the ullage.

(3) Blowback from the bottom of the aspirator (at base of tube).

These features were characteristic of the initial SA tests and merit discussion.

The bright flame was not confined to the tube interior, but occurred outside the base of the aspirator tube because of the blowback (3 above). This blowback occurred even before visible ignition; upon ignition, hydrogen was forcibly ejected from both ends of the tube, destroying the aspirator effect. Burning continued outside the tube after blowback and displayed on oscillatory expansion and contraction of the cloud at the tube base with a frequency of 1000-500 cps (the frequency dropped as the cloud got larger).

The initial SA design was simply a relatively large-diameter straight tube. The LH_2 flow annulus was apparently too large relative to the F_2 flow area, resulting in initial blowback of the injectant through the annulus upon expansion of the injectant into the larger tube. This expansion slowed the velocity of the F_2 to less than the flame velocity, resulting in the flame being fixed at the expansion region (which is the "pumping" region). The flame created a local high-pressure region which expelled LH_2 from both ends of the tube; it also spread outside the tube and ignited the F_2 which had previously been blown back through the annulus.

In the supplemental testing, a modified SA injector, configured as shown in fig. 6B, was tested over a wide range of conditions shown in Table VIII. The key modifications in the SA injector design were as follows:

(1) A converging section (bottom) with a much smaller LH_2 flow annulus to provide more efficient LH_2 acceleration and pumping; and to reduce the possibility of initial F_2 blowback.

(2) A much smaller diameter straight section to keep the F_2 flow velocity above the flame velocity, thus driving the flame front away from the vicinity of the pumping region.

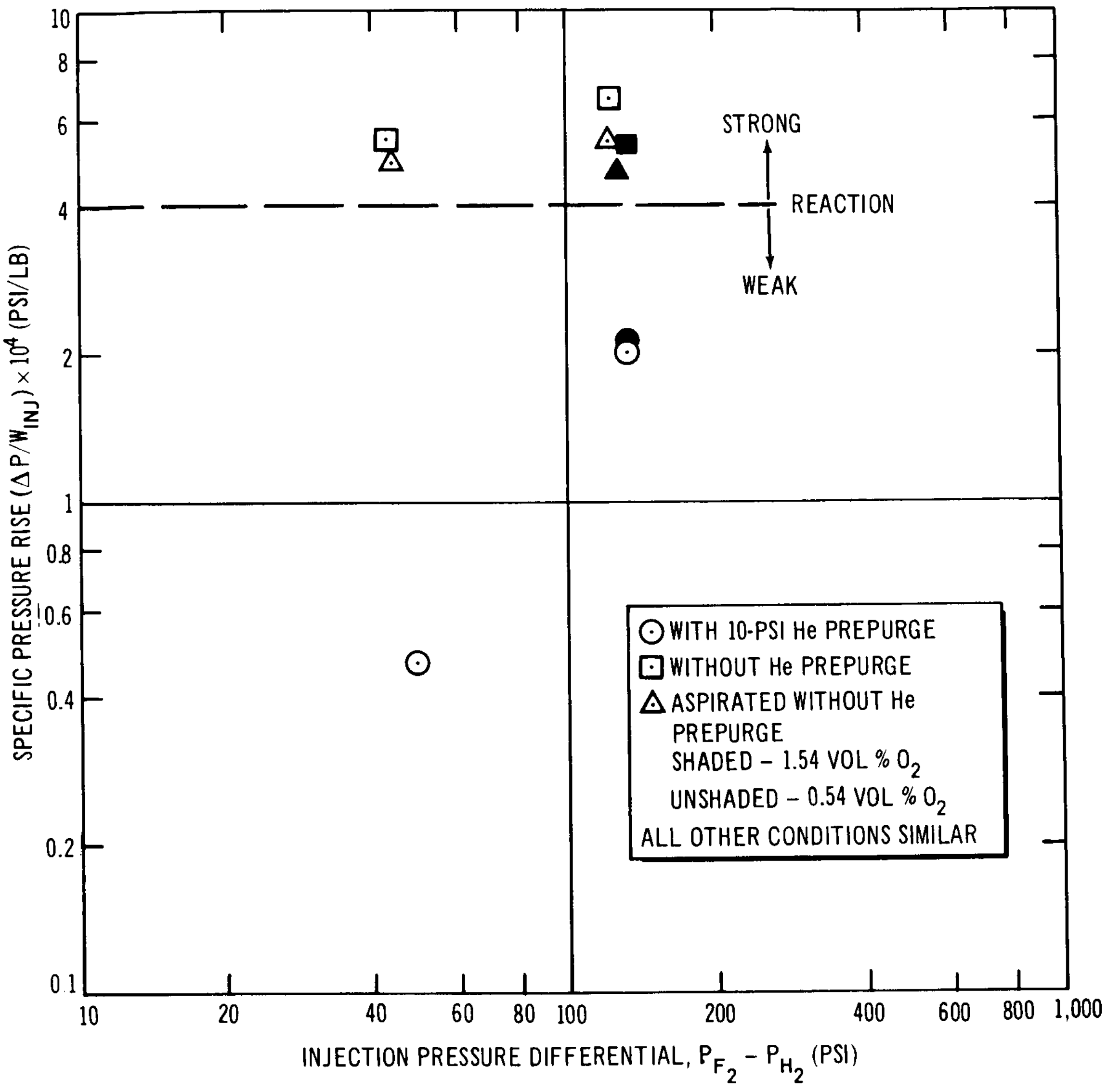

Figure 20. Specific Pressure Rise vs Injection Pressure Differential (Submerged Injection with Warm Gas for Different Injection Modes)

(3) A diverging section (top) to expand the F_2 flow to a velocity below the flame velocity, resulting in a flame holding region separate from the pumping region.

The tests of this configuration were very successful: there was only a small amount of blowback and the flame burned at the base in the blowback region only briefly (~5 msec) before jumping to the upper diverging section where it held stably for the remainder of the injection. There was no oscillation observed and the aspirator pumped smoothly following the ~5 msec startup transient.

As expected, the amount of blowback decreased with decreasing F_2 injectant static pressure, and it is felt that this effect may be an ever-present part of the startup transient for the aspirator. The performance of the modified aspirator, as measured by the specific pressure rise, was essentially indistinguishable from that of the previous SS and SA tests.

Detonation Supplemental Tests: As described previously, there were occasional detonations in the course of the US tests, all of which followed liquid F_2 injections, and all possibly related to O_2 inhibition of reaction rate. However, detonation was never observed in the initial submerged tests. It was expected that this was due to the use of the long injection line in the submerged configuration, which resulted in warming of the injectant prior to injection. To check this thesis, a short series of tests were run (see Table VIII) in which cold gas/liquid F_2 was injected, with the entire external injection loop cooled with LN_2 to prevent warming of the injectant. The O_2 level remained at 0.54 vol %. Of the four tests, three detonated shortly after injection (4 to 9 msec delay). Again, these detonations were visible for less than 1/4000 sec. The fourth test failed to react, but detonated 2.940 sec later, after the frozen F_2 had settled to the Dewar bottom. It appears that injection of cold gas or liquid gives a dense slug of F_2 which, coupled with O_2 imposed reaction inhibition, leads to a condition where detonation can occur following the initial nonreaction.

Statistical Results.—A fundamental assumption in the factorial design of the test series is that the dependent variables of hypergolicity such as ignition delay time, pressure rise, etc., must be "continuous" quantitative responses to the independent variables. This is required because the statistical tests of significance of the main effects and interactions require the assumption that the response is normally distributed (which presupposes a homogeneous sample). If this assumption is not met, and some of the responses are continuous and others are Go/No-Go, then no unambiguous quantitative statements can be made about the main effects and interactions. The only recourse is to make a point-to-point interpretation of the data--the "eyeball technique."

To clarify this point, consider the following hypothetical data as an example:

	LOA	HIA
LOB	100	200 (∞, i.e., no response)
HIB	300	500

The treatments are A and B, and the response is reaction time (in μsec) for a certain process. Ignoring first the ∞ value, and assuming experimental error to be negligible, the following values are derived for the main effects and interactions:

A effect: $1/2\ ([200 - 100] + [500 - 300]) = 150$

B effect: $1/2\ ([300 - 100] + [500 - 200]) = 250$

AB (interaction) effect: $1/2\ ([500 + 100] - [300 + 200]) = 50$

These are all straightforward, saying for example, that on the average, considering the A effect above, HIA is 150 greater than LOA. Substituting ∞ for 200 in the example, and using the same technique as above, one obtains:

A effect: $1/2\ ([\infty - 100] + [500 - 300]) = \infty$

B effect: $-\infty$

AB effect: $-\infty$

This is obviously meaningless. The "eyeball technique" can only provide qualitative information such as: LOA seems to yield a response, while HIA might not unless accompanied by HIB; and HIB "always" yields a response. Such information is unsatisfactory in statistical studies which attempt to provide quantitative information.

The fact that the test matrices were effectively incomplete due to "non-responses" (no reaction) prevented a full-scale statistical analysis. However, there were test samples complete enough to perform limited statistical significance tests. In the US testing, where the effect of O_2 addition was noted, there were sufficient data to allow t-tests of significance to be performed contrasting k_1 (0.1 vol % O_2) and k_2 (1.1 vol % O_2) (see Table I.)

For US injection with GF_2, the test numbers in the k_1 group were #5, 13B, 6, 8. The tests in the k_2 group were #12A, 9, 11. All tests were at f_1, e_1, and h_1, and the effect of i (helium ullage dilution) and j (HF content) were ignored. The calculated t value was 10.3 with 3 degrees of freedom. The t-test indicated with 99% confidence that tests using k_1 gave higher pressure rise than those using k_2.

Similarly, for US injection with LF_2, the tests in the k_1 group were #18, 23, 23A, 24, and 26. The tests in the k_2 group were #17, 22, 25, and 27. All tests were at f_1 and similar injected quantity, and the level of d was ignored (i.e., no differentiation was made between saturated vapor and liquid injectant). The calculated t value was 14.5 with 4 degrees of freedom. The t-test indicated with 99% confidence that tests using k_1 gave higher pressure rise than those using k_2. An example of the point-to-point comparison or "eyeball technique" is shown in Table XII to illustrate how qualitative deductions can be made; in this case, to verify the existence of the injectant pressure effect with O_2 addition (ek effect--see Table I) for warm gas US injection.

TABLE XII

PRESSURE RISE COMPARISON USING POINT-TO-POINT TECHNIQUE
(Warm Gas US Injection)

Independent variables fixed or ignored	Contrasting test no. contrasting variables pressure rise (minus enthalpy)		Difference	
	No. 9 vs.	No. 14		
$f_1\ i_1\ h_1\ j$	$e_2\ k_2$	$e_1\ k_2$		
	13.0	0.5	12.5	$e_2\ k_2$ more potent than $e_1\ k_2$
	No. 12	No. 12A		
$f_1\ i_1\ h_1\ j$	$e_2\ k_2$	$e_1\ k_2$		
	6.0	1.0	5	
	No. 16	No. 11		
$f_1\ i_2\ h_1\ j$	$e_2\ k_2$	$e_1\ k_2$		
	16.0	1.0	15	

This comparison ignores the effect of j (HF content). It can be seen that the comparison gives the unambiguous conclusion that the conditions e_2k_2 (high injection pressure with added O_2) give higher pressure rise than the conditions of e_1k_2 (low injection pressure with added O_2).

Table XIII shows use of this technique applied to the SS injection with prepurge to verify the pressure and phase effect previously mentioned. The first comparison shows that e_2 (high pressure gas injection) gives higher

TABLE XIII

PRESSURE RISE COMPARISON USING POINT-TO-POINT TECHNIQUE
(SS Injection With Purge)

Independent Variables Fixed or Ignored	Contrasting Test No Contrasting Variables Pressure Rise (minus enthalpy)			Difference	
	No. 37	vs	No. 33		
$f_1 k_1 g_1 h_1$	e_2		e_1		
	3.5		0.8	2.7	e_2 more potent than e_1
	No. 36		No. 35		
$f_1 k_1 g_2 h_2$	e_2		e_1		
	0.0		0.0	0.0	
	No. 37		No. 44A		
$f_1 k_1 g_1 h$	e_2		d_2		
	3.5		11.0	-7.5	d_2 more potent than e_2
	No. 36		No. 43		
$f_1 k_1 g_2 h$	e_2		d_2		
	0.0		16.9	-16.9	
	No. 33		No. 40		
$f_1 k_1 g_1 h$	e_1		d_3		
	0.8		5.3	-4.5	d_3 more potent than e_1
	No. 35		No. 42		
$f_1 k_1 g_2 h$	e_1		d_3		
	0.0		3.5	-3.5	

TABLE XIII. - (Cont'd)

PRESSURE RISE COMPARISON USING POINT-TO-POINT TECHNIQUE
(SS Injection With Purge)

Independent Variables Fixed or Ignored	Contrasting Test No Contrasting Variables Pressure Rise (minus enthalpy)			Difference	
	No. 33	vs	No. 34		
$f_1\ k_1\ g_1\ h$	e_1		d_1		
	0.8		1.5	-0.7	d_1 more potent than e_1
	No. 35		No. 38		
$f_1\ k_1\ g_2\ h$	e_1		d_1		
	0.0		9.3	-9.3	
	No. 38		No. 49		
$d_1\ k_1\ g_2\ h_1$	f_1		f_2		
	9.3		7.1	2.2	f_1 more potent than f_2
	No. 43		No. 51		
$d_2\ k_1\ g_2\ h_1$	f_1		f_2		
	16.9		14.0	2.9	
	No. 41		No. 48		
$d_3\ k_1\ g_1\ h_1$	f_1		f_2		
	U		5.2	U	

TABLE XIII - (Concluded)

PRESSURE RISE COMPARISON USING POINT-TO-POINT TECHNIQUE
(SS Injection With Purge)

Independent Variables Fixed or Ignored	Contrasting Test No Contrasting Variables Pressure Rise (minus enthalpy)		Difference	
(SS INJECTION WITHOUT PREPURGE)				
	No. 53	No. 59		
$d_1\ k_1\ g_2\ h_1$	f_1	f_2		
	52.4	25.9	26.3	f_1 more potent than f_2
	No. 55	No. 68		
$d_3\ k_1\ g_1\ h_1$	f_1	f_2		
	21.1	U	U	

pressure rise than e_1 (low pressure gas injection). The second, third and fourth comparison shows that liquid or cold gas injectant (d_1, d_2, d_3) gives higher pressure rise than warm gas injectant at the same pressure (e_1, e_2, e_1). Examination of the second, third, and fourth comparisons also shows that high pressure liquid injectant (d_2) gives higher pressure rise than low pressure liquid (or cold gas) injectant (d_1, d_3).

This technique revealed an effect which had not been noticed previously, as shown in the fifth comparison and for corroboration, using data for SS injection with prepurge (sixth comparison). These comparisons show that injection into low pressure LH_2 (f_1) gives higher pressure rise than similar injection into high pressure LH_2 (f_2). A plausible explanation of this unexpected effect is that the high pressure LH_2 is not really saturated, but is slightly subcooled, with the result that part of the reactive energy must be used to raise the LH_2 temperature to the boiling point, giving a lower net pressure rise for this case.

The point-to-point comparison can be used to provide quantitative statistical data if there are sufficient samples. This is shown in Table XIV where the pressure rises for SS injection with and without prepurge are compared. Based on this comparison it can be stated at the 98% confidence level that SS injection without prepurge gives higher reactive pressure rise than SS injection with prepurge.

TABLE XIV

PRESSURE RISE COMPARISON USING POINT-TO-POINT TECHNIQUE
(SS Injection with Cold Gas or Liquid)

Independent Variables Fixed or Ignored	Contrasting Test No. Pressure Rise (minus enthalpy)		Difference
	With Prepurge vs.	Without Prepurge	
$f_1 h_1 d_1 k_1 g_1$	No. 34	No. 54	
	1.5	22.8	21.3
$f_1 h_1 d_1 k_1 g_2$	No. 38	No. 53	
	9.3	52.4	43.1
$f_1 h_1 d_2 k_2 g_2$	No. 47	No. 56	
	5.2	36.9	31.7
$f_1 h_1 d_3 k_1 g_1$	No. 41	No. 55	
	U	21.1	U
$f_1 h_1 d_3 k_1 g_2$	No. 42	No. 52	
	3.5	40.5	37.0
$f_2 h_1 d_3 k_1 g_1$	No. 48	No. 68	
	5.2	U	U
$f_2 h_1 d_1 k_1 g_2$	No. 49	No. 59	
	7.1	25.9	18.8

Comparison of Observed and Expected Pressure Rise.—For MTI, there are three simple models which describe how the reaction heat release can be used for tank pressurization:

(1) All of the reaction heat goes to uniformly raising the temperature (and thus pressure) of the ullage gas.

(2) All of the reaction heat goes to vaporization (but not superheating) of LH_2 and the resultant vapor mass addition raises the pressure.

(3) The reaction heat goes into vaporizing some of the LH_2 and raising the temperature of the remainder such that the resulting GH_2-LH_2 system is saturated and at equilibrium.

Model (1) gives the highest specific pressure rise (pressure rise per mass injected) but is subject to pressure collapse due to heat transfer from the warmer ullage to the surroundings. Model (2) is perhaps more desirable for certain applications because it gives the highest pressure rise without pressure collapse, and leaves the LH_2 slightly subcooled. Model (3) is undesirable because it gives the lowest pressure rise and leaves the LH_2 in a saturated condition.

Based on the characteristics of the hypergolicity test apparatus, the three models are shown in fig. 21, together with data from all tests which showed reaction. It must be emphasized that it is very risky to draw general steady-flow pressurization criteria from these data, which are for very small quantities "slug-injected" in a very short time. The following general observations are made, restricted by the previous considerations:

(1) Warm gas US injection gives the highest specific pressure rise, generally accompanied by a temperature rise. This would be expected for this mode, but these data do not reflect the subsequent pressure collapse, which sharply reduces the high pressures noted.

(2) Cold gas or liquid US injection gives lower specific pressure rise, but does not generally show a temperature rise, and has much less subsequent pressure collapse.

(3) The most repeatable pressurization is provided by cold gas or liquid SS injection without prepurge. These give the highest specific pressure rise with minimum pressure collapse. The fact that many of the data points lie above the theoretical line B-B may be explained by (a) non-steady state and non-equilibrium effects, (b) unobserved "enthalpic" effects which were included, or (c) discrepancies in the physical assumptions on which the model B-B was based.

(4) Warm gas SS injection tests without prepurge and cold gas or liquid SS injection tests with prepurge are definitely lower in specific pressure rise, indicating that the probable reaction inhibition effect of heat transfer to the LH_2 (without vaporization) has occurred.

(5) The test data lying below line C-C are definitely "weak" or inhibited reactions which are most inefficient in providing pressurization.

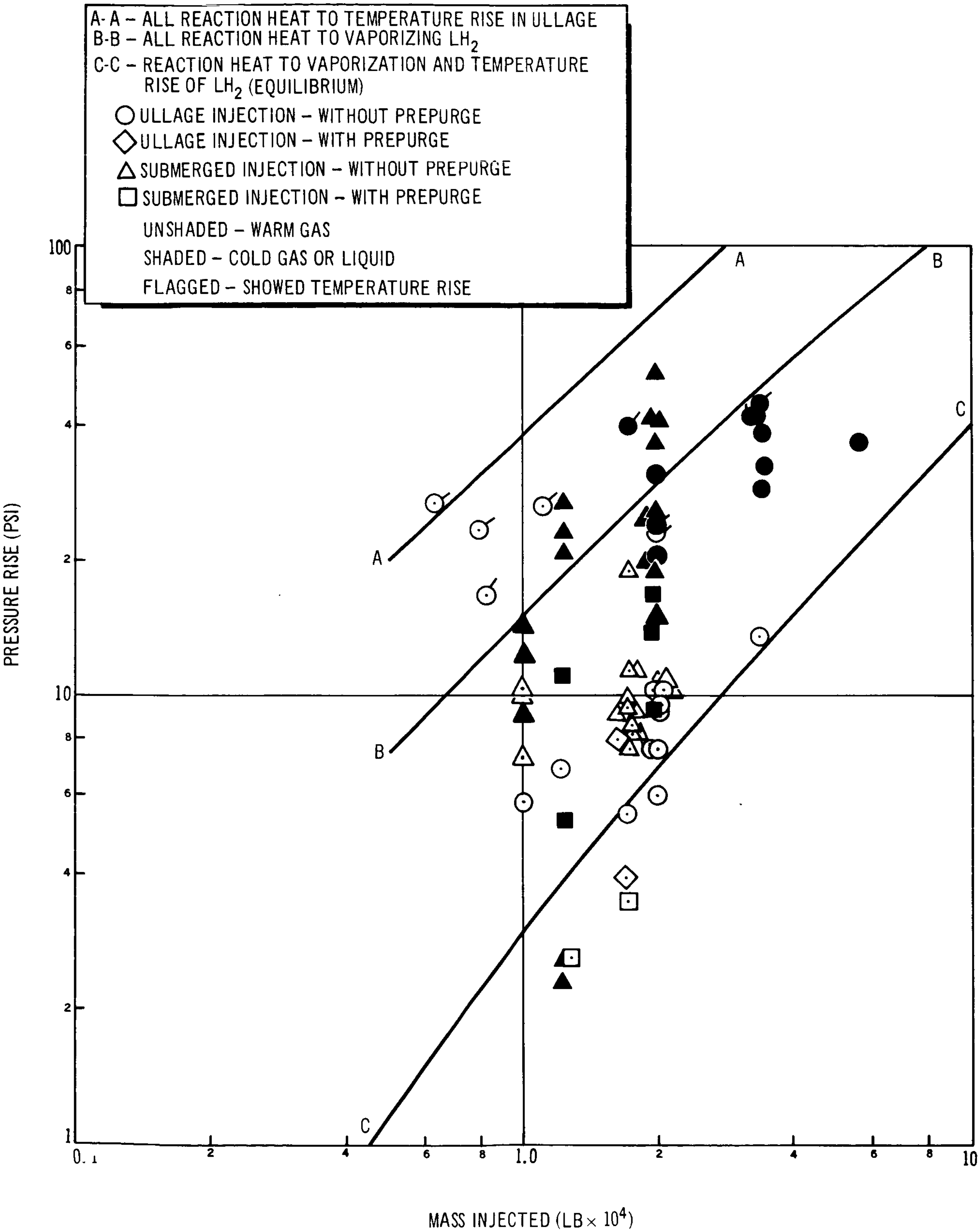

Figure 21. Pressure Rise vs Injected Mass for Three Heat Transfer Models

REACTION PRODUCT FREEZING

Peculiar to the use of MTI with deep cryogenic systems, such as LH_2, is the problem of reaction product freezing. An additional problem which may occur in the LH_2 tank is the freezing of the F_2 injectant when reaction does not occur. These phenomena have several impacts on the design of an MTI system. First, the reaction products, themselves, cannot be used for pressurization, as is the case with other MTI systems, because they rapidly condense out and freeze. Rather, the heat release from the chemical reaction and product condensation must be directed to vaporizing LH_2 or to heating the ullage gas to effect pressurization. Further, the reaction product, HF, becomes a contaminant in the propellant, and may have deleterious effects on the operation of the propellant transfer system. Finally, unreacted frozen F_2 must be avoided at all costs (i. e., reaction must be assured), since frozen F_2 in LH_2 is very hazardous and is likely to explode with little or no provocation. It is necessary, therefore, to determine the characteristics and behavior of both the reaction product (HF) and the unreacted product (F_2) in the LH_2 tank.

Reacted Product

The behavior of the frozen reaction product HF was observed visually in each of the approximately 60 tests in which reaction occurred. The HF particles are apparently very fine, and render the LH_2 cloudy-looking. In an attempt to determine the approximate size of the HF particles, a Tyndall-cone apparatus was installed next to the test Dewars. This apparatus consisted simply of an intense light beam source and a remotely operated camera. The setup was such that the beam could also be observed visually. The Tyndall-cone effect appears if colloidal particles ($\sim 1\mu$) are present in the path of the light beam through the fluid. The beam becomes visible with a somewhat milky appearance due to light scattering. Larger particles appear as bright points of light or as recognizable individual particles. Solutions appear clear. The apparatus was checked out with tap water which showed a strong Tyndall-cone effect. Immediately after filling the Dewar, the pure LH_2 was examined to see if there was a Tyndall-cone effect. There was not. Following several runs, in which reaction occured, both photographs (fig. 22) and visual observation showed no Tyndall-cone effect, indicating that the frozen HF crystals are not colloidal sized ($\sim 1\mu$) and are probably much larger ($\sim 100\mu$).

It was observed that the HF crystals plated out on all available surfaces, forming a frosty film (fig. 23A). This was observed to take place before and

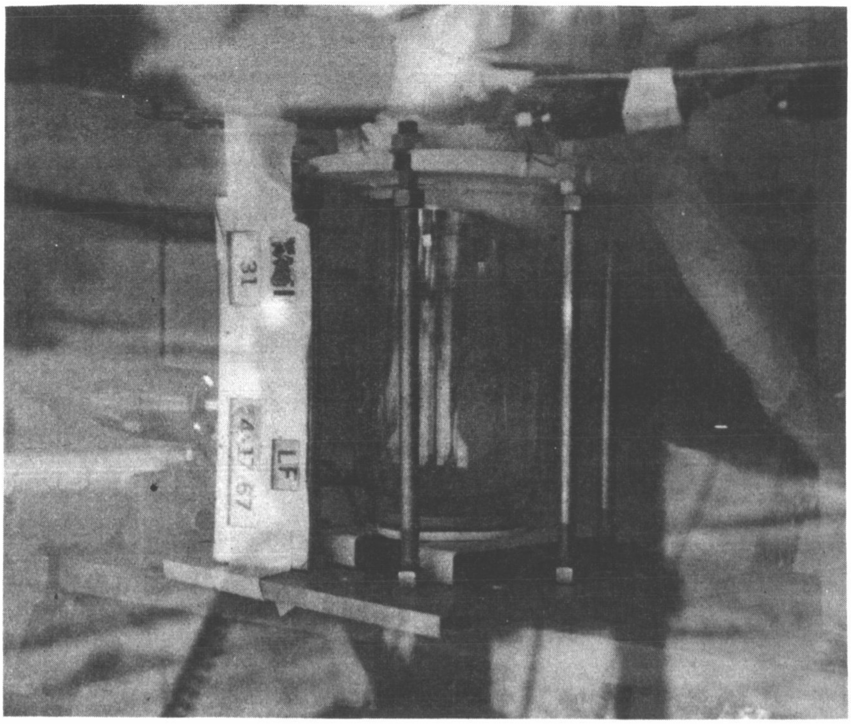

Figure 22. Photograph Showing Absence of Tyndall Effect After Reaction

during expulsion of the LH_2 from the Dewar. High-power examination of the HF film verified the conclusions regarding size drawn from the Tyndall-cone experiment. This also agreed with previous observations of HF crystals condensed on aluminum from GF_2 vapor (done under a Douglas IRAD program) which indicated that the HF crystal size was of the order of 200μ.

Attempts were made to collect the HF solids on a stainless steel mesh by filtering the LH_2 during expulsion from the reactor at the end of pressurizing experiments. Materials collecting on the filter were then to be distilled into a trap and analyzed. No increase in pressure drop across the filter was observed during the LH_2 flow, and attempts to analyze products collected in the trap gave erratic results. It was concluded that no appreciable quantity of HF collected on the filter; this may have been due to difficulties in filtering HF from LH_2 or else the observed plating out of HF in the Dewar reactor was complete and no HF reached the filter. Some recent experiments on a Douglas IRAD program have shown that filtration of solid HF from LF_2 at -320°F is difficult--the crystals are not stopped by a 10μ filter.

The HF crystals did not noticeably sink in the LH_2 during several minutes of observation. They remained suspended, and continued to plate out on all internal Dewar surfaces, but preferentially above the LH_2 surface. Following expulsion of the LH_2 and subsequent purging of the Dewar with warm gaseous helium, at least 5 min of purging were required before the HF crystals melted and disappeared. This, of course, is mainly a function of the warmup time of this particular apparatus.

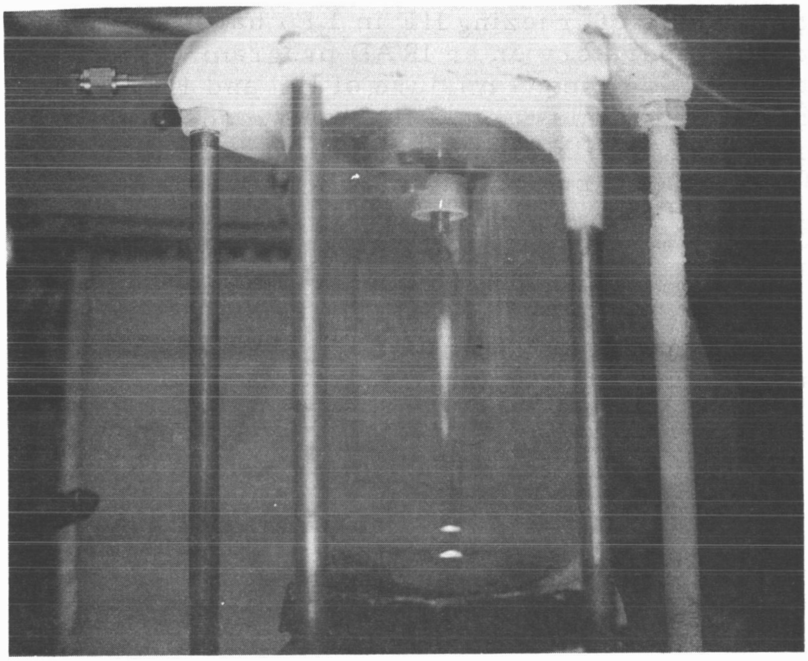

(A)

HF DEPOSITION AFTER REACTION

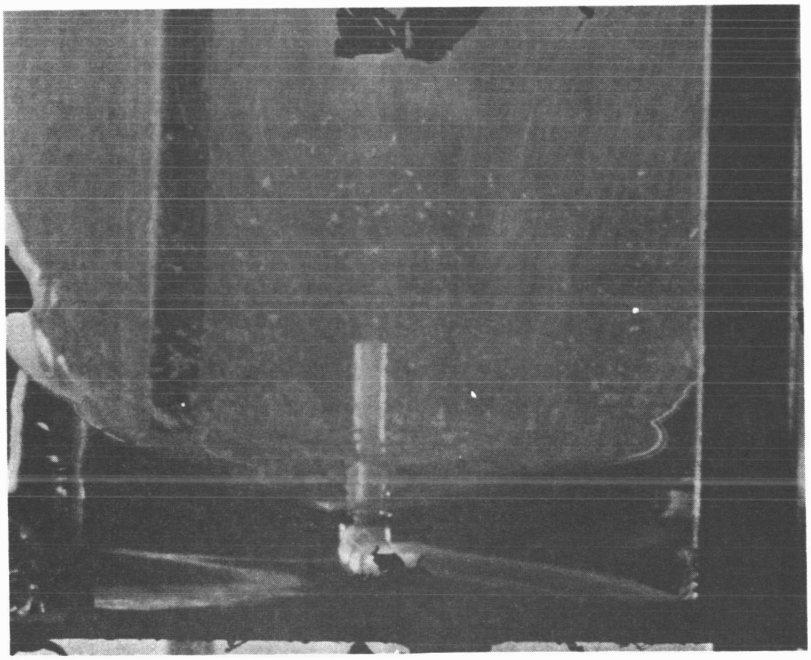

(B)

FROZEN F_2 SETTLED IN DEWAR BOTTOM AFTER NONREACTIVE INJECTION

Figure 23. Reaction-Product Effects

Experimental studies of freezing HF in LF_2 have been conducted at Douglas Astropower Laboratory on an IRAD program, and the results have been very interesting. A gaseous mixture of HF and F_2, containing 1.2 vol% of HF was led through a stainless steel tube and condensed in the bottom of a 20 mm diam glass tube at LN_2 temperature. A very cloudy suspension was formed and a flocculent precipitate slowly settled, leaving the clean supernatant LF_2 above. No solids were observed to float on the LF_2. When examined under low-power magnification (20x), individual crystals could not be resolved. The precipitate was easily dispersed by gentle agitation of the solution, and appeared to be made up of fluffy particles about 0.1 to 0.2 mm diam consisting of agglomerates of much finer crystallites. The quantity of HF appears to have an effect on the agglomeration process. Very small quantities of HF form a very fine film; larger quantities form fine crystallites which break off, settle, and agglomerate.

During the submerged injection test series, frozen HF was a particularly bothersome problem. It tended to plate out on the inside of the injector tube, leading occasionally to injector plugging, and twice to plugging of the injector valve in such a way that it did not allow it to close, thus letting pressurizing He into the Dewar following injection. This HF film was particularly stubborn, requiring long periods of purging before the injector tube warmed up enough to allow the HF to melt and disappear. It was noted that the frozen HF in the injector continued to attack the glass, etching and weakening the injector tube until it broke during chilldown (in 1 case) or reaction (in 2 cases) (fig. 24).

The 10 psi He prepurge used in many of the SS tests was expected to reduce problems of injector plugging. This prepurge was found to be quite effective in most cases, though some gradual HF build-up occurred. Post injection purge with GHe did not prevent clogging of the system with HF ice.

The difference in effectiveness is probably closely related to the mechanical effects of the propellant being purged. The prepurge with GHe efficiently drove light, free flowing H_2 from the injector, replacing it with GHe, so that the F_2 had to leave the injector before it contacted H_2 to produce HF. Post injection purge GHe would have to cleanse the injector completely of dense, viscous LF_2 before any H_2 diffused back in. It would appear that this purge was not effective in removal of all F_2.

Because extended purging of the injector with warm He is not practical in an actual vehicle propellant tank, and the entire injector penetration from the outside to the inside of the LH_2 tank will certainly be below the boiling point of HF (238°K or 429°R)--and probably below the freezing point of HF (161°K or 290°R)--collection and freezing of HF in the injector is likely to be a very troublesome problem.

To further attempt to define this problem area, two supplemental tests were made in which pure HF was injected into the LH_2 Dewar through the injection loop. To obtain the required injectant driving pressure, the HF was heated to 630°R (170°F). One test was made in the US configuration and one in the SA configuration. Continuous HF injection lasted for 2.0 to 2.75 sec before the freezing HF completely plugged the injector, stopping further flow. Again, the HF plated out heavily on all internal Dewar surfaces,

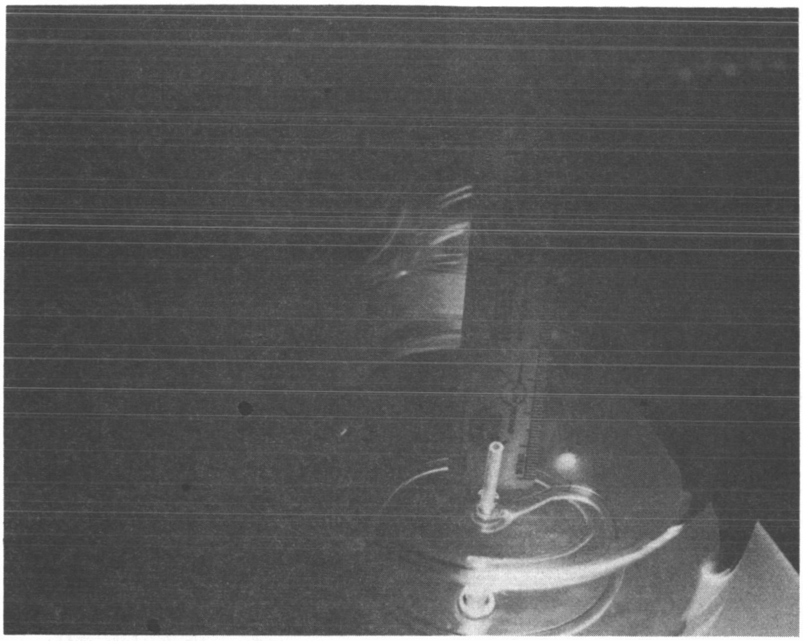

(A)

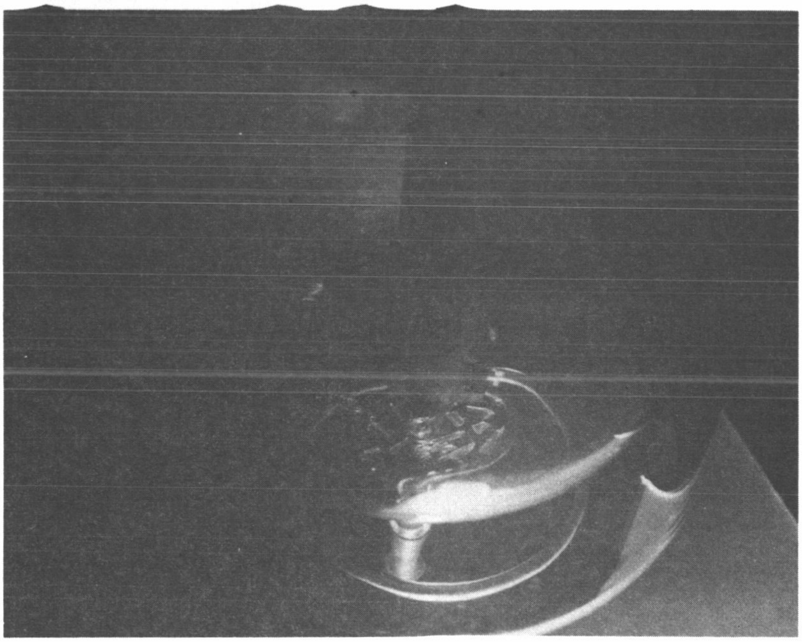

(B)

Figure 24. Injector Damage Caused by HF Attack

preferentially above the LH_2 level (i. e., in the ullage). However, the large quantities of HF injected did crystallize and collect on the Dewar bottom. As noted above, this settled HF may also be a very troublesome pressurization system problem.

Unreacted Product

The behavior of frozen F_2 in LH_2 was observed visually (with mirrors) in each of the approximately 30 tests in which reaction did not occur. The behavior of the frozen F_2 is markedly different from that of frozen HF. The particles are not suspended in the LH_2, but are rapidly agglomerated into spherical snow-like particles about 1 mm diam which settle to the bottom of the LH_2 tank (fig. 23B). The agglomeration process takes just a few seconds and the settling rate is quite slow (~0. 5 FPM). The F_2-snow (fluow ?) is readily resuspended and is easily swirled about by agitation of the LH_2. It does not adhere to the walls of the Dewar, but will repose on sloping walls up to about 25°. The action is very similar to the behavior of the "snow" in the spherical glass, water-filled scenic toy. Its innocent appearance is belied, however, by the ferocity of the reaction when the F_2-snow H_2 system decides to explode. There were only two instances of explosion of frozen F_2 in the 30 tests in which the F_2 did not react. The first case occurred after all the LH_2 had been dumped except a small puddle of a few cc's which was below the bottom of the fill/dump tube. As was the normal case, most of the frozen F_2 (about 0. 1 gram) was settled in or near the puddle in the bottom of the Dewar. This small quantity exploded violently, throwing pieces of the glass Dewar over 50 ft. The second case occurred at the very start of the dumping procedure, before any of the liter or so of LH_2 in the Dewar had been dumped. The frozen F_2 again was partially settled in the Dewar bottom. This explosion was very violent, since the full liter of LH_2 detonated in the air after the Dewar was broken. It must be emphasized that in all 30 cases the dumping procedure was the same, and that the 2 that exploded were not different in any known way from the 28 that didn't explode. Further, agitation of the frozen F_2 was not a factor, since normal dumping of the LH_2 resulted in violent agitation of the F_2 particles caused by burps and bubbles from the fill/dump tube. One of the explosions occurred before the agitation started; the other after this agitation. Following the LH_2 dumping, in all cases, was a warm He purge. The frozen F_2 only lasted several seconds after this purge (in contrast to the frozen HF, which lasted several minutes) before it melted and disappeared.

It had been planned to study the reacted and unreacted products with a mass spectrometer to determine their exact composition. Although the reacted products were readily shown to be HF, the hazards associated with the frozen F_2-LH_2 system made mass spectrometry too dangerous, and it was dropped as an analytical technique in such cases. However, as has been pointed out, in two cases there was proof-positive that the unreacted products were solid F_2, and such products must be avoided.

CONCLUSIONS

As a result of this test program it has been found that F_2 and H_2 are generally hypergolic under conditions relevant to the use of MTI pressurization for the LH_2 tank. Normally, reliable ignition and smooth pressure rise were found; however, some physical and chemical variables inhibited the reaction, resulting in nonignition and subsequent freezing of the injectant F_2 in the LH_2. The following particular effects were noted:

(1) In the simple ullage injection mode (US), it was found that adding O_2 to the F_2 injectant to the order of 1.0 vol % caused reaction inhibition such that increased injectant total enthalpy was required to overcome this inhibition and give reliable ignition before freezing of the injectant occurred. There was no discernible effect due to HF in the F_2, 50% helium in the ullage, or catalysis from an aluminum or copper surface in the apparatus. In this mode there was no enthalpic pressure rise due to injection of a relatively warmer fluid. Following reactive pressurization a rapid pressure collapse generally occurred.

(2) In the simple submerged injection mode (SS) there was a significant enthalpic pressure rise, and very little pressure collapse following reaction. In this mode a helium prepurge had an inhibiting effect, but helped alleviate the problem of HF freezing in the injector. SS injection without a helium prepurge gave reliable ignition even with O_2 levels of as high as 1.54 vol %.

(3) The aspirated submerged injection mode (SA), in the modified configuration, gave excellent pressurization control with no sacrifice in pressure rise. This technique holds considerable promise as a method for obtaining predictable full-scale injection and pressurization.

(4) Comparison of observed pressure rise with simple pressurization models indicated that US injection tended to give ullage heating, while SS and SA injection tended to provide more effective pressurization by vaporization of LH_2 with no ullage heating.

(5) Actual ignition delay time was found to be very short (0 to 3 msec) and the maximum fluorine/hydrogen flame velocity was found to be approximately 130 ft/sec.

(6) Reaction Product (HF) freezing occurred after H_2-F_2 reaction and HF particles became suspended in the LH_2. The particles have an apparent size ~100µ and tended to plate out on all internal Dewar surfaces with a frosty appearance. This plating out resulted in severe problems of injector plugging during the SS mode tests without a helium prepurge.

(7) Following tests with no reaction, the injectant F_2 froze in the LH_2 forming white flocculent snow-like particles ~1 mm in diameter. These particles settled in the LH_2 at about 0.5 ft/min, but were easily dispersed by agitation of the LH_2. They did not stick to Dewar walls but reposed at angles up to about 25° in the Dewar bottom. This frozen F_2 in LH_2 was very hazardous and resulted in several vigorous detonations.

The submerged injection mode gives the most reliable ignition and effective pressure rise, with the SA configuration providing maximum pressurization control with no apparent loss of pressurization efficiency. However, problems of HF freezing in the injector are most severe in this mode (unless a reaction-inhibiting helium prepurge is used) and may be most troublesome with pulsed (or restart) operation because HF may plate out in the injector between pulses. It is felt that steady-state injection and pressurization tests can now be safely and effectively undertaken to provide necessary data on MTI system problems of control and optimum injector design.

REFERENCES

1. Kenny, R., Winkler, J., Bingham, P.: (U) Main-Tank-Injection Pressurization of High-Energy Propellants, Final Report, Technical Report AFRPL-TR-66-65, Martin Company, Denver, Colo., July 1966. Confidential

2. Levy, Joseph B., and Copeland, B. K. Westley: The Kinetics of the Thermal, Hydrogen-Fluorine Reaction. I. Magnesium Reactor. J. Phys. Chem. Vol. 67, 2156, Oct. 1963.

3. Levy, Joseph B., and Copeland, B. K. Westley: The Kinetics of the Hydrogen-Fluorine Reaction. II. The Oxygen-Inhibited Reaction. J. Phys. Chem. Vol. 69, 408, Feb. 1965.

4. Davies, O. L., Ed., The Design and Analysis of Industrial Experiments, 1960.

5. Brokaw, Richard S.: A Suggested Mechanism for the Hydrogen-Fluorine Reaction. J. Phys. Chem. Vol. 69, 2488, 1965.

6. Brokaw, Richard S.: A Suggested Mechanism for the Hydrogen-Fluorine Reaction. II. The Oxygen-Inhibited Reaction. J. Phys. Chem. Vol 69, 2808, 1965.

7. Hu, J. H., White, D., Johnston, H.: Condensed Gas Calorimetry. V. Heat Capacities, Latent Heats and Entropies of Fluorine From 13 to 85°K.; Heats of Transition, Fusion, Vaporization and Vapor Pressure of the Liquid. J. Am. Chem. Soc. Vol. 75, 5642, 1953.

(3) Partially miscible solid solutions.

(A) Peritectic solid solution.

(B) Eutectic solid solution.

For nonpolar compounds to form solid solutions, the following conditions must generally be satisfied:

(1) Analogous chemical constitutions.

(2) Similar crystal structures.

(3) Nearly equal molecular volumes.

While little is known of crystal structures of F_2 and OF_2, it is certain that conditions 1 and 3 are not satisfied, and it is unlikely that solid solutions will form. There is no known tendency toward compound formation between OF_2 and F_2. Thus, simple eutectic or monotectic systems are probable--and the latter are rarely encountered.

If it is assumed that the system would be a simple eutectic, with the solution of each component in the other obeying Raoult's law, and the liquidus curves conforming to equations for ideal solutions, the following considerations would apply.

From the Clausius-Clapeyron equation, it can be shown that for equilibrium between solid solvent and vapor, at constant pressure,

$$\frac{d\ell n P_s}{dT} = \frac{L_s}{RT^2}$$

For an equilibrium between liquid and vapor, the corresponding equation is

$$\frac{d\ell n P_L}{dT} = \frac{L_e}{RT^2}$$

If it is assumed that the equations hold for supercooled solution in contact with solid, then

$$\frac{d\,\ell n(P_s/P_L)}{dT} = \frac{L_s - L_e}{RT^2} = \frac{L_f}{RT^2}$$

Appendix A

FREEZING-POINT DEPRESSION IN LF_2 SYSTEMS

INTRODUCTION

To alleviate potential problems of injectant freezing during MTI, a program was initiated to lower the freezing point of LF_2 without appreciably affecting its chemical reactivity. The use of an eutectic mixture with another cryogenic oxidizer seemed the method of choice, and consideration of physical and chemical properties led to the selection of oxygen difluoride, OF_2, for the other component. Oxygen was also suggested, but reports were noted of the considerable effect oxygen has on the LF_2-LH_2 reaction (ref. A-1), an effect which was found during the hypergolicity testing and was also reported in the OF_2-H_2 reaction (ref. A-2). Oxygen was dropped from further consideration.

Theoretical calculations for the F_2-OF_2 system suggested that experimental investigation was warranted. An experimental plan and apparatus were designed and the tests were conducted.

THEORETICAL

The equilibrium or phase diagram of a two-component solid-liquid system may assume several general forms according to the nature of the components (ref. A-3); these forms may be classified as follows:

(1) Eutectic systems.

   (A) Simple eutectic.

   (B) Monotectic (special form of simple eutectic).

   (C) Compound formation with congruent melting point.

   (D) Compound formation with incongruent melting point.

(2) Completely miscible solid solutions.

   (A) Continuous solid solution.

   (B) Minimum melting solid solution.

   (C) Maximum melting solid solution.

At the freezing point of the solution, the vapor pressure of the solid solvent must equal that of the solution, hence,

$$\frac{d\ell n (P_1/P_L)}{dT} = \frac{L_f}{RT^2}$$

Since $P_1/P_L = X_1$ (mol fraction of solvent in solution) if Raoult's law is applicable

$$\frac{d\ell n X_1}{dT} = \frac{L_f}{RT^2}$$

If this is integrated between T and T_o (where $X_1 = 1$),

$$\ell n X_1 = \frac{L_f}{R}\left(\frac{1}{T} - \frac{1}{T_o}\right)$$

where T is the freezing point of the solution at concentration X_1. This assumes that L_f is independent of temperature. This assumption is not strictly true, but this approximation was accepted because the normal variation of L_f with temperature would increase the temperature depression to contrast to the real nonideality of the solutions which tends to decrease the depression.

From the last equation, T was calculated for various concentrations of F_2 in OF_2 and OF_2 in F_2. A value of 122 cal/mole was used for the heat of fusion of F_2 (ref. A-4). However, no value for the heat of fusion of OF_2 could be found in the literature. With a value of 6.5 assumed for the entropy of fusion, a provisional value of 320 cal/mole was used for the calculations involved for constructing the phase diagram. A minimum temperature of 39°K at a F_2 mole fraction of 0.65 resulted.

Solid F_2 is reported to undergo a transition at 45.55°K with a heat of transition of 173.9 cal/mole. (ref. A-4). Because the solid F_2 can exist in two forms above the predicted eutectic temperature, the equilibrium diagram becomes more complicated. The theoretical phase diagram was recalculated with a value of 122 cal/mole as the heat of fusion of F_2 until the transition temperature was reached, after which the liquidus curve was assumed to undergo a change in slope corresponding to the heat of fusion plus the heat of transition. This curve was continued to meet the OF_2-rich liquidus curve leading to a theoretical minimum freezing point of 40°K at 0.54 mole fraction F_2.

APPARATUS

A Pyrex apparatus was designed and built for this experiment (fig. A-1). Essentially, it consists of a central volume for the test chamber, fitted with inlet and outlet tubing, a solenoid operated stirrer, and a thermowell. The central tube is surrounded by an annulus in which the pressure can be controlled to control heat transfer rates, an annulus for LHe to cool the fluids in test, an evacuated annulus, an annulus for LN_2 (heat shield), and an evacuated annulus. The evacuated annuli were silvered except for strips for observation of the interior.

Liquid helium is supplied to the cooling bath from 25-liter transport Dewars connected to the apparatus by insulated lines. Liquid nitrogen was poured into the heat shield when needed.

Temperatures were measured with a copper-constantan thermocouple inserted in the thermowell with an external reference junction at LN_2 temperature. Thermoelectric potentials were measured with a Grey type E-3067 potentiometer and temperatures were estimated from the tables and data of Powell, Bunch, and Corruccini (ref A-5). The thermocouple calibration was checked against boiling LN_2 and LH_2 as fixed points. At 50°K, the thermoelectric emf for copper-constantan is about 12.1 μV/deg. With a sensitivity of 5 μV or better for the potentiometer, the sensitivity of temperature reading is about 0.4°.

MATERIALS

The oxidizers tested were obtained in the gaseous state from commercial suppliers. Fluorine was supplied by Air Products and Chemicals. It was passed over a NaF absorption scrubber to reduce the HF content to 0.02 vol %. Oxygen difluoride was supplied by Allied Chemicals Division of General Chemical. It also was treated with NaF to remove HF.

PROCEDURE

The quantities of F_2 and OF_2 were measured by volume in the liquid state; weights were calculated from reported densities (refs. A-6 and A-7). A glass ampoule of calibrated volume was attached to the oxidizer supply manifold. The system was evacuated, the measuring apparatus and the ampoule were chilled with LN_2 to 77°K, the test apparatus was valved off, and the oxidizer supply was valved open. When sufficient oxidizer had condensed in the ampoule, the supply was shut off, the line to the test unit was valved open, and the LN_2 was removed from around the ampoule, causing the oxidizer to distill into the test apparatus. When distillation was complete, the ampoule was valved off.

After condensation of oxidizer was complete, the solenoid stirrer was activated, LH_e was supplied to the cooling bath, and the pressure in the heat-transfer annulus was adjusted to attain a cooling rate of about 1°K/min. The

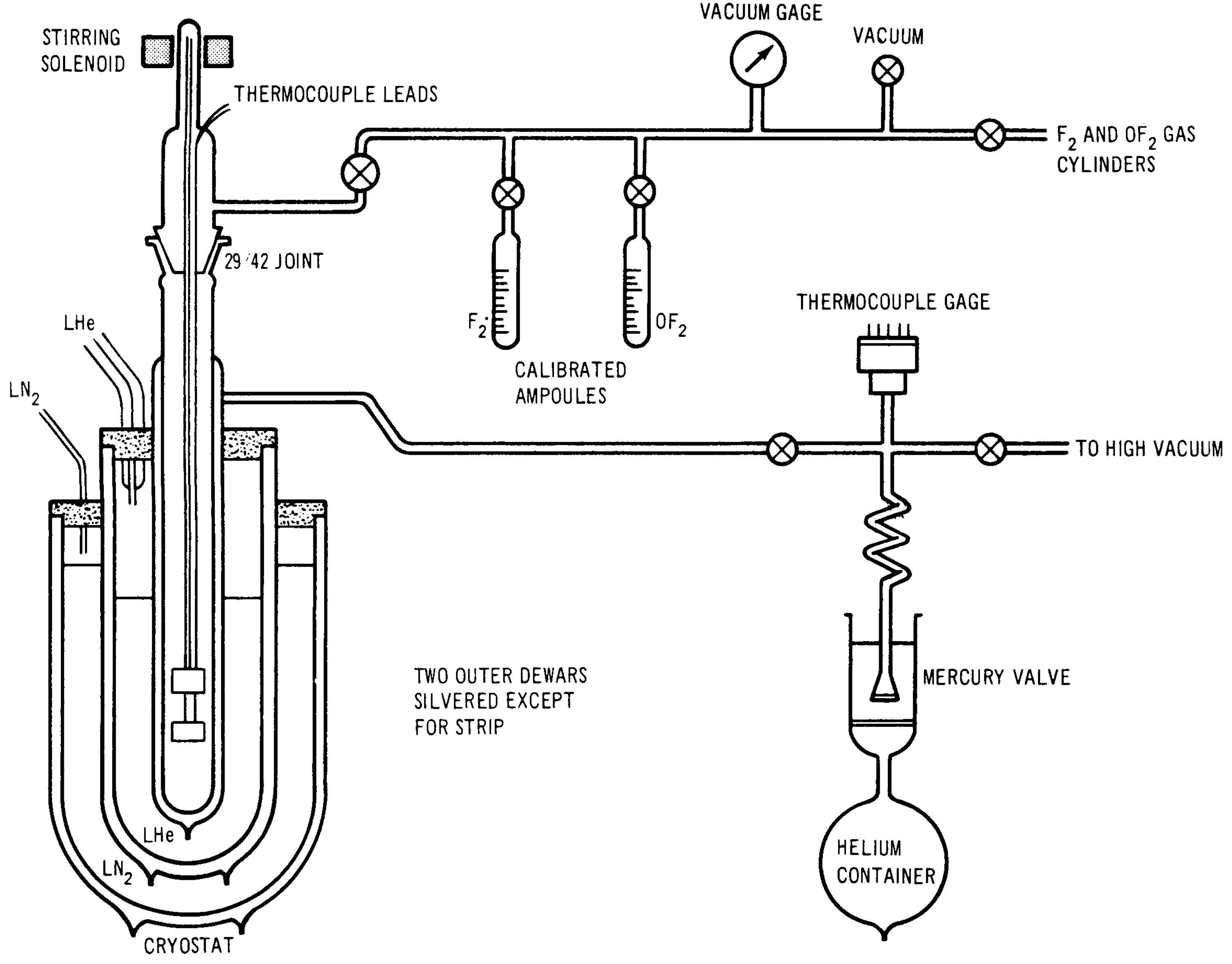

Figure A-1. Freezing-Point Apparatus

emf of the thermocouple was continuously monitored, and the value recorded at 30-sec intervals. The appearance of the oxidizer was observed visually during the experiment.

The experiments were conducted with F_2, with OF_2, and with several mixtures. The recorded thermocouple potentials were converted to temperatures. Cooling curve graphs, temperatures versus time, were plotted for each solution concentration. Figure A-2 is a typical example. Temperatures at which breaks in the curves occurred were identified, and these were plotted on a temperature versus concentration graph to provide a typical phase diagram (fig. A-3). The data used for plotting the phase diagram are tabulated in Table A-I).

RESULTS AND DISCUSSION

It was determined that, within the accuracy of the experiments, the binary system F_2-OF_2 exhibited typical eutectic formation with a probable break in the F_2-rich liquidus curve caused by a solid phase transition. The eutectic temperature was found to be 43°K; the transition occurred at 45°K. The accuracy of the temperature measurements was about ±0.5°K; when the temperature-composition curves were plotted and extrapolated to their intersection (the eutectic); this resulted in an error of ±2 mol %. This variation is indicated on the graphs by the bars through the experimental points.

It can be seen that the eutectic mixture would provide a margin of about 10°K (18°R) before freezing, compared to F_2 alone. However, it was found during the hypergolicity testing that freezing of the injectant in the injector was not a problem and therefore the eutectic was dropped from consideration as an injectant for the test program.

TABLE A-I

OBSERVED FREEZING POINTS, OF_2-F_2 MIXTURES

Runs	Mole (% F_2)	Initial freezing point (°K)	Transition temperature (°K)	Eutectic freezing point (°K)
1	100	53.0	--	--
2	80	48.3	45.0	43.5
3	69.5	--	45.0	42.4
4	46	45.6	--	43.3
5	28	47.8	--	43.4
6	0	49.2	--	--

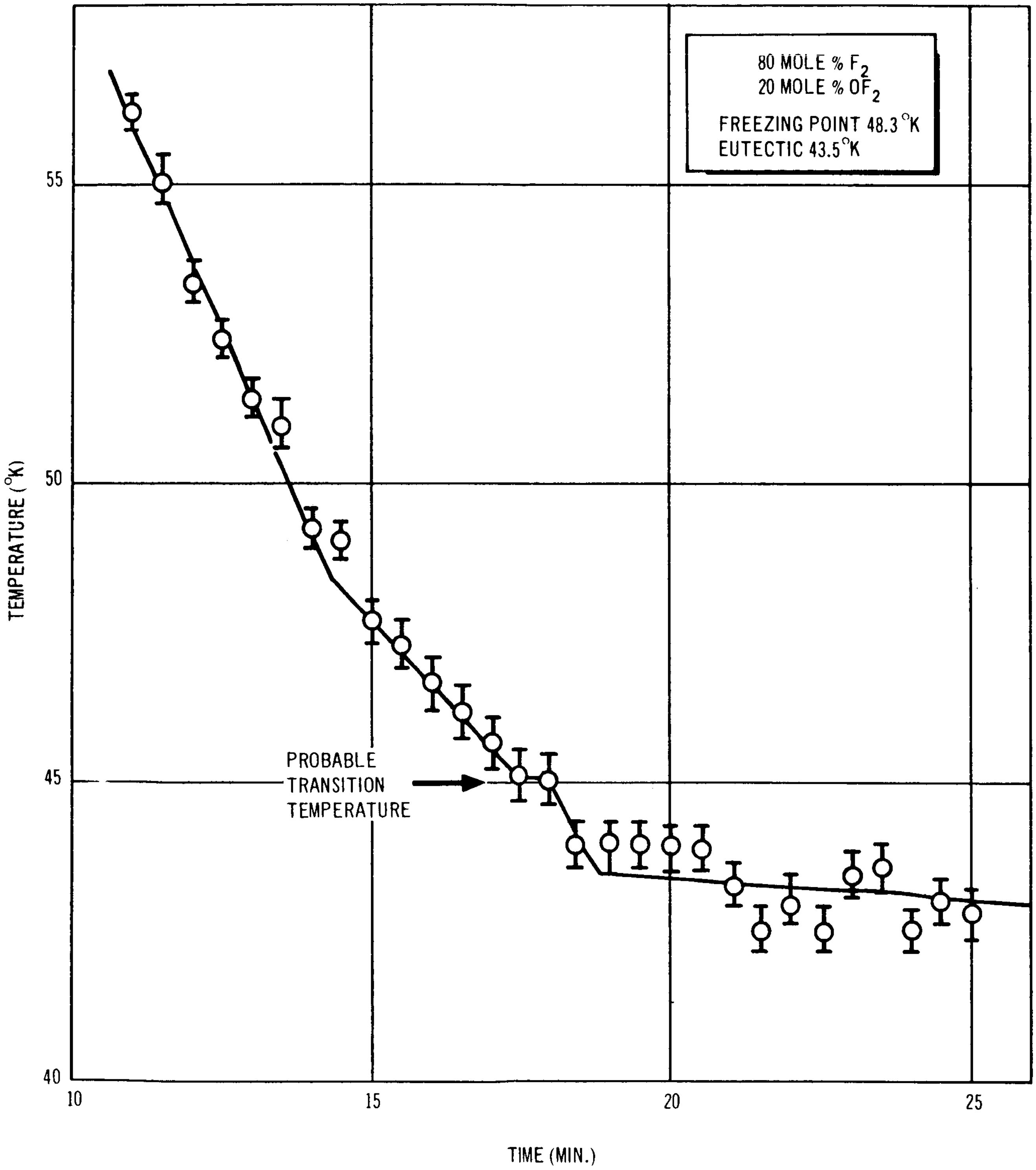

Figure A-2. Typical Cooling Curve

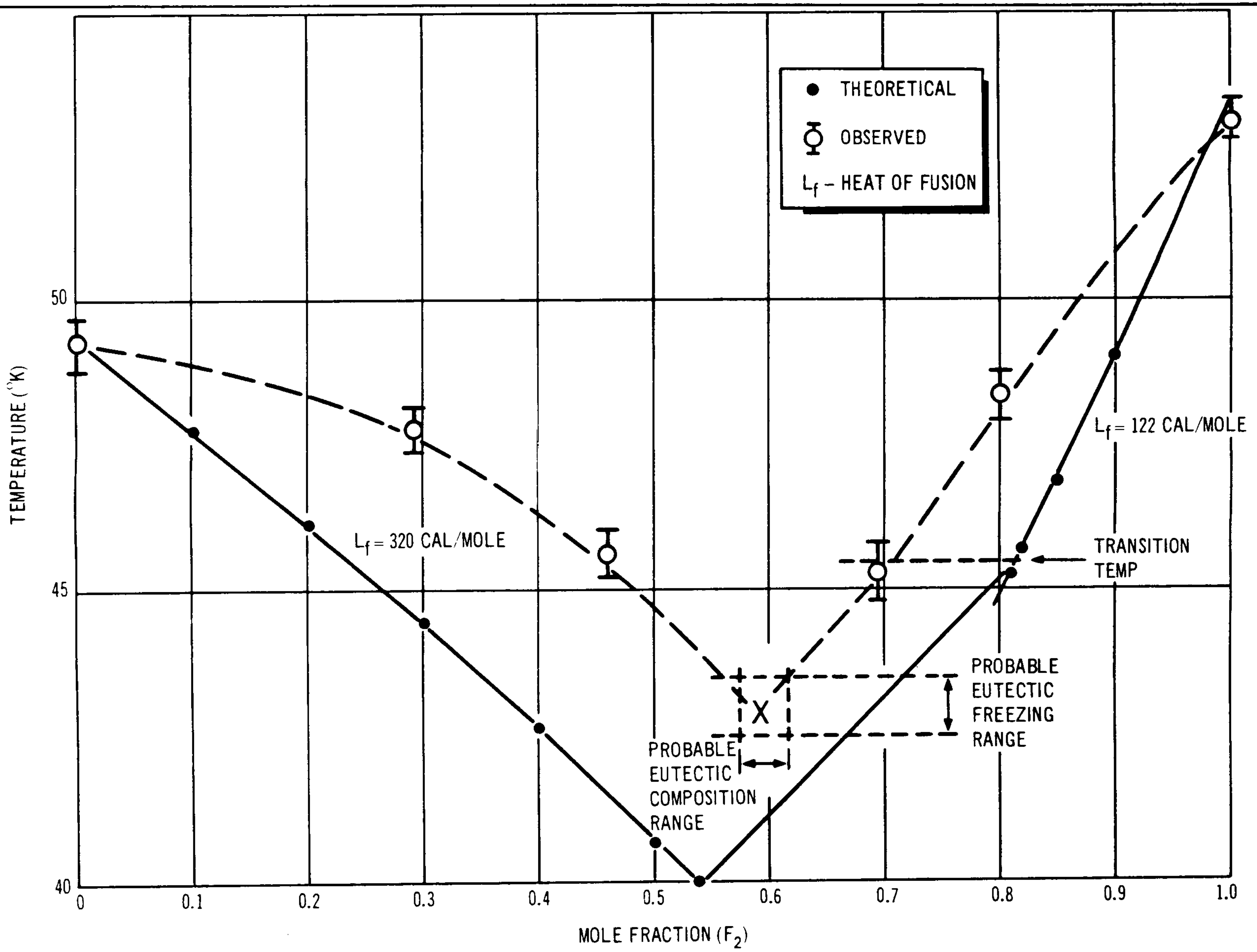

Figure A3. Phase Diagram $OF_2 - F_2$

SYMBOLS

P = vapor pressure

L = latent heat

R = gas constant

T = temperature, °K

Subscripts

s = solid state or solid-gas transition

L = liquid state or liquid-gas transition

f = fusion

l = solution

o = freezing point of pure solvent

e = equilibrium

PRECEDING PAGE BLANK NOT FILMED.

REFERENCES

A-1. Levy, J. B. and Copeland, B. K. W.: J. Phys. Chem., 67, 2156 (1963), 69, 408 (1965). Brokaw, R. S., ibid. 69, 2488, (1965), 69, 2808 (1965).

A-2. Solomon, W. C., et al: Exploratory Propellant Chemistry, Semiannual Report. Air Force Rocket Propulsion Laboratory, Edwards, California, AFRPL-TT-66-238, October 1966.

A-3. Glasstone, S.: Textbook of Physical Chemistry. D. Van Nostrand & Co., New York 1940, Chapter X.

A-4. Jih-Heng, H., White, D. and Johnston, H. L.: Am. Chem. Soc., Vol. 75, pages 5642-5, 1953.

A-5. Powell, R. O., Bunch, M. O., and Corraccini, R. J.: Cryogenics, Vol. 2, pages 139-50, 1961.

A-6. Jarry, R. L. and Miller, H. C.: J. Am. Chem. Soc., Vol 78, page 1553, 1956.

A-7. Ruff, O. and Menzel, W.: Z. Anorg. Chem. Vol 198, page 39, 1931.

PRECEDING PAGE BLANK NOT FILMED.

An experimental program is described which determined the effects of physical and chemical variables on the hypergolicity of F_2-H_2 under conditions relevant to MTI pressurization of the LH_2 tank. A concurrent program describes the characteristics of reacted HF and unreacted F_2 freezing in the LH_2 tank. Testing was done in small (5-in. diam) glass Dewars. Generally, hypergolic ignition was found with some variables inhibiting the reaction to the point of nonignition and freezing of the F_2. Several injection modes were tested and criteria for reliable ignition and effective pressure rise were determined.

An experimental program is described which determined the effects of physical and chemical variables on the hypergolicity of F_2-H_2 under conditions relevant to MTI pressurization of the LH_2 tank. A concurrent program describes the characteristics of reacted HF and unreacted F_2 freezing in the LH_2 tank. Testing was done in small (5-in. diam) glass Dewars. Generally, hypergolic ignition was found with some variables inhibiting the reaction to the point of nonignition and freezing of the F_2. Several injection modes were tested and criteria for reliable ignition and effective pressure rise were determined.

An experimental program is described which determined the effects of physical and chemical variables on the hypergolicity of F_2-H_2 under conditions relevant to MTI pressurization of the LH_2 tank. A concurrent program describes the characteristics of reacted HF and unreacted F_2 freezing in the LH_2 tank. Testing was done in small (5-in. diam) glass Dewars. Generally, hypergolic ignition was found with some variables inhibiting the reaction to the point of nonignition and freezing of the F_2. Several injection modes were tested and criteria for reliable ignition and effective pressure rise were determined.

An experimental program is described which determined the effects of physical and chemical variables on the hypergolicity of F_2-H_2 under conditions relevant to MTI pressurization of the LH_2 tank. A concurrent program describes the characteristics of reacted HF and unreacted F_2 freezing in the LH_2 tank. Testing was done in small (5-in. diam) glass Dewars. Generally, hypergolic ignition was found with some variables inhibiting the reaction to the point of nonignition and freezing of the F_2. Several injection modes were tested and criteria for reliable ignition and effective pressure rise were determined.

DISTRIBUTION LIST FOR INTERIM REPORT NASA CR-72253 "HYPERGOLICITY OF F_2-H_2 AND REACTION PRODUCT FREEZING UNDER MAIN TANK INJECTION PRESSURIZATION CONDITIONS"

CONTRACT NAS3-7963

DOUGLAS AIRCRAFT COMPANY
MISSILE AND SPACE SYSTEMS DIVISION
SANTA MONICA, CALIFORNIA

National Aeronautics and Space Administration
Lewis Research Center
21000 Brookpark Road
Cleveland, Ohio 44135
Attention: Contracting Officer, MS 500-210 (1)
Liquid Rocket Technology Branch, MS 500-209 (8)
Technical Report Control Office, MS 5-5 (1)
Technology Utilization Office, MS 3-16 (1)
AFSC Liaison Office, MS 4-1 (2)
Library (2)
Office of Reliability & Quality Assurance, MS 500-203 (1)
E. W. Conrad, MS 100-1 (1)
D. L. Nored, MS 500-209 (1)
W. E. Roberts, MS 3-17 (1)

National Aeronautics and Space Administration
Washington, D.C. 20546
Attention: - Code MT (1)
RPX (2)
RPL (2)
SV (1)

Scientific and Technical Information Facility (6)
P. O. Box 33
College Park, Maryland 20740
Attention: NASA Representative
Code CRT

Office of the Director of Defense Research & Engineering (1)
Washington, D. C. 20301
Attention: Dr. H. W. Schulz,
Office of Asst. Dir.
(Chem. Technology)

Defense Documentation Center (1)
Cameron Station
Alexandria, Virginia 22314

RTD(RTNP) (1)
Bolling Air Force Base
Washington, D. C. 20332

Arnold Engineering Development Center (1)
Air Force Systems Command
Tullahoma, Tennessee 37389
Attention: AEOIM

Advanced Research Projects Agency (1)
Washington, D. C. 20525
Attention: D. E. Mock

Air Force Missile Test Center (1)
Patrick Air Force Base, Florida
Attention: L. J. Ullian

Air Force Systems Command (SCLT/Capt. S. W. Bowen) (1)
Andrews Air Force Base
Washington, D. C. 20332

Air Force Rocket Propulsion Laboratory (RPR) (1)
Edwards, California 93523

Air Force Rocket Propulsion
Laboratory (RPM) (1)
Edwards, California 93523

Air Force FTC (FTAT-2) (1)
Edwards Air Force Base,
California 93523
Attention: Col. J. M. Silk

Air Force Office of Scientific
Research (1)
Washington, D.C. 20333
Attention: SREP, Dr. J. F. Masi

Office of Research Analysis (OAR) (1)
Holloman Air Force Base
New Mexico 88330
Attention: RRRT

U.S. Air Force (1)
Washington 25, D.C.
Attention: Col. C. K. Stambaugh
Code AFRST

Commanding Officer (1)
U.S. Army Research Office (Durham)
Box CM, Duke Station
Durham, North Carolina 27706

U.S. Army Missile Command (1)
Redstone Scientific Information Center
Redstone Arsenal, Alabama 35808
Attention: Chief, Document Section

Bureau of Naval Weapons (1)
Department of the Navy
Washington, D.C.
Attention: J. Kay, Code RTMS-41

Commander (1)
U.S. Naval Missile Center
Point Mugu, California 93041
Attention: Technical Library

Commander
U.S. Naval Ordnance Test Station
China Lake, California 93557
Attention: Code 45 (1)
Code 753 (1)
W. F. Thorm,
Code 4562 (1)

Commanding Officer (1)
Office of Naval Research
1030 E. Green Street
Pasadena, California 91101

Director (Code 6180) (1)
U.S. Naval Research Laboratory
Washington, D.C. 20390
Attention: H. W. Carhart

Picatinny Arsenal (1)
Dover, New Jersey
Attention: I. Forsten, Chief
Liquid Propulsion
Laboratory

U.S. Atomic Energy Commission (1)
Technical Information Services
Box 62
Oak Ridge, Tennessee
Attention: A. P. Huber, Code ORGDP
Box P

Air Force Aero Propulsion
Laboratory (1)
Research & Technology Division
Air Force Systems Command
United States Air Force
Wright-Patterson AFB, Ohio 45433
Attention: APRP (C. M. Donaldson)

Aerojet-General Corporation (1)
P.O. Box 296
Azusa, California 91703
Attention: Librarian

Aerojet-General Corporation (1)
11711 South Woodruff Avenue
Downey, California 90241
Attention: F. M. West
Chief Librarian

Aerojet-General Corporation (1)
P.O. Box 1947
Sacramento, California 95809
Attention: Technical Library
2484-2015A

Aeronutronic Division of
Philco Corporation (1)
Ford Road
Newport Beach, California 92600
Attention: Technical Information
Department

Aeroprojects, Incorporated (1)
310 East Rosedale Avenue
West Chester, Pennsylvania 19380
Attention: C. D. McKinney

Aerospace Corporation (1)
P.O. Box 95085
Los Angeles, California 90045
Attention: Library-Documents

Arthur D. Little, Inc. (1)
Acorn Park
Cambridge 40, Massachusetts
Attention: A. C. Tobey

Astropower Laboratory (1)
Douglas Aircraft Company
2121 Campus Drive
Newport Beach, California 92663

Astrosystems, Incorporated (1)
1275 Bloomfield Avenue
Caldwell Township, New Jersey
Attention: A. Mendenhall

ARO, Incorporated (1)
Arnold Engineering Development Center
Arnold AF Station, Tennessee 37389
Attention: Dr. B. H. Goethert
Chief Scientist

Atlantic Research Corporation (1)
Shirley Highway & Edsall Road
Alexandria, Virginia 22314
Attention: Security Office for Library

Battelle Memorial Institute (1)
505 King Avenue
Columbus, Ohio 43201
Attention: Report Library, Room 6A

Beech Aircraft Corporation (1)
Boulder Facility
Box 631
Boulder, Colorado
Attention: J. H. Rodgers

Bell Aerosystems, Inc. (2)
Box 1
Buffalo, New York 14205
Attention: T. Reinhardt
W. M. Smith

Bendix Systems Division (1)
Bendix Corporation
Ann Arbor, Michigan
Attention: John M. Bureger

The Boeing Company (2)
Aero Space Division
P.O. Box 3707
Seattle, Washington 98124
Attention: Ruth E. Peerenboom (1190)
J. D. Alexander

Chemical Propulsion Information Agency (1)
Applied Physics Laboratory
8621 Georgia Avenue
Silver Spring, Maryland 20910

Chrysler Corporation (1)
Missile Division
Warren, Michigan
Attention: John Gates

Chrysler Corporation (1)
Space Division
New Orleans, Louisiana
Attention: Librarian

Curtiss-Wright Corporation (1)
Wright Aeronautical Division
Woodridge, New Jersey
Attention: G. Kelley

University of Denver (1)
Denver Research Institute
P.O. Box 10127
Denver, Colorado 80210
Attention: Security Office

Fairchild Stratos Corporation (1)
Aircraft Missiles Division
Hagerstown, Maryland
Attention: J. S. Kerr

General Dynamics/Astronautics (1)
P.O. Box 1128
San Diego, California 92112
Attention: Library & Information Services (128-00)

Convair Division
General Dynamics Corporation (1)
P.O. Box 1128
San Diego, California 92112
Attention: Mr. W. Fenning
Centaur Resident Project Office

General Electric Company (1)
Re-Entry Systems Department
P.O. Box 8555
Philadelphia, Pennsylvania 19101
Attention: F. E. Schultz

General Electric Company (1)
Flight Propulsion Lab.. Department
Cincinnati 15, Ohio
Attention: D. Suichu

Grumman Aircraft Engineering Corporation (1)
Bethpage, Long Island,
New York
Attention: Joseph Gavin

Hercules Powder Company (1)
Allegheny Ballistics Laboratory
P.O. Box 210
Cumberland, Maryland 21501
Attention: Library

IIT Research Institute (1)
Technology Center
Chicago, Illinois 60616
Attention: C. K. Hersh
Chemistry Division

Kidde Aero-Space Division (1)
Walter Kidde & Company, Inc.
675 Main Street
Belleville 9, New Jersey
Attention: R. J. Hanville
Director of
Research Engineering

Lockheed Missiles & Space Company (1)
P.O. Box 504
Sunnyvale, California
Attention: Technical Information Center

Lockheed-California Company (1)
10445 Glen Oaks Blvd.
Pacoima, California
Attention: G. D. Brewer

Lockheed Propulsion Company (1)
P.O. Box 111
Redlands, California 92374
Attention: Miss Belle Berland
Librarian

Lockheed Missiles & Space Company (1)
Propulsion Engineering Division (D. 55-11)
1111 Lockheed Way
Sunnyvale, California 94087

Marquardt Corporation (1)
16555 Saticoy Street
Box 2013 - South Annex
Van Nuys, California 91404
Attention: Librarian

Martin-Marietta Corporation (1)
Martin Division
Baltimore 3, Maryland
Attention: John Calathes (3214)

Martin-Marietta Corporation (1)
Martin Company
Denver Division
Denver, Colorado 80201

McDonnell Aircraft Corporation (1)
P.O. Box 6101
Lambert Field, Missouri
Attention: R. A. Herzmark

North American Aviation, Inc. (1)
Space Division
12214 Lakewood Boulevard
Downey, California 90242
Attention: Technical Information Center, D/096-722 (AJ01

Northrop Space Laboratories (1)
1001 East Broadway
Hawthorne, California
Attention: Dr. William Howard

Purdue University (1)
Lafayette, Indiana 47907
Attention: Technical Librarian

Radio Corporation of America (1)
Astro-Electronics Division
Defense Electronic Products
Princeton, New Jersey
Attention: S. Fairweather

Republic Aviation Corporation (1)
Farmingdale, Long Island
New York
Attention: Dr. William O'Donnell

Rocket Research Corporation (1)
520 South Portland Street
Seattle, Washington 98108

Rocketdyne Division of
North American Aviation, Inc. (1)
6633 Canoga Avenue
Canoga Park, California 91304
Attention: Library
Department 596-306

Rohm and Haas Company (1)
Redstone Arsenal Research Division
Huntsville, Alabama 35808
Attention: Librarian

Space-General Corporation (1)
777 Flower Street
Glendale, California
Attention: C. E. Roth

Stanford Research Institute (1)
333 Ravenswood Avenue
Menlo Park, California 94025
Attention: Thor Smith

Texaco Experiment, Incorporated (1)
P. O. Box 1-T
Richmond, Virginia 23202
Attention: Librarian

Thiokol Chemical Corporation (1)
Alpha Division, Huntsville Plant
Huntsville, Alabama 35800
Attention: Technical Director

Thiokol Chemical Corporation (1)
Reaction Motors Division
Denville, New Jersey 07834
Attention: Librarian

Thiokol Chemical Corporation (1)
Redstone Division
Huntsville, Alabama
Attention: John Goodloe

TRW Systems, Incorporated (1)
1 Space Park
Redondo Beach, California 90200
Attention: STL Tech. Lib. Doc.
Acquisitions

TRW, Incorporated (1)
TAPCO Division
23555 Euclid Avenue
Cleveland, Ohio 44117
Attention: P. T. Angell

United Aircraft Corporation (2)
Corporation Library
400 Main Street
East Hartford, Connecticut 06118
Attention: Dr. David Rix
Erle Martin

United Aircraft Corporation (1)
Pratt and Whitney Division
Florida Research and Development
Center
P. O. Box 2691
West Palm Beach, Florida 33402
Attention: Library

United Aircraft Corporation (1)
United Technology Center
P. O. Box 358
Sunnyvale, California 94088
Attention: Librarian

Vought Astronautics (1)
Box 5907
Dallas 22, Texas
Attention: Warren C. Trent

National Aeronautics and Space
Administration (1)
Ames Research Center
Moffett Field, California 94035
Attention: Library

National Aeronautics and Space
Administration (1)
Flight Research Center
P. O. Box 273
Edwards, California 93523
Attention: Library

National Aeronautics and Space
Administration (1)
Goddard Space Flight Center
Greenbelt, Maryland 20771
Attention: Library

National Aeronautics and Space
Administration (1)
John F. Kennedy Space Center
Cocoa Beach, Florida 32931
Attention: Library

National Aeronautics and Space
Administration (1)
Langley Research Center
Langley Station
Hampton, Virginia 23365
Attention: Library

National Aeronautics and Space
Administration (1)
Manned Spacecraft Center
Houston, Texas 77001
Attention: Library

National Aeronautics and Space
Administration (2)
George C. Marshall Space Flight
Center
Huntsville, Alabama 35812
Attention: Library
Keith Chandler,
R-P&VE-PA

Jet Propulsion Laboratory (1)
4800 Oak Grove Drive
Pasadena, California 91103
Attention: Library